PB 182988

INFRARED SPECTROSCOPIC STUDY OF GAS-SOLID INTERACTIONS

FINAL REPORT

JANUARY 1969

Process Control Engineering Division
National Air Pollution Control Administration
Consumer Protection and Environmental Health Services
Public Health Service
U. S. Department of Health, Education and Welfare

Contract No. PH 86-68-78

Submitted by

General Technologies Corporation
1821 Michael Faraday Drive
Reston, Virginia 22070

by

James S. Burton

Reproduced by the
CLEARINGHOUSE
for Federal Scientific & Technical
Information Springfield Va. 22151

111

INFRARED SPECTROSCOPIC STUDY OF GAS-SOLID INTERACTIONS

FINAL REPORT

JANUARY 1969

Process Control Engineering Division
National Air Pollution Control Administration
Consumer Protection and Environmental Health Services
Public Health Service
U. S. Department of Health, Education and Welfare

Contract No. PH 86-68-78

Submitted by

General Technologies Corporation
1821 Michael Faraday Drive
Reston, Virginia 22070

by

James S. Burton

Acknowledgment. The author wishes to thank Dr. R. G. Shaver, Vice President of Engineering, General Technologies Corporation, for his assistance in the statistical analysis of the adsorption data.

ABSTRACT

Infrared spectroscopy was applied to the study of gas-solid interactions between sulfur dioxide in a simulated flue gas and various solid adsorbents. In situ spectroscopic studies have been conducted in a high-temperature infrared cell up to 300°C. By measuring the integrated intensities of the sulfate absorption band of the reacted product, it was possible to calculate the rates at which limestone Sample No. BCR 1699-202 adsorbed sulfur dioxide from a simulated flue gas at 262°C. An activation energy of 11.8 kcal/mole was calculated for the adsorption process. These studies combined with the recorded spectra of various limestone samples before and after exposure to sulfur dioxide at 750 and 1800°F. showed that the most probable reaction mechanism of samples exposed at 750°F. was the adsorption of sulfur dioxide as sulfite and the oxidation of the sulfite to sulfate. At temperatures above 1800°F., the oxidation of sulfite to sulfate was very rapid and only sulfate was detected in the spectrum of the reacted samples. In addition, a proposed design is presented for conducting the infrared studies in the 1600 - 2000°F. temperature region.

Preliminary investigations were also conducted on the mechanism of "dead-burning." The results have shown that the silicates probably play a role in the "dead-burning" process. ( )

TABLE OF CONTENTS

Page

I INTRODUCTION AND SUMMARY 1

II EXPERIMENTAL SECTION 4

1. EXPERIMENTAL APPARATUS 4

  a. Flow-Through Infrared Cell for Preliminary Examination of Adsorbed Species 4
  b. Flow-Through High Temperature Infrared Cell 4
  c. Pyrex Resistance Furnace 7
  d Infrared Recording Equipment 7

2. GAS-HANDLING EQUIPMENT 8

3. CHEMICALS IN THIS STUDY 8

  a. Gases 8
  b. Solid Adsorbents 8

4. EXPERIMENTAL PROCEDURES 15

  a. Preparation of Samples 15
  b. Calculation of the Integrated Intensities of the Sulfate Ion 15

III RESULTS AND DISCUSSION OF RESULTS 18

1. PRELIMINARY INFRARED SPECTROSCOPIC STUDIES OF THE GAS-SOLID INTERACTION BETWEEN SULFUR DIOXIDE IN A FLUE GAS AND VARIOUS SOLID ADSORBENTS 18

2. INFRARED SPECTRA OF LIMESTONE SAMPLES REACTED WITH FLUE GAS AT THE NATIONAL AIR POLLUTION CONTROL ADMINISTRATION 24

  a. Infrared Spectra of Slaked Limestone Samples Before and After Exposure to Flue Gas 24

  b. Infrared Spectra of Limestone Samples Before and After Exposure to Flue Gas at 1800°F 43

3 INFRARED SPECTRA OF THE REACTION OF FLUE GAS WITH VARIOUS LIMESTONE SAMPLES IN HIGH-TEMPERATURE INFRARED CELL 63

TABLE OF CONTENTS (cont.)

Page

a. Infrared Spectra of the Reaction of Flue Gas with Limestone Sample No. BCR 1699-202 63
b. Mechanism of the Adsorption of Sulfur Dioxide from a Flue Gas by Limestone Adsorbents 74
c. Analysis of Infrared Spectroscopic Data Obtained from the Exposure of Slaked Limestone Sample No. BCR 1699-202 to Flue Gas at 201-302°C. 74
d. Analysis of Data Obtained at 262°C with Limestone Sample No. BCR 1699-202 79
e. Infrared Spectrum of Sample No. BCR 1362-201 After Reaction with a Simulated Flue Gas at Elevated Temperatures 85
f. Infrared Spectrum of Alkalized Alumina Before and After Reaction with Flue Gas at Elevated Temperatures 85

4. PRELIMINARY STUDIES ON THE UTILIZATION OF INFRARED SPECTROSCOPY TO INVESTIGATE "DEAD BURNING" 88

5. PROPOSED DESIGN OF INFRARED CELL FOR CONDUCTING INFRARED SPECTROSCOPIC STUDIES OF GAS-SOLID INTERACTIONS IN THE TEMPERATURE RANGE OF 1600 - 2000°F. 91

IV CONCLUSIONS AND RECOMMENDATIONS 95

V REFERENCES 97

VI APPENDIX — REYNOLD'S "ANALOGY" EQUATIONS FOR MASS TRANSFER FROM A GAS STREAM TO A FLAT PLATE 99

LIST OF ILLUSTRATIONS

Figure		Page
1	Infrared Cell for Studying Gas-Solid Interactions at Room Temperature	5
2	Infrared Cell for Studying Gas-Solid Interactions at Elevated Temperatures	6
3	Stainless Steel Infrared Cell Positioned in the Beckman IR 10	9
4	Portable Vacuum System	10
5	Flow System for Synthetic Flue Gas	11
6	Aluminum Hydroxide, $Al(OH)_3$	21
7	Infrared Spectrum of CaO Deposit on Irtran Window before Reaction with Simulated Flue Gas	22
8	Infrared Spectrum of CaO Deposit after Reaction with Simulated Flue Gas for One Hour	23
9	Spectrum of Sample No. BCR 1684-198 (Unreacted Material)	25
10	Spectrum of Sample No. BCR 1684-198 (Reacted Material)	26
11	Spectrum of Sample No. BCR 1362-201 (Unreacted Material)	27
12	Spectrum of Sample No. BCR 1362-201 (Reacted Material)	28
13	Infrared Spectrum of Sample No. BCR 1342-199 (Unreacted Material)	29
14	Infrared Spectrum of Sample No. BCR 1342-199 (Reacted Material)	30
15	Infrared Spectrum of Sample No. BCR 1361-200 (Unreacted Material)	31
16	Infrared Spectrum of Sample No. BCR 1361-200 (Reacted Material)	32
17	Infrared Spectrum of Sample No. BCR 1699-202 (Unreacted Material)	33

LIST OF ILLUSTRATIONS (cont.)

Figure		Page
18	Infrared Spectrum of Sample No. BCR 1699-202 (Reacted Material)	34
19	Infrared Spectrum of Sample No. BCR 1343 (Calcined Material)	44
20	Infrared Spectrum of Sample No. BCR 1343 (Reacted Material)	45
21	Infrared Spectrum of Sample No. 1351 (Calcined Material)	46
22	Infrared Spectrum of Sample No. BCR 1351 (Reacted Material)	47
23	Infrared Spectrum of Sample No. BCR 1352 (Calcined Material)	48
24	Infrared Spectrum of Sample No. BCR 1352 (Reacted Material)	49
25	Infrared Spectrum of Sample No. BCR 1360 (Calcined Material)	50
26	Infrared Spectrum of Sample No. BCR 1360 (Reacted Material)	51
27	Infrared Spectrum of Sample No. BCR 1697 (Calcined Material)	52
28	Infrared Spectrum of Sample No. BCR 1697 (Reacted Material)	53
29	Infrared Spectrum of Sample No. BCR 1699-DB (Calcined Material)	54
30	Infrared Spectrum of Sample No. BCR 1699 Run No. 34 DB (Reacted Material)	55
31	Infrared Spectrum of Sample No. BCR 1360-DB (Unreacted Material)	56

LIST OF ILLUSTRATIONS (cont.)

Figure		Page
32	Infrared Spectrum of Sample No. BCR 1360-Run No. 31 DB (Reacted Material)	57
33	Infrared Spectra of Sample No. BCR 1699-202 Before and After Reaction with Sulfur Dioxide in a Flue Gas at 262°C.	66
34	Infrared Spectrum of Sample No. BCR 1699-202 Exposed to 2800 ppm of SO_2 at 750°F. Sample Plated on Irtran 4 Windows of Infrared Cell	68
35	Infrared Spectra of Limestone Sample No. BCR 1699-202 Reacted With a SO_2-N_2-H_2O Mixture at 261°C.	70
36	Infrared Spectrum of Limestone Sample No. BCR 1699-202	71
37	Infrared Spectra of Limestone Sample No. BCR 1699-202 During Exposure to Flue Gas	72
38	Effect of Temperature on Adsorption Rate	75
39	Comparison of Temperature Dependency of Adsorption Rate with Predicted Diffusion Dependency	78
40	Effect of O_2 Concentration	81
41	Effect of H_2O Concentration	82
42	Effect of CO_2 Concentration	83
43	Effect of Total Gas Flow Rate on Adsorption Rate	84
44	Sample No. BCR 1362-201 Before and After Reaction with SO_2 in a Synthetic Flue Gas. a. Spectral Scan of Sample No. BCR 1362-201 Before Reaction. b. Spectral Scan of Sample No. BCR 1362-201 After Reaction with Sulfur Dioxide in a Flue Gas for 1.8 Hours at 250°C.	86
45	Infrared Spectra of Alkalized Alumina Deposit. a. Infrared Spectrum of Alkalized Alumina Before Reaction with SO_2 in a Flue Gas. b. Infrared Spectrum of Alkalized Alumina After Reaction with SO_2 in a Flue Gas for Two Hours at 204°C.	87

LIST OF ILLUSTRATIONS (cont.)

Figure		Page
46	Infrared Spectrum of Sample No. BCR 1363. a. Sample No. BCR 1363 Containing Adsorbed SO_2. b. Sample No. BCR 1363 (Dead Burned)	89
47	Infrared Spectrum of Limestone Sample No. BCR 1363. a. Sample No. BCR 1363 Containing Adsorbed SO_2. b. Sample No. BCR 1363 (Dead Burned)	90
48	Infrared Spectrum of Limestone Sample No. BCR 1369-DB	91
49	High-Temperature Cell for the Study of Gas-Solid Interactions at Temperatures in Excess of 1800°F.	93

LIST OF TABLES

Table		Page
I	Solids Applicable to the Removal of Sulfur Dioxide from a Flue Gas	12
II	Typical Analysis of Four Limestone Samples Obtained from the Standard Lime and Refractories Company	14
III	Limestone Samples Obtained from the National Air Pollution Control Administration	15
IV	Reaction Conditions for Investigating the Interactions Between SO_2 in a Simulated Flue Gas and Various Solids	19
V	Infrared Absorption Bands of a Simulated Flue Gas Reacted with CaO at 403°C.	20
VI	Infrared Absorption Bands of Sample No. BCR 1684-198	35
VII	Infrared Absorption Bands of Sample No. BCR 1362-201	36
VIII	Infrared Absorption Bands of Sample No. BCR 1342-199	37
IX	Absorption Bands of Sample No. BCR 1361-200	38
X	Infrared Absorption Bands of Sample No. BCR 1699-202	40
XI	Infrared Absorption Bands of $CaSO_4$ and $CaSO_4 \cdot 2H_2O$	42
XII	Fundamental Frequencies of the Sulfate Ion in Alkali Halides (cm.$^{-1}$)	42
XIII	Infrared Absorption Bands of Sample No. BCR 1343	58
XIV	Infrared Absorption Bands of Sample No. BCR 1351	59
XV	Infrared Absorption Bands of Sample No. BCR 1352	60
XVI	Infrared Absorption Bands of Sample No. BCR 1360	61
XVII	Infrared Absorption Bands of Sample No. BCR 1697	62
XVIII	Summary of Experimental Results of the Exposure of Sample No. BCR 1699-202 to Flue Gas in the Stainless Steel Infrared Cell	64

SECTION I

INTRODUCTION AND SUMMARY

Currently, dry-solid sorbent processes are being considered for the removal of sulfur dioxide from power plant stack gases(1, 2). As a result, there is a great need to obtain fundamental data on the mechanism and rate at which solid adsorbents might fix sulfur dioxide from a flue gas. This study was concerned with the utilization of infrared spectroscopy to obtain this type of information. The objective of this work was to use infrared spectroscopy to investigate the basic processes occurring between sulfur dioxide in a simulated flue gas and various limestone or other selected adsorbents. An attempt was made to postulate the mechanism of the gas-solid interaction by determining the molecular structure of the adsorbed species, measuring the reaction rates at several flow rates and temperatures between 25°C and 400°C and calculating the thermodynamic data for the gas-solid interaction. In addition, the feasibility of applying the infrared techniques at temperatures in the 1600°-2000°F range was evaluated. The composition of the synthetic flue gas used in these studies consisted of the following: 3%O_2, 12%CO_2, 0.2%SO_2, 78.3% to 79.9%N_2 and 4.2% to 5.97%H_2O.

This particular approach is based on previous work in the area of application of infrared spectroscopy to study gas-solid interactions(3-6). In these studies, infrared spectroscopy has provided a direct means of observing the perturbations and interactions of the adsorbate at the surface during adsorption. Specific information obtained in the infrared spectroscopic study of adsorption phenomena includes: (1) the distinction between physical adsorption and chemical adsorption, (2) determination of the molecular structure of the adsorbed species, and (3) determination of adsorption energies and adsorption equilibria(7,8). Examples of the infrared spectroscopic study of gas-solid interactions include the following studies: (1) CO, CO_2, O_2 and H_2O adsorbed on silica-supported iron(9), (2) H_2O and CO_2 on beryllium oxide(10), (3) CO_2, HCl and other molecules on dry silica-alumina(11), and (4) CO_2 adsorbed on zeolite X(12).

Very little work has been done on the infrared spectra of sulfur dioxide adsorbed on solid adsorbents. In one of the few studies of this nature, Crawford(13) reported an average displacement of 115 cm^{-1} to lower frequencies for the fundamental hydroxyl absorption band when SO_2 was adsorbed on porous silica glass at 24°C. The shift to lower frequencies was attributed to the perturbation of surface hydroxyl groups by the sulfur dioxide adsorbate due to hydrogen-bonding taking place between the polar adsorbate and surface hydroxyl groups.

In studies described in this report, it was found that the slaked limestone samples adsorbed sulfur dioxide from a simulated flue gas according to a two-step reaction. The first step consisted of adsorbing sulfur dioxide as sulfite followed by the oxidation of the sulfite to sulfate. On the other hand, limestone samples exposed at temperatures around 1800°F showed only infrared bands attributed to sulfate. Thus, very rapid oxidation of adsorbed sulfite to sulfate at 1800°F is apparent.

A statistical analysis of the adsorption data on Limestone Sample No. BCR 1699-202 showed that a two-fold gas flow rate change had no significant effect on adsorption rate, but changed the initial toe portion of the adsorption-time curves wherein steady-state conditions were being established. For sample No. BCR 1699-202, the relative adsorption rate was found to be 5.5×10^{-9} moles cm^{-2} min^{-1} for flow rates of 627-633 cc/min and 5.3×10^{-9} moles cm^{-2} min^{-1} for flow rates of 1253-1315 cc/min. The temperature effect on adsorption rate was found to correspond to an activation energy of 11.8

kcal./mole. Examination of the fluid dynamic equations governing the diffusion coefficient in this situation lead to the prediction that adsorption should be proportional to temperature to the 0.57 power, if the reaction was diffusion controlling. However, the temperature effect found was too great to be consistent with this diffusion-limiting situation. From these results we concluded that the absorption cell was not diffusion-mechanism rate-controlled.

Further evidence for this conclusion was ascertained from a comparison of the measured activation energy for the sorption of sulfur dioxide onto various limestones with values determined by Borgwardt(14) at the National Air Pollution Control Administration using fixed-bed reactors. He measured an activation energy of 14.2 kcal./gm. mole for the sorption of sulfur dioxide onto Limestone No. BCR 1343 which has a composition similar to Limestone Sample No. BCR 1699-202. The agreement of these two values indicates that the same sorption processes were occurring in both experiments.

Calcium oxide and aluminum hydroxide adsorbed sulfur dioxide from a simulated flue gas at 400°C. Sulfite and a small amount of sulfate were found in the reacted calcium oxide sample and only sulfate was found in the reacted $Al(OH)_3$ sample.

Preliminary studies were conducted in the infrared spectra of "dead-burned" samples. There was spectral evidence for the presence of silicates in these samples indicating that silicates may play an important role in "dead-burning" phenomena. Finally, a design is presented for an infrared cell for conducting the gas-solid interactions in the temperature range of 1600-2000°F.

SECTION II

EXPERIMENTAL SECTION

1. EXPERIMENTAL APPARATUS

a. Flow-Through Infrared Cell for Preliminary Examination of Adsorbed Species

Figure 1 shows the infrared cell used in the preliminary examination of the interactions between sulfur dioxide and various solid adsorbents. The cell consisted of an outer Pyrex tube 4 inches long and 1-1/2 inches in diameter. During the reaction, the two 1-inch diameter inner tubes are sealed to each end of the outer Pyrex tube. The solid adsorbent is deposited on one of the KBr windows which has been attached to the inner tubes by Glyptal sealant. Two 4 mm.-bore stopcocks are attached to the cell to provide the cell with the capability of being evacuated or used as a flow-through cell. The distance between the KBr windows is approximately 0.5 cm to eliminate infrared absorption by gas-phase molecules.

b. Flow-Through High Temperature Infrared Cell

The infrared cell used to conduct infrared investigations at elevated temperatures is shown in Figure 2. This cell is constructed from type 304 stainless steel. Essentially, it consists of three parts: an outer part 3-3/4 inches long and 1-3/4 inches in diameter and two inner parts 1-57/64 inches long and 1-31/64 inches in diameter. The cell is sealed using two stainless steel end caps and Viton O-rings. Water is circulated through the end caps in order to protect the Viton O-rings at temperatures in excess of 260°C. (500°F.). Viton O-rings are stable up to these temperatures. The cell is designed to be used as a flow-through cell as well as a vacuum cell by the utilization of stopcocks connected to the cell by means of Kovar metal-to-glass seals. Irtran 4 (ZnSe) windows

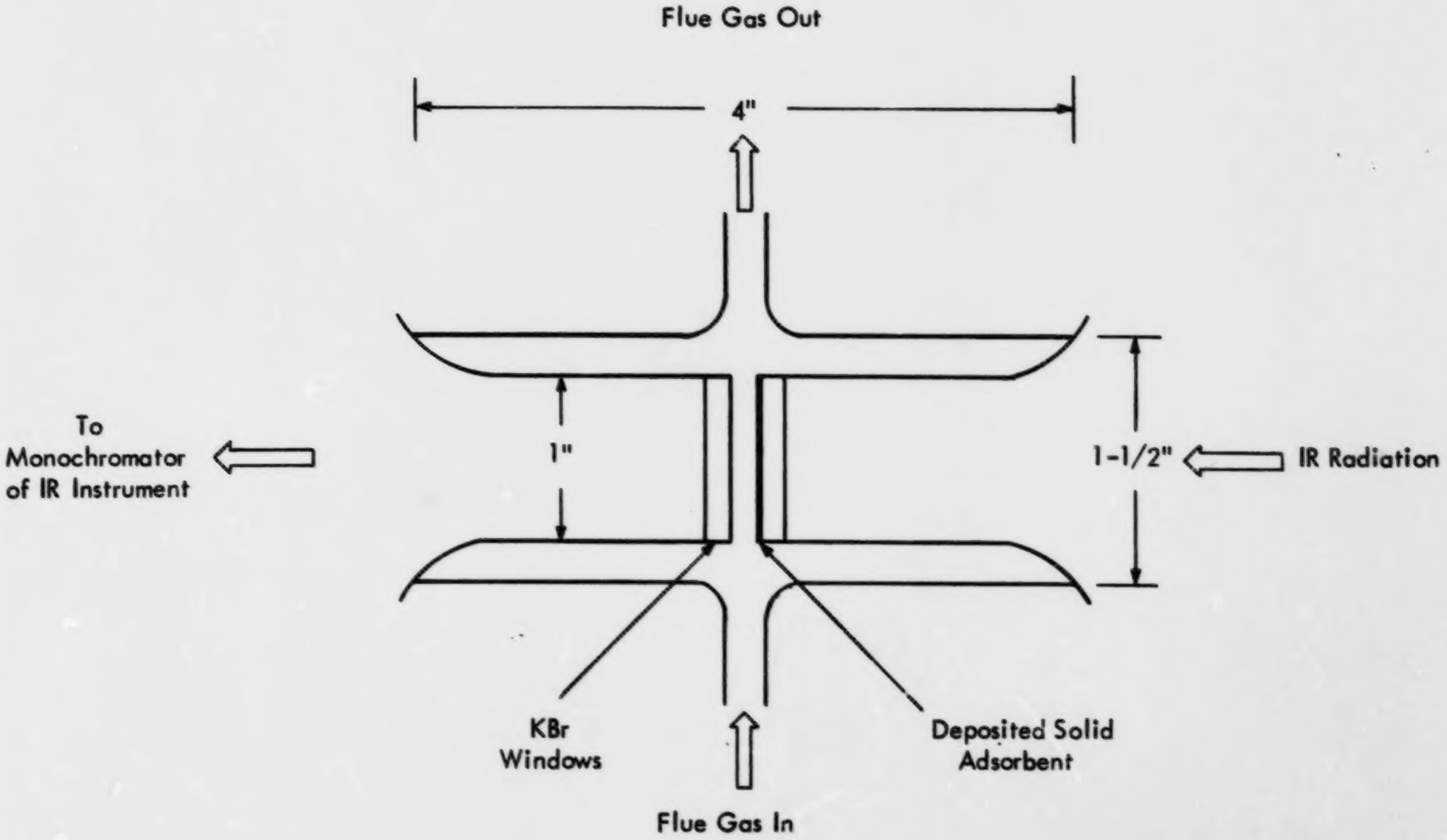
Flue Gas Out
4"
To
Monochromator
of IR Instrument
1"
1-1/2"
IR Radiation
KBr
Windows
Deposited Solid
Adsorbent
Flue Gas In

Figure 1. Infrared Cell for Studying Gas-Solid Interactions at Room Temperature

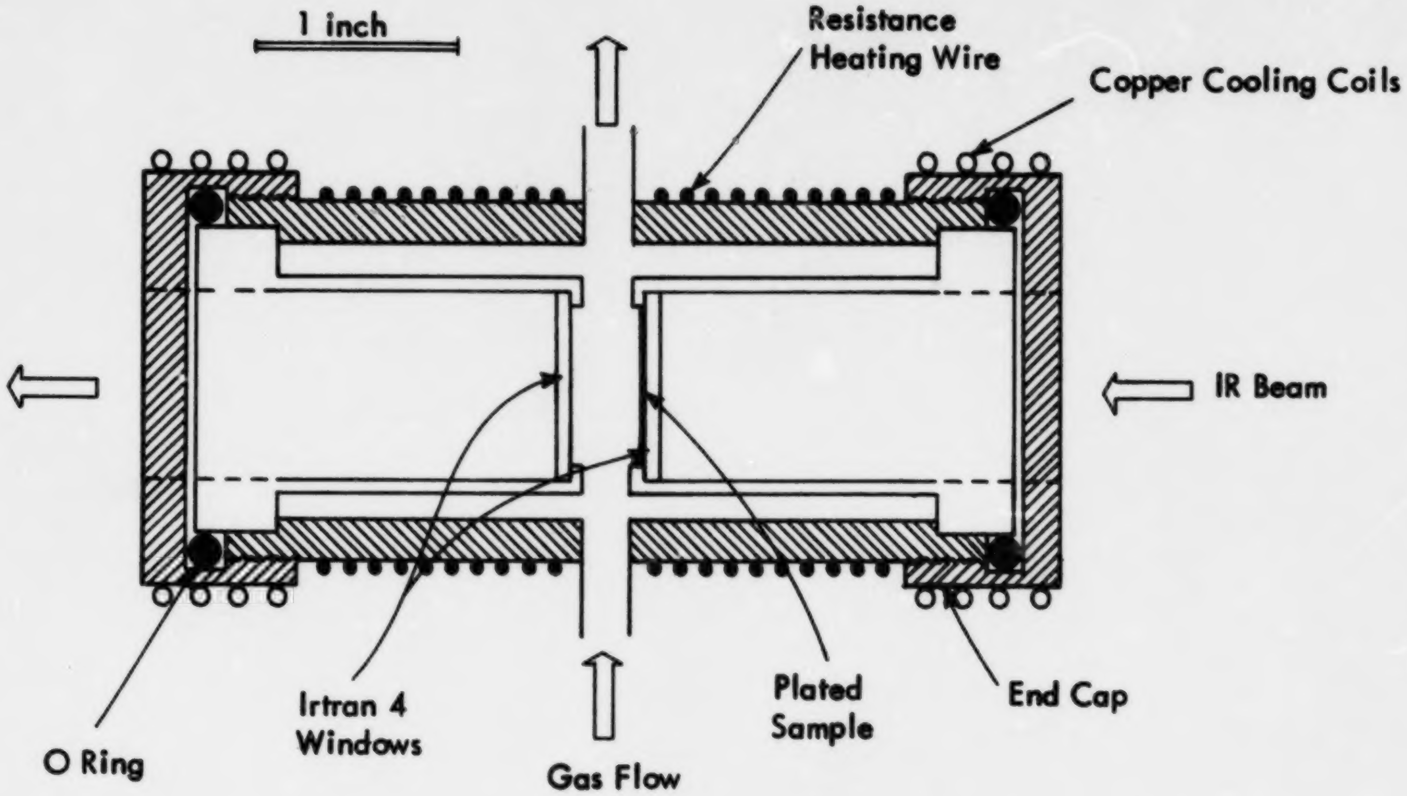
1 inch
Resistance Heating Wire
Copper Cooling Coils
IR Beam
O Ring
Irtran 4 Windows
Gas Flow
Plated Sample
End Cap

Figure 2. Infrared Cell for Studying Gas-Solid Interactions at Elevated Temperatures

are used in the cell and these are attached to the two inner bodies by Dow Corning Silastic RTV 732 adhesive. Irtran 4 transmits infrared radiation from 0.48 to 21.8μ. It has a melting point of 1520°C., which makes it useful at elevated temperatures. The path length of the cell is 0.56 cm. to decrease absorption due to gas-phase molecules.

The Dow Corning Silastic RTV 732 adhesive decomposed at temperatures around 400°C. and another sealant, High Vacuum Leak Sealant, a silicone resin produced by Space Environment Laboratories, Inc., was used to seal the windows to the cell. However, it was found that the Viton O-rings could not be cooled sufficiently at the temperatures around 400°C. and as a result, decomposed to contaminate the sample. Hence, this particular cell was only useful at temperatures around 300°C.

c. Pyrex Resistance Furnace

Preliminary studies of the exposure of various solids to a simulated flue gas were also conducted in a Pyrex resistance furnace. The Pyrex furnace was wound with Kanthol resistance wire. This apparatus was used to expose reaction boats containing the solid adsorbent as well as Irtran 4 windows containing the plated solid adsorbent to flue gas. When reaction boats containing various solid adsorbents were exposed to flue gas, the spectrum of the unreacted and reacted material was recorded using the KBr pellet technique(15).

d. Infrared Recording Equipment

The infrared spectra of the interaction between sulfur dioxide in a flue gas and various solid adsorbents were recorded with a Beckman IR-10 infrared spectrophotometer. This is a grating infrared spectrophotometer and possesses both double-beam and single-beam operational modes. The spectrophotometer scans the infrared region from 4000 cm.$^{-1}$ to 300 cm.$^{-1}$ or 2.5μ to 33.3μ. A photograph of this instrument with the high temperature infrared cell positioned in the sampling area is shown in Figure 3.

An external recorder (Beckman Model 100500 10-inch recorder) was used to expand portions of the spectra as recorded on the IR-10 spectrophotometer. This recorder was calibrated using polystyrene film, atmospheric H_2O and CO_2.

2. GAS-HANDLING EQUIPMENT

The high-vacuum line for evacuating the flow-through infrared cell to distinguish between physical and chemical adsorption is shown in Figure 4. This system is capable of evacuating the cell to less than 10^{-5} mm. of Hg.

The flow system for passing the flue gas mixture over the various adsorbents is shown in Figure 5. The flow meter for measuring SO_2 flow was calibrated by the Matheson Company, and the flows for the remaining gases were measured using calibrated flow charts furnished by the Matheson Company.

3. CHEMICALS USED IN THIS STUDY

a. Gases

The following gases were used to make up the simulated flue gas without any further purification:

(1) Prepurified grade nitrogen (99.997% min. purity)

(2) Coleman Instrument-grade carbon dioxide (99.99% min. purity)

(3) Ultra-high-purity oxygen (analysis: 0.0 ppm CO_2, 0.003 ppm N_2O, 10.1 ppm Kr, 0.7 ppm Xe, 5.3 ppm N_2, 0.0 ppm Ar, 5.5 ppm H_2O, 0.0 ppm CH_4)

(4) Anhydrous grade sulfur dioxide (99.98% min. purity)

These gases were purchased from the Matheson Company.

b. Solid Adsorbents

The solid adsorbents investigated in this study are presented in Table 1.

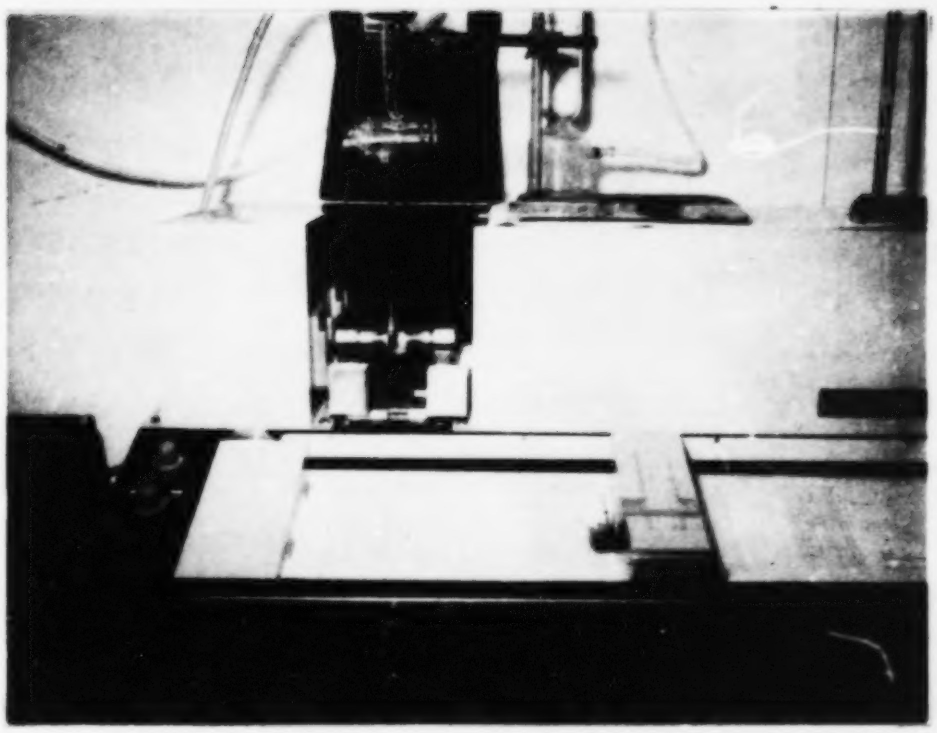

Figure 3. Stainless Steel Infrared Cell Positioned in the Beckman IR 10

GTC 136-5

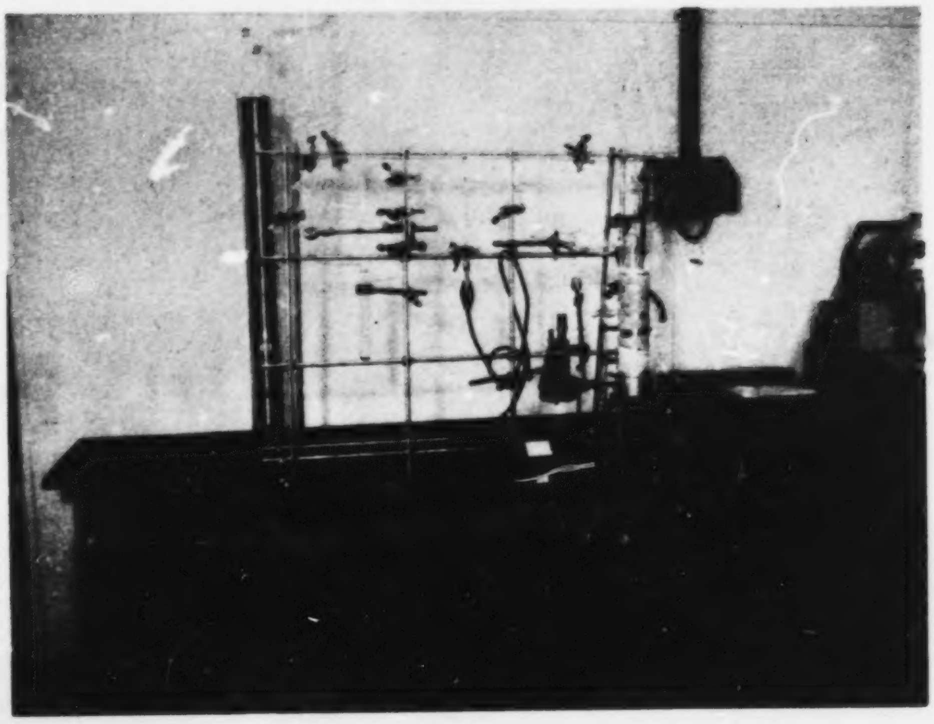

Figure 4. Portable Vacuum System

GTC 136-4

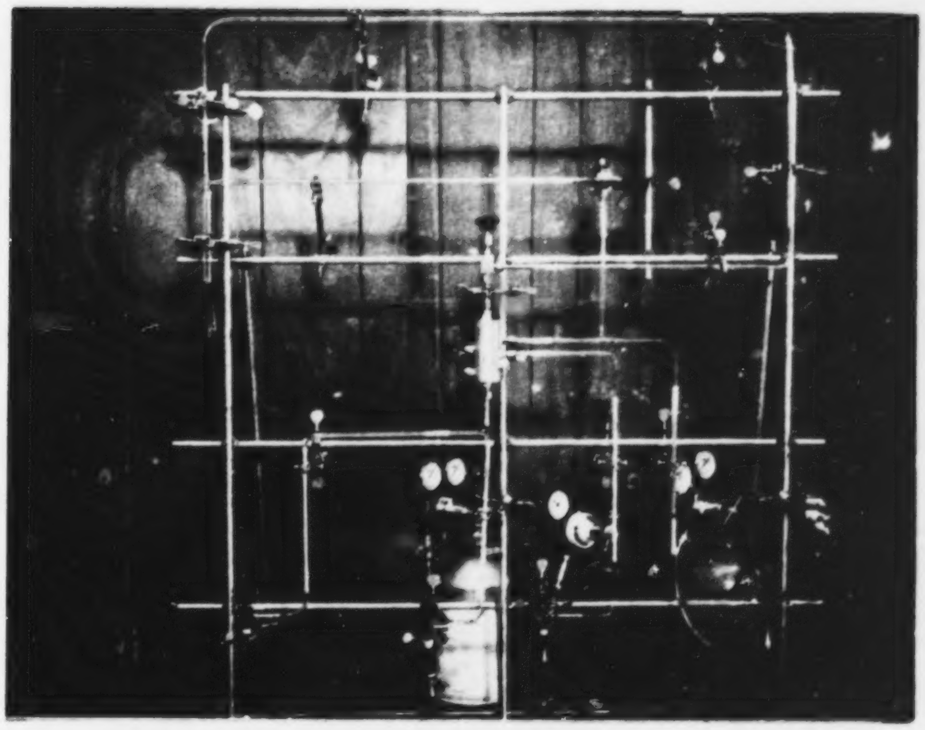

Figure 5. Flow System for Synthetic Flue Gas

Table I Solids Applicable to the Removal of Sulfur Dioxide from a Flue Gas

Material	Composition	Source
1. Limestones		
Code 90 Stone	See Table II	Standard Lime and Cement Co., Baltimore, Maryland
CAL AG	See Table II	Standard Lime and Cement Co., Baltimore, Maryland
Dolo Stone	See Table II	Standard Lime and Cement Co., Baltimore, Maryland
Dolomite Fines (DBD Stack Dust)	See Table II	Standard Lime and Cement Co., Baltimore, Maryland
BCR No.		
1342	See Table III	National Air Pollution Control Administration
1343	"	"
1351	"	"
1352	"	"
1360	"	"
1361	"	"
1362	"	"
1363	"	"
1684	"	"
1697	"	"
1699	"	"
2. Montmorillonites		
Ben-A-Gel*	highly purified magnesium montmorillonite	National Lead Company

---

*The Ben-A-Gel has the following average chemical analysis, dry basis.

SiO	56.5%	CaO	2.8%	Cl	2.5%
Al_2O_3	0.2%	Na_2O	2.5%	F	1.0%
Fe_2O_3	0.2%	K_2O	0.1%	ignition loss	7.7%
MgO	25.8%	Li_2O	1.1%		

Table I (cont.) Solids Applicable to the Removal of Sulfur Dioxide from a Flue Gas

Material	Composition	Source
2. Montmorillonites (cont.)		
Bentone 34	dimethyldioctadecyl ammonium bentonite	National Lead Company
Bentone 38	organic derivative of a special magnesium montmorillonite	National Lead Company
Bentone 27	organic derivative of a special magnesium montmorillonite	National Lead Company
3. Other Solid Adsorbents		
Urea		Fisher Certified Grade
Mercuric Chloride		Fisher Certified Grade
$Al(OH)_3$		Baker Analyzed Reagent
Diphenyl Carbazide		Fisher Reagent Chemical
CaO		Fisher Certified Reagent Grade
Florisil		Matheson Company, Inc.
Alkalized Alumina		National Air Pollution Control Administration

The analysis of the limestone samples obtained from the Standard Lime Company are given in Table II.

From information obtained from the Standard Lime Company, all but the Code 90 stone are stack dusts from rotary kilns. Code 90 is a fine, high-calcium limestone. CAL AG and Dolo Stone Fines are from lime kilns (high calcium and dolomitic respectively). Dolomitic Fines are from dead-burned dolomitic kilns. The CAL AG and Code 90 stone are from Pleasant Gap, Pa., and the Dolo Stone Fines and Dolmitic Fines are from Woodville, Ohio. All are originally full carbonates (the ignition loss is almost entirely CO_2, by weight), but the three stack dusts all exhibit partial burning, significantly more from the lime kilns than the DBD kilns.

Table II Typical Analysis of Four Limestone Samples Obtained from the Standard Lime and Refractories Company

	Limestone			
Composition	CAL AG	Code 90	Dolo Stone Fines	Dolomite Fines
SiO_2	7.0	.6	3.2	1.0
Fe_2O_3	1.4	.1	.5	1.9
Al_2O_3	4.7	.4	2.2	1.4
CaO	56.0	55.0	35.7	29.7
MgO	.6	.6	24.9	21.2
Ign	30.3	43.3	34.0	44.8
AOAC				
Neutralizing Powder	100	---	111	99
% Pass #8	98	---	100	
20	92	84	99	98
60	76	---	96	88
100	67	7	91	76
200	56	---	79	49

Table III Limestone Samples Obtained From the National Air Pollution Control Administration*

BCR No.	Loss on Ignition	CaO	MgO	Fe_2O_3	SiO_2	Al_2O_3
1343	42.5	94	0.85	0.66	2.98	0.73
1351	50.3	54	28.5	7.0	8.2	1.55
1352	43.3	56	31.0	1.74	7.4	2.48
1360	44.5	81	13.0	1.25	3.65	0.27
1363	36.1	66	1.42	2.50	21.0	6.60
1697	47.3	55	43.0	0.36	0.78	0.14
1699	43.7	96	1.10	< 0.20	1.26	< 0.30
1342	39.1	60.0	28.0	0.19	10.4	0.09
1361	40.3	75.0	7.15	5.10	8.20	2.37
1362	33.9	57.0	39.0	0.84	2.53	< 0.30
1684	46.3	57.0	39.0	0.84	2.53	< 0.30

4. EXPERIMENTAL PROCEDURE

a. Preparation of Samples

Preliminary studies of the interaction of flue gas with various solids at elevated temperatures were conducted by placing reaction boats containing the samples into a Pyrex resistance furnace described in Section II-1-c. The furnace was heated to the required temperature under an atmosphere of nitrogen and the samples were exposed to flue gas at the reaction temperatures up to 408°C. The infrared spectra of the samples were recorded before and after exposure to flue gas using the KBr pellet technique.

The Pyrex resistance furnace was also used to expose solid samples plated onto Irtran 4 windows to sulfur dioxide in a flue gas. The samples CaO and $Al(OH)_3$ were plated onto Irtran 4 windows from an acetone suspension and the infrared spectra were measured before and after exposure to flue gas. The window containing the plated sample was allowed to cool to room temperature before recording the spectrum.

---

*Analytical results obtained from National Air Pollution Control Administration.

The infrared spectra of solids exposed to the synthetic flue gas in the room temperature and high temperature infrared cell were recorded using the following procedure. The solid adsorbent was ground in a vibrator-grinder from 30 to 60 seconds and plated on the Irtran 4 window of the stainless steel infrared cell from an acetone suspension. The cell was assembled and evacuated to approximately 24_μ while heating the samples to 100°C. This procedure was followed in order to clean the surface of the limestone deposit. In some cases the cell was pressurized with N_2 and heated to the reaction temperature and in others, the cell was heated to the reaction temperature while under vacuum. After the cell had reached equilibrium, the flue gas was allowed into the cell and the spectrum was scanned repeatedly.

b. Calculation of the Integrated Intensities of the Sulfate Ion

In order to determine the relative amount of sulfate on the surface of the limestone samples after exposure to flue gas at various temperatures, the integrated intensity was measured of the sulfate band. The experimentally determined integrated intensity of an absorption band is given by the equation (1),

$$A = \frac{1}{c\ell} \int_{\nu_1}^{\nu_2} \ln\left(\frac{I_o}{I}\right) d\nu \qquad (1)$$

where I_o = intensity of the incident radiation,

I = intensity of the transmitted radiation,

ν = wavenumbers, cm.$^{-1}$,

c = moles cm.$^{-3}$,

ℓ = path length in cm.

Another intensity unit used in this study for the representation of integrated intensities for absorption bands of adsorbed molecules is given by equation (2),

$$A = \frac{1}{\bar{c}} \int_{\nu_1}^{\nu_2} \ln \left(\frac{I_o}{I}\right) d\nu \qquad (2)$$

where the concentration and path length are combined and expressed as moles cm.$^{-2}$ and is represented by $\bar{c}$. This unit was employed because it is difficult to know the exact path length through an adsorbed molecule.

The integral, $\int_{\nu_1}^{\nu_2} \ln \left(\frac{I_o}{I}\right) d\nu$ was evaluated by replotting the ν_3 absorption band of the sulfate ion in terms of $\ln \left(\frac{I_o}{I}\right)$ versus frequency in wavenumbers. The area under the curve was measured with a polar planimeter. The value of A was taken from the integrated intensity of the $\nu_3(b_1)$ SO stretching mode for $BaSO_4$(16), which was 28 x 10^6 cm.$^{+1}$ mole^{-1}. The calculated concentration of adsorbed sulfate was expressed in terms of moles/cm^2.

SECTION III

RESULTS AND DISCUSSION OF RESULTS

1. PRELIMINARY INFRARED SPECTROSCOPIC STUDIES OF THE GAS-SOLID INTERACTION BETWEEN SULFUR DIOXIDE IN A FLUE GAS AND VARIOUS SOLID ADSORBENTS

The preliminary experiments in the exposure of various solids to flue gas are summarized in Table IV. In experiment 9, Code 90 and the CAL AG stone were contained in ceramic reaction boats and reacted with simulated flue gas in an electrically heated Pyrex oven. As stated in Section II-1-c, KBr pellets were prepared of the unreacted and reacted samples. Experiments 11 through 16 were conducted by contacting the compounds with simulated flue gas and the sulfur dioxide-nitrogen mixture in the stainless steel infrared cell. Runs at 125°C. were conducted using the stainless steel cell fitted with KBr windows. The aluminum hydroxide, Ben-A-Gel and Code 90 stone were deposited from an acetone suspension. The Bentone 34 and diphenyl carbazide were deposited from methanol solutions. The Code 90 stone and CaO in experiment 17 were reacted with the simulated glue gas in a Pyrex resistance furnace. The materials were placed in ceramic reaction boats. The weight of CaO used was 204 mg. and that of Code 90 stone was 219 mg. Florisil in experiment 20 was reacted with the simulated flue gas in the stainless steel cell. The florisil was deposited from an acetone suspension. In experiment number 21, the $Al(OH)_3$ and CaO were deposited from acetone suspensions onto Irtran 4 (ZnSe) windows. The windows were placed in the Pyrex resistance oven and reacted with simulated flue gas at 403°C. Preliminary experiments indicated that the flue gas had very little effect on the windows at 400°C. Some sublimation of window material occurred and a slight darkening of the windows was observed. This, however, did not interfere significantly with the infrared transmittance of the windows.

Table IV Reaction Conditions for Investigating the Interactions between SO_2 in a Simulated Flue Gas and Various Solids

Experiment Number	Solid Absorbent	Reaction Time	Gas Flows: CO_2 (cc./min.)	O_2 (cc./min.)	SO_2 (cc./min.)	N_2 (cc./min.)	H_2O* (cc./min.)	N_2 Through Vaporizer (cc./min.)	Temperature of Vaporizer (°C.)	Reaction Temperature (°C.)	Total Flow (cc./min.)	Remarks
9a	Code 90 stone	2 hr.	79	23	1.2	549	-	-	-	401	652	no significant changes in the spectrum
9b	CAL AG stone	2 hr.	79	23	1.2	549	-	-	-	401	652	no significant changes in spectrum
10	$Al(OH)_3$	47 min.	-	-	1.3	672	-	-	-	room temp.	673	no significant changes detected in spectrum
11	Diphenyl carbazide	1 hr. 30 min.	78	22	1.2	548	-	-	-	room temp.	649	inconclusive results due to the nature of the deposit
12a	Ben-A-Gel	1 hr. 15 min.	78	22	1.3	548	-	-	-	room temp.	649	no visible changes in the spectrum
12b	Ben-A-Gel	1 hr. 3 min.	-	-	1.2	659	-	-	-	room temp.	660	no visible changes in the spectrum
13	Bentone 34	2 hr.	-	-	1.4	655	-	-	-	room temp.	656	no changes observed in the spectrum
14	Bentone 34	40 min.	-	-	1.4	600	-	-	-	room temp.	601	no significant changes in the spectrum
15	Code 90 stone	1 hr.	-	-	1.4	663	-	-	-	125	664	no significant changes in the spectrum
16	Code 90 stone	3 hr. 45 min.	-			160	-	-	-	126	164	no changes in the spectrum
17a	Code 90 stone	4 hr. 3 min.	79			459	20	51	70	408	632	no changes observed in the spectrum of the reacted product incorporated in a KBr pellet
17b	CaO	4 hr.	79	22	1.2	459	20	51	70	408	632	new IR bands observed at 1424, 1134, 932 cm.$^{-1}$
20	Florisil	3 hr. 17 min.	79	22	1.3	459	21	54	70	room temp.	636	no significant changes observed in the spectrum
21a	$Al(OH)_3$	1 hr.	77	21	1.2	481	21	58	69	403	659	new infrared bands observed in spectrum of the reacted product
21b	CaO	1 hr.	77	21	1.2	481	21	58	69	403	659	new bands observed in the spectrum of the reacted product

---

* Calculated from ideal gas law (assuming saturation of gas phase).

In these series of experiments, the only compounds found to adsorb sulfur dioxide at reaction temperatures around 400°C. were CaO and $Al(OH)_3$. The infrared spectra of $Al(OH)_3$ before and after exposure to flue gas at 400°C. is given in Figure 6. The $Al(OH)_3$ was plated on an Irtran 4 window. The spectrum of the unreacted $Al(OH)_3$ shows an absorption band at 1012 $cm.^{-1}$ for the unreacted material which was assigned to the deformation or bending mode of vibration of the hydroxyl groups. Upon reaction with flue gas, an absorption band was observed at 1064 $cm.^{-1}$ which was assigned to the sulfate ion.

The spectrum of CaO before reaction with a simulated flue gas is shown in Figure 7, and the spectrum of CaO after reaction with a simulated flue gas is shown in Figure 8. The infrared bands for these spectra are presented in Table V.

Table V Infrared Absorption Bands of a Simulated Flue Gas Reacted with CaO at 403°C.

$cm.^{-1}$	Relative Intensity*	Assignment
1422	b	$CO_3^=$
1109	vwb	$SO_4^=$
987	sh	?
928	m	$SO_3^=$
873	wsh	?
646	m	?

---

*b = broad, vw = very weak, sh = shoulder, and m = medium

The 1422 $cm.^{-1}$ band was assigned to carbonate, the 1109 $cm.^{-1}$ band to sulfate and the 928 $cm.^{-1}$ band to $SO_3^=$.

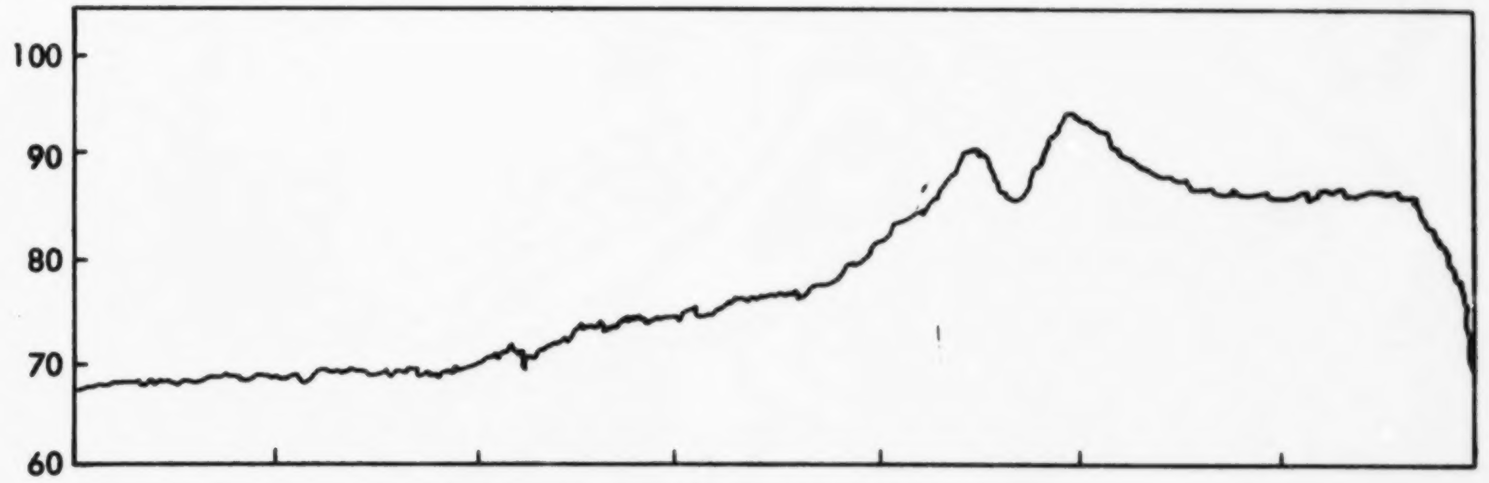

b. After Reaction with a Humidified Flue Gas

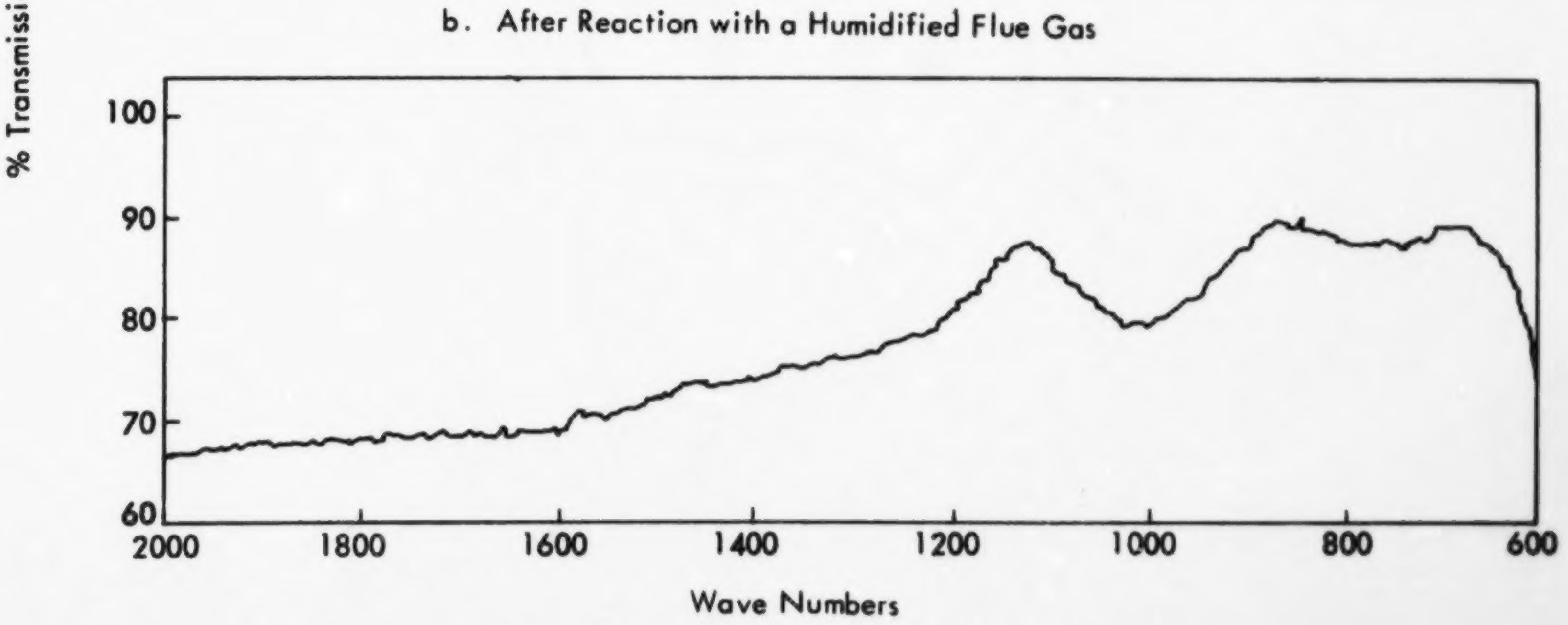

a. Before Reaction with a Humidified Flue Gas

Figure 6. Aluminum Hydroxide, Al $(OH)_3$

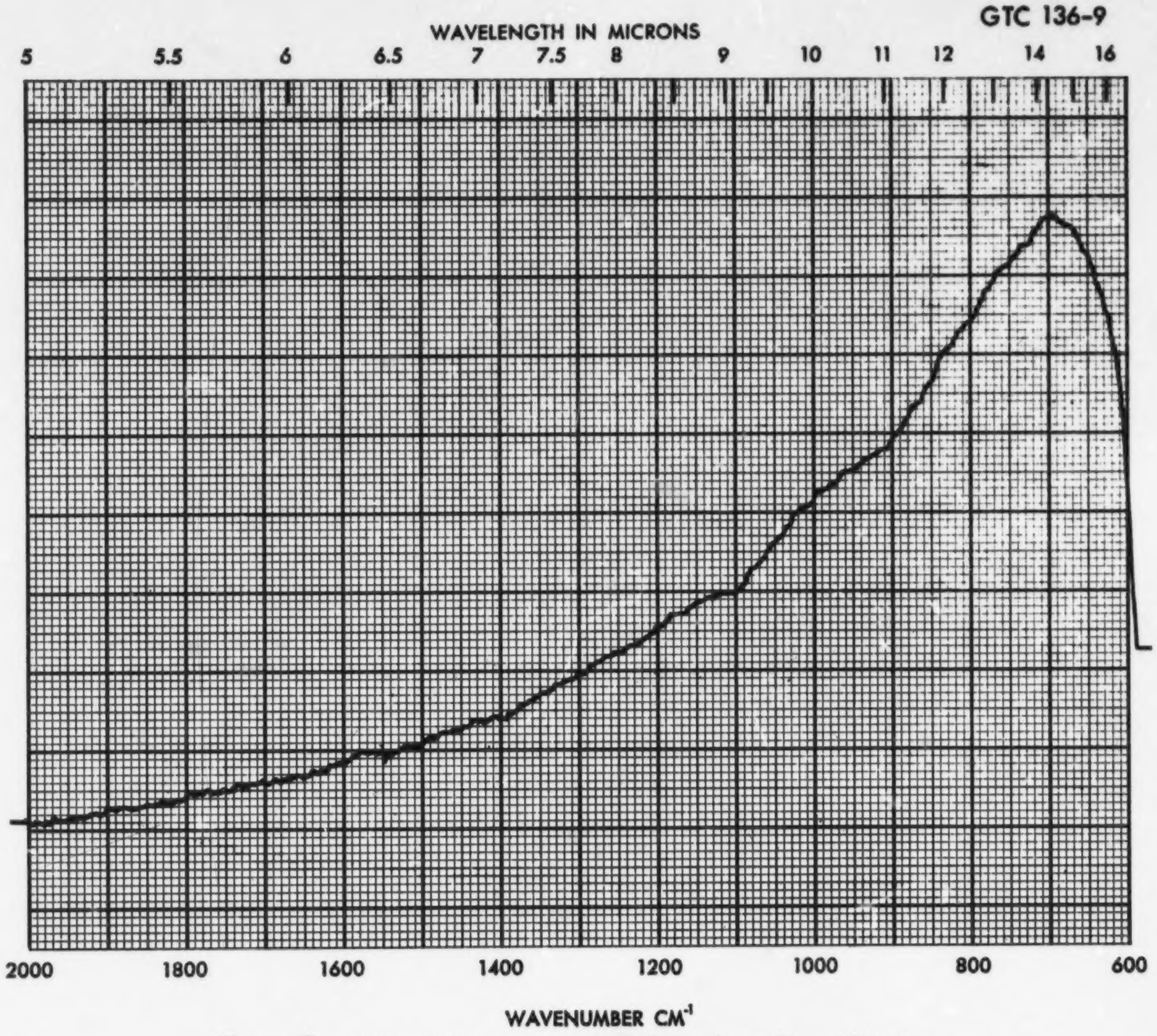

Figure 7. Infrared Spectrum of CaO Deposit on Irtran Window before Reaction with Simulated Flue Gas

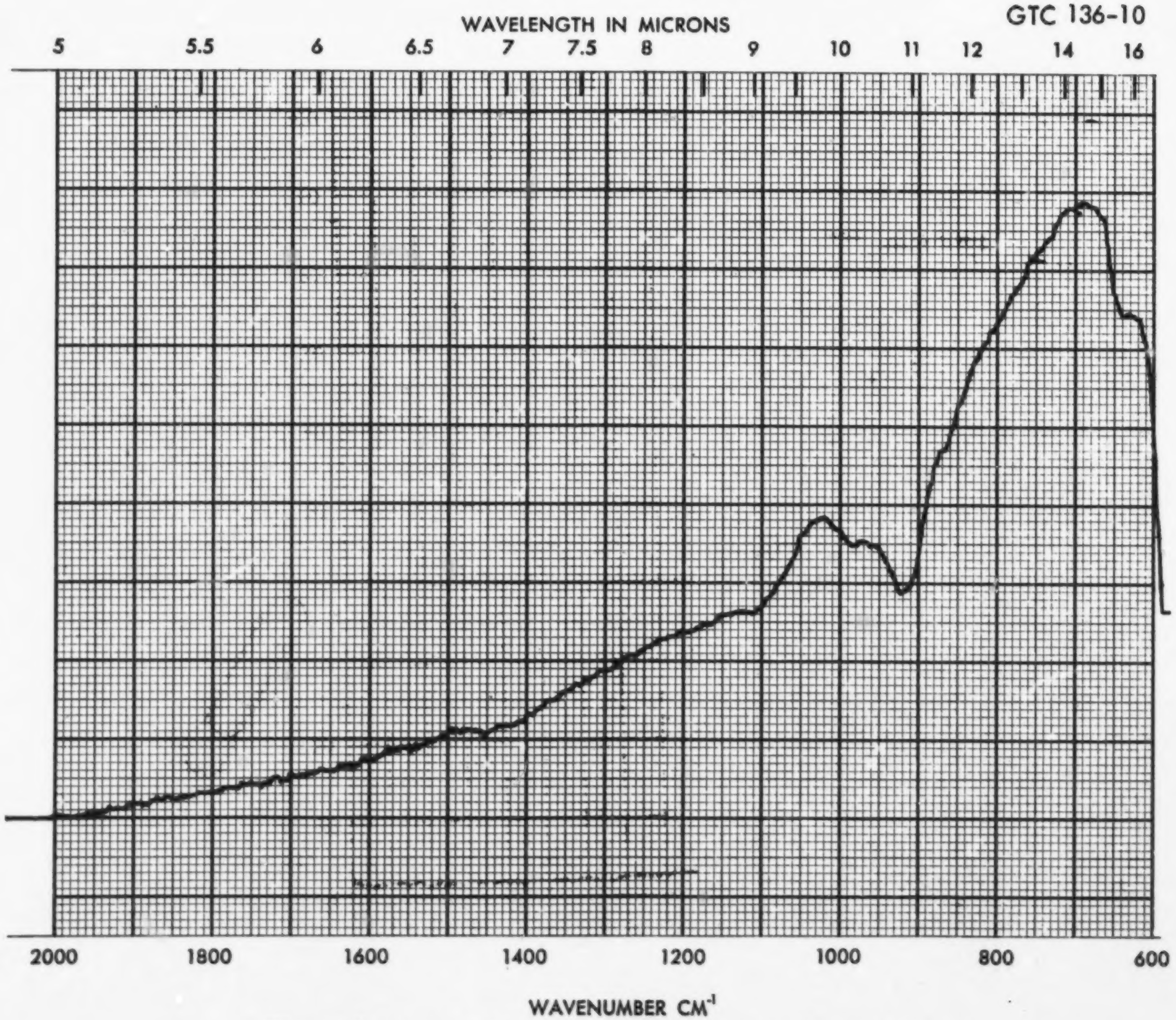

Figure 8. Infrared Spectrum of CaO Deposit after Reaction with Simulated Flue Gas for One Hour

Urea and diphenyl carbizide were exposed to sulfur dioxide to determine whether the amide groups, 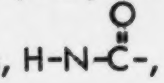 $H-N-\overset{\overset{O}{\|}}{C}-$, had an affinity for sulfur dioxide. No reaction was observed when these compounds were exposed to flue gas at room temperature.

The mercuric chloride was considered as a possible adsorbent for sulfur dioxide because of the possible formation of Lewis Acid-Base complexes with sulfur dioxide. However, no reaction was observed between $HgCl_2$ and sulfur dioxide at room temperature.

2. INFRARED SPECTRA OF LIMESTONE SAMPLES REACTED WITH FLUE GAS AT THE NATIONAL AIR POLLUTION CONTROL ADMINISTRATION

a. Infrared Spectra of Slaked Limestone Samples Before and After Exposure to Flue Gas

The infrared spectrum of limestone samples before and after exposure to flue gas at the National Air Pollution Control Administration were measured in order to serve as controls in the development of the infrared spectroscopic technique to study the gas-solid interactions occurring between sulfur dioxide in a simulated flue gas and various limestone adsorbents. The infrared spectra of slaked limestone samples Nos. BCR 1684-198, 1362-201, 1342-199, 1361-200 and 1699-202 before and after exposure to 2800 ppm of SO_2 at 750°F. are presented in Figures 9 through 18. The unreacted samples were prepared by calcining in a rotary kiln at 1800°F. for two hours and then slaking in distilled water. The assignments for the infrared absorption bands of these samples are presented in Tables VI through X. The primary absorption bands present in the spectra of the limestone samples after exposure to sulfur dioxide is the $CO_3^=$ absorption bands in the 2990-2520 cm.$^{-1}$ region, the ν_3 vibrational mode of $CO_3^=$ in the 1450-1398 cm.$^{-1}$ region, the C-O stretching vibrational mode of $CO_3^=$ at 1798 cm.$^{-1}$, the deformation vibrational mode of $CO_3^=$ in the 878-716 cm.$^{-1}$ region, the ν_3 vibrational mode of $SO_4^=$ in the 1190-1110 cm.$^{-1}$ region and the deformation mode of $SO_4^=$ in the 673-610 cm.$^{-1}$ region.

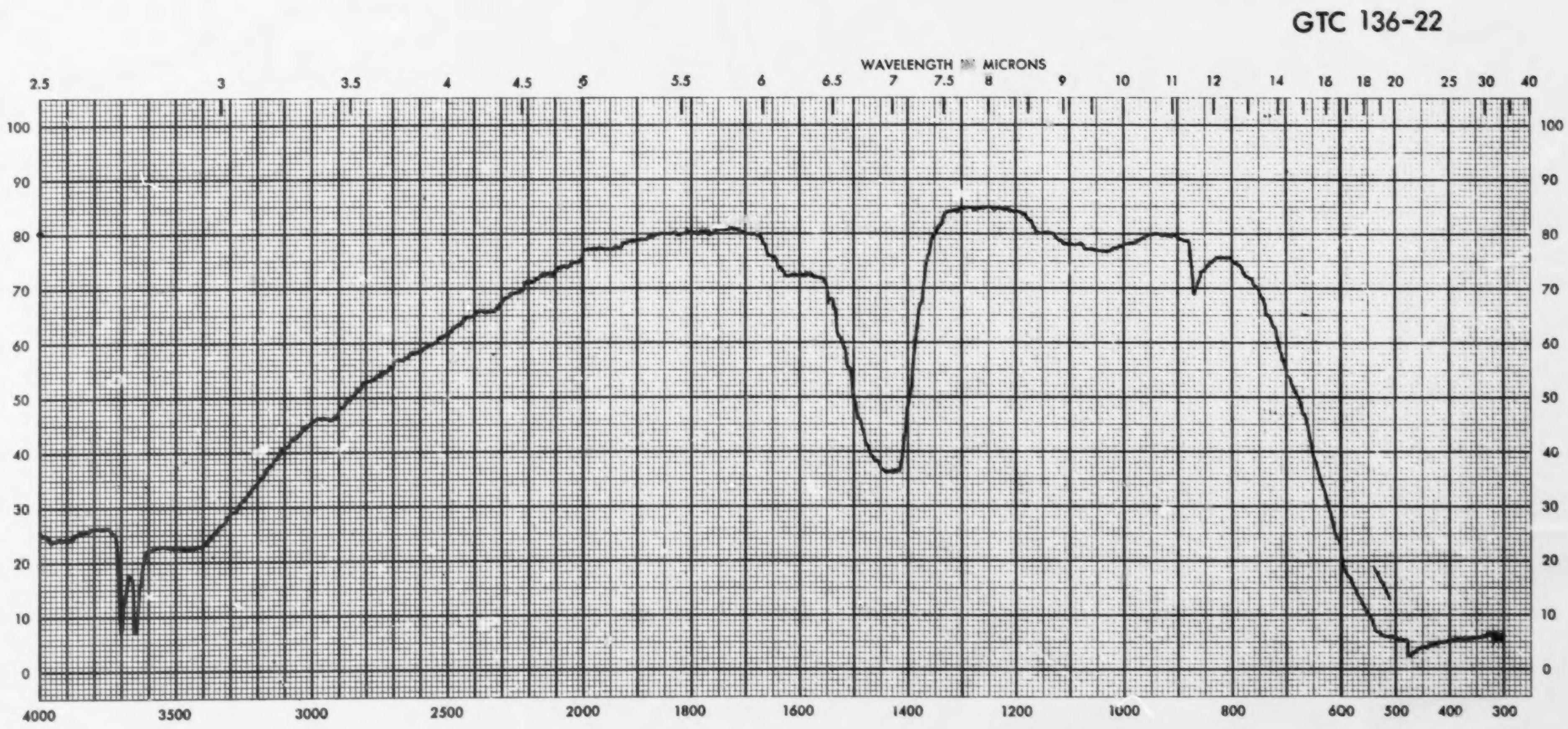

Figure 9. Spectrum of Sample No. BCR 1684-198 (Unreacted Material)

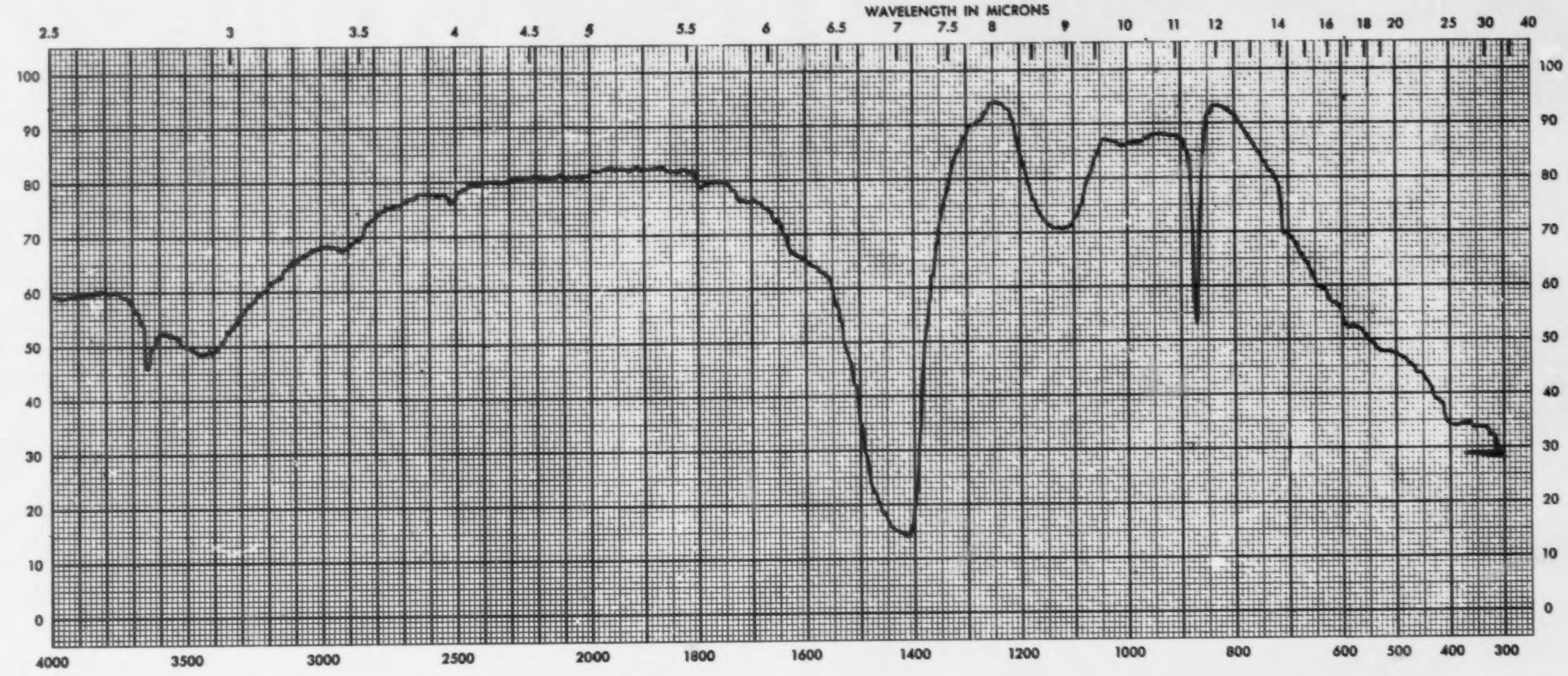

Figure 10. Spectrum of Sample No. BCR 1684-198 (Reacted Material)

GTC 136-24

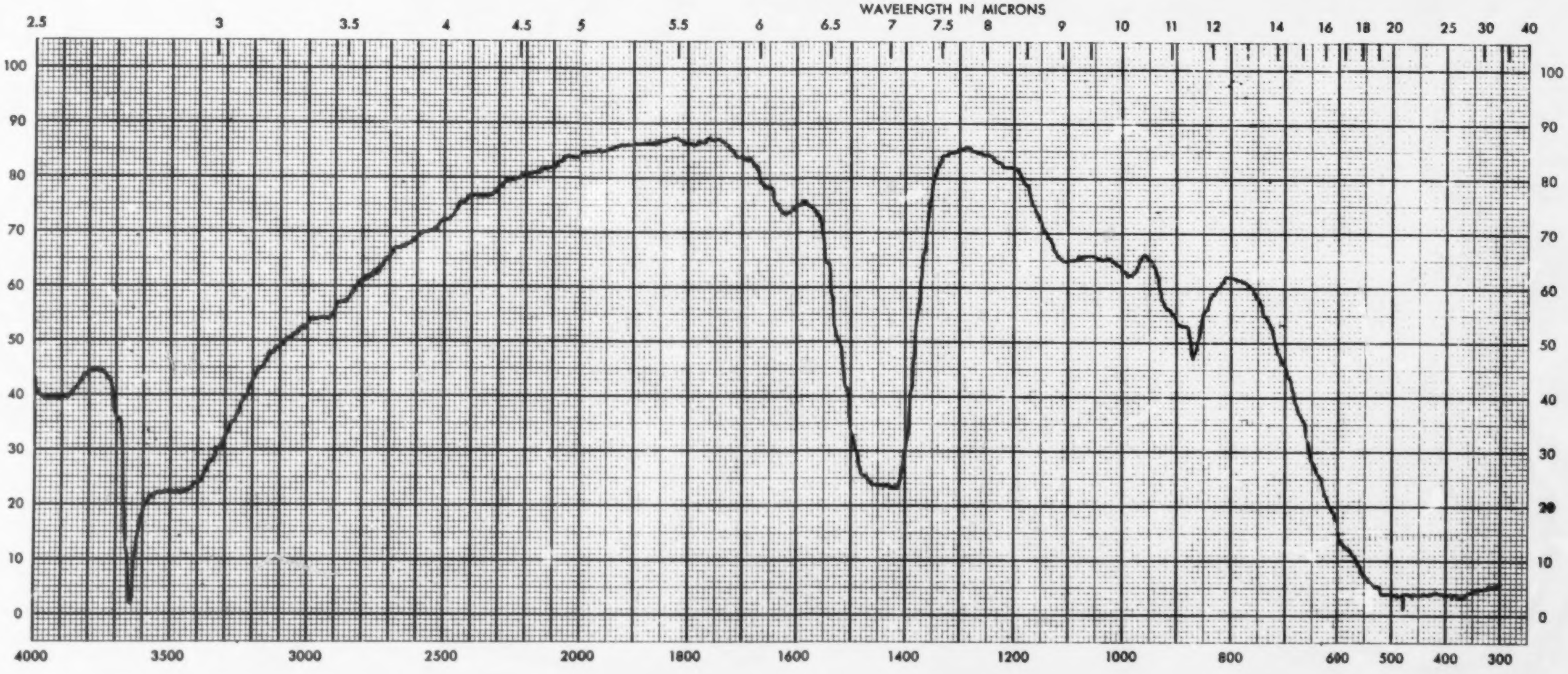

Figure 11. Spectrum of Sample No. BCR 1362-201 (Unreacted Material)

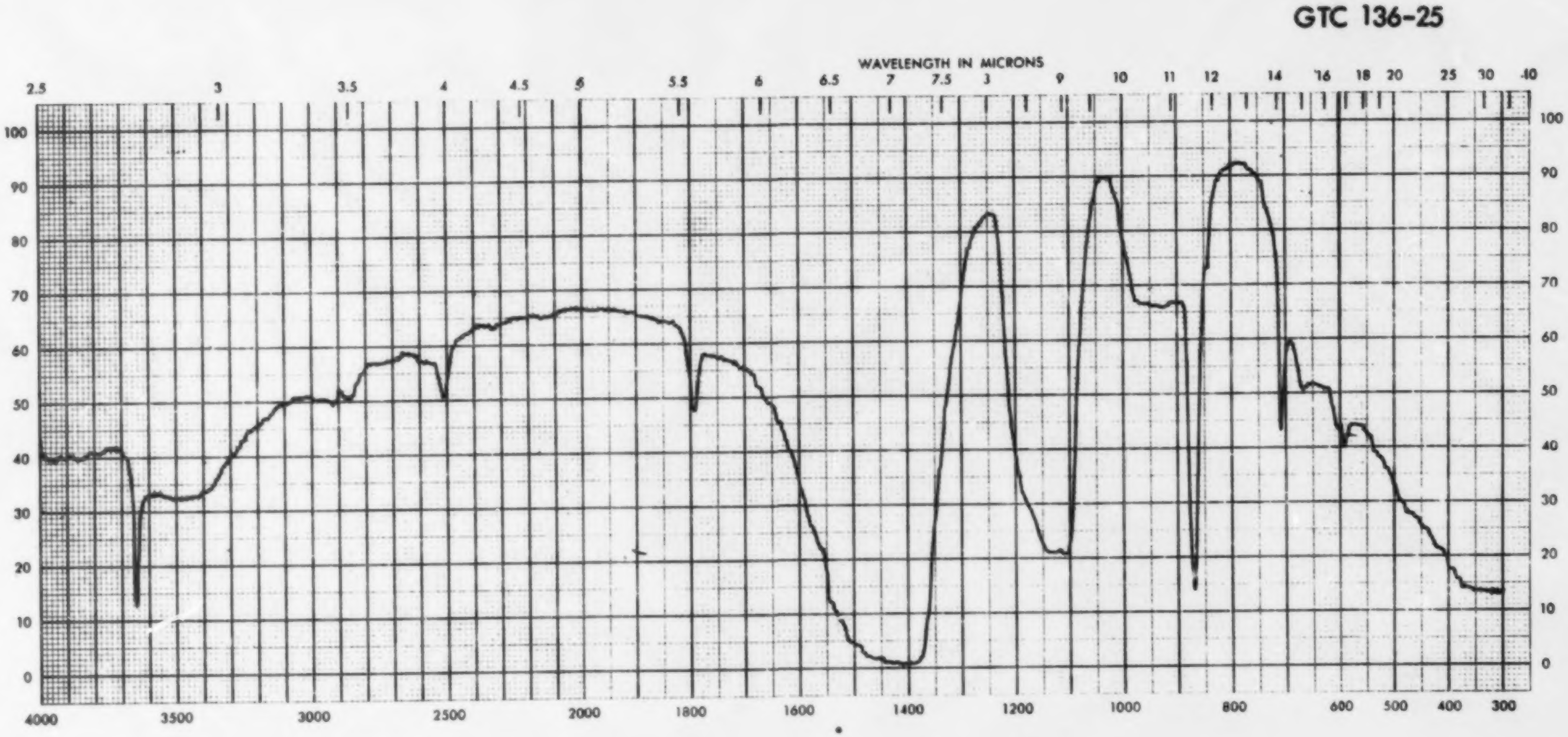

Figure 12. Spectrum of Sample No. BCR 1362-201 (Reacted Material)

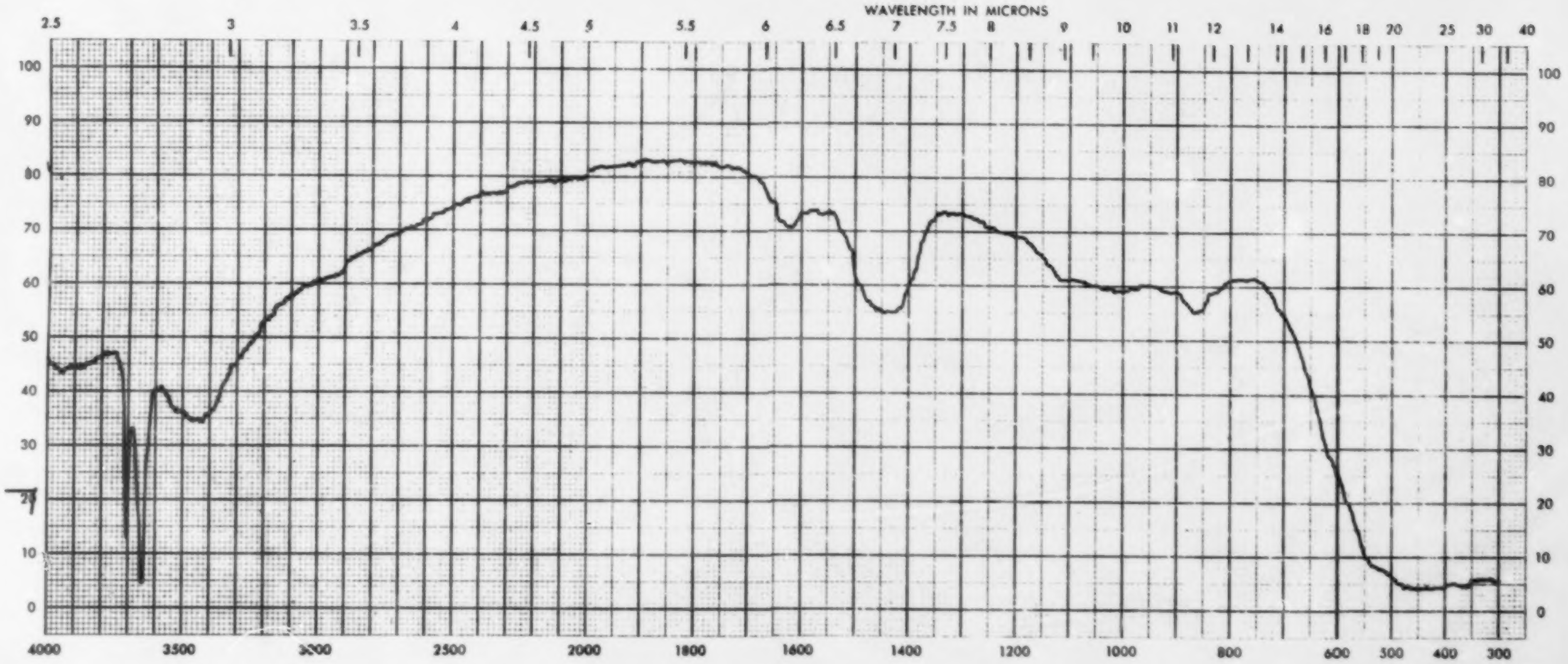

Figure 13. Infrared Spectrum of Sample No. BCR 1342-199 (Unreacted Material)

GTC 136-27

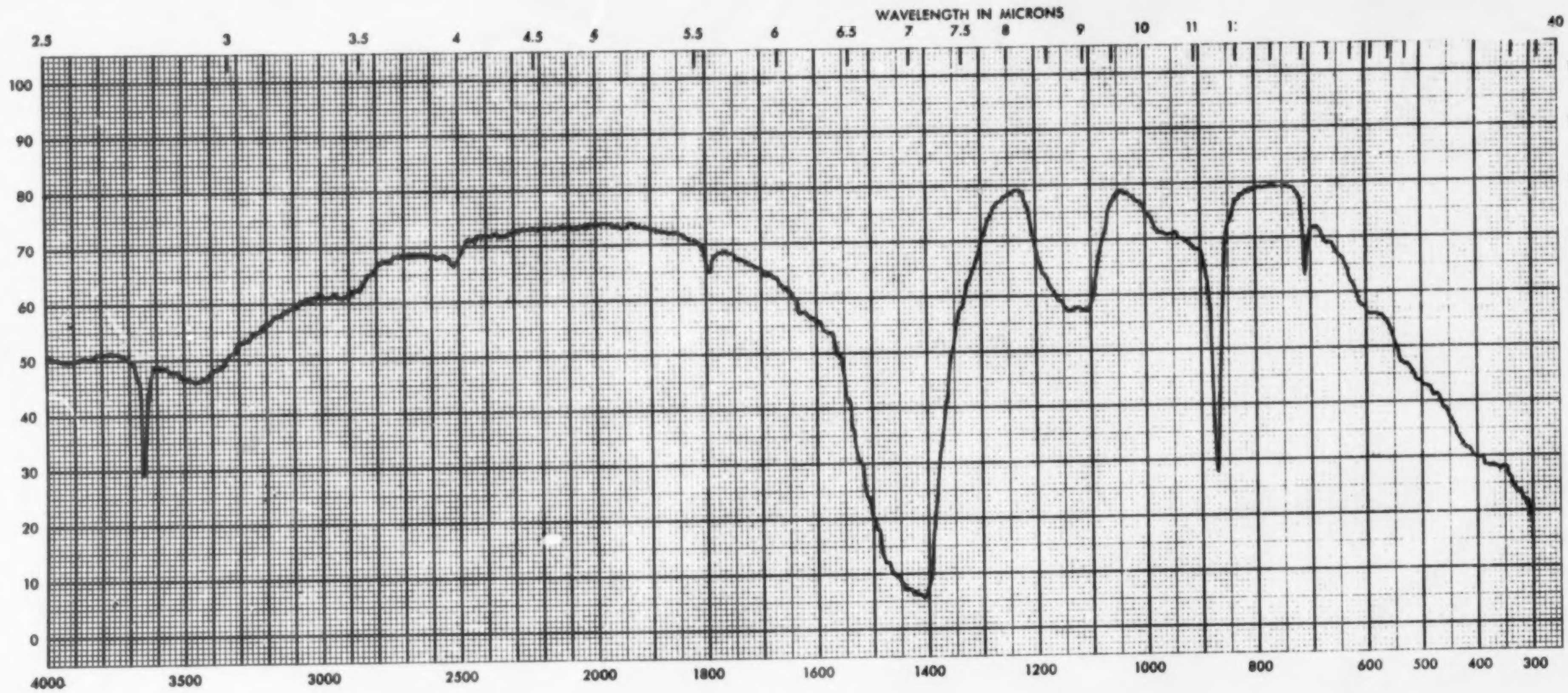

Figure 14. Infrared Spectrum of Sample No. BCR 1342-199 (Reacted Material)

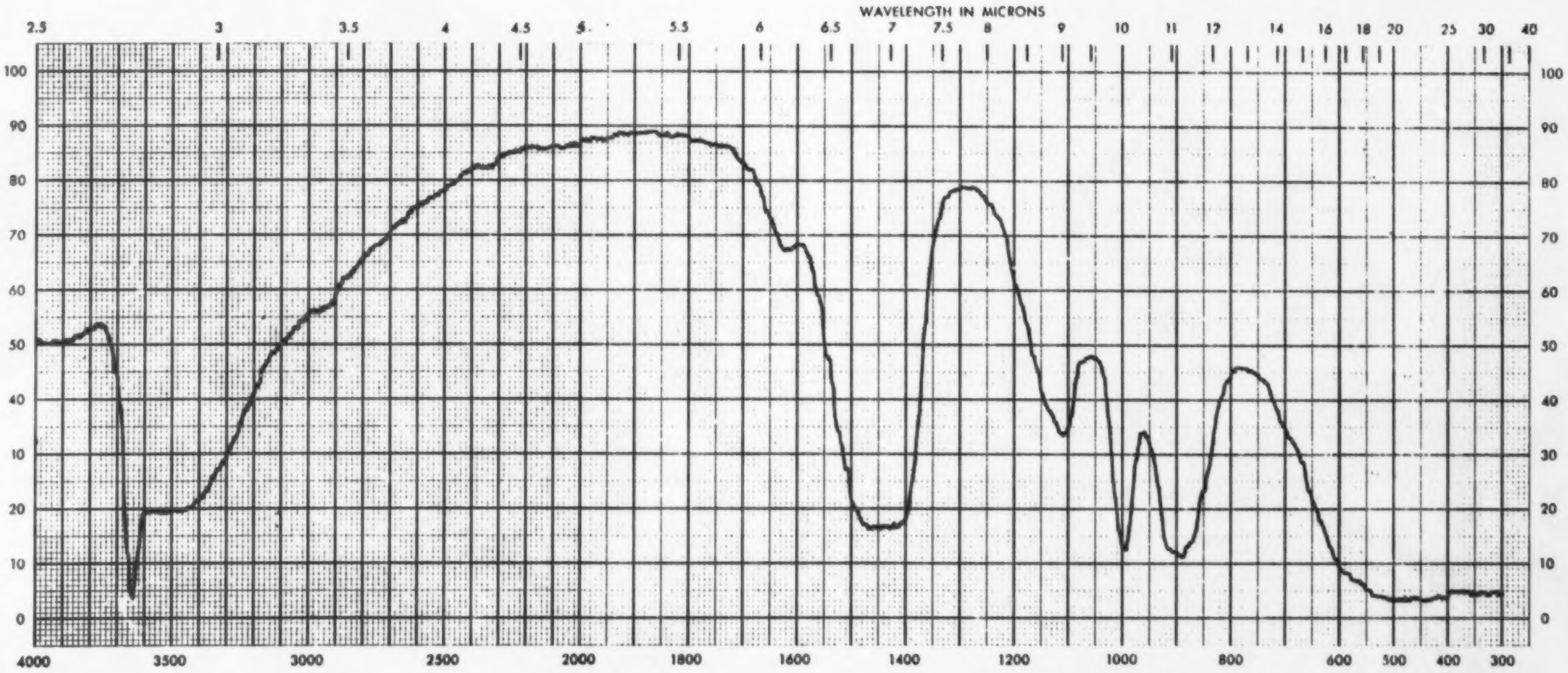

Figure 15. Infrared Spectrum of Sample No. BCR 1361-200 (Unreacted Material)

GTC 136-29

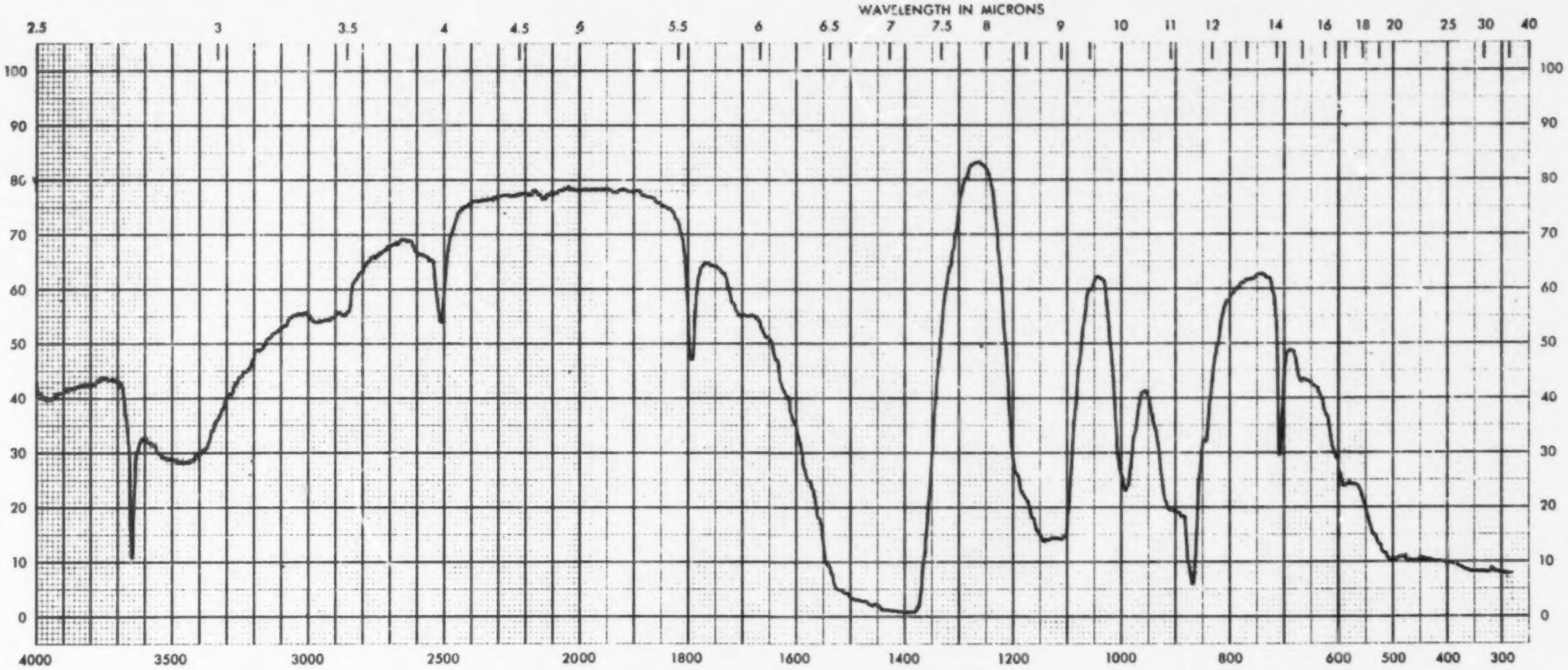

Figure 16. Infrared Spectrum of Sample No. BCR 1361-200 (Reacted Material)

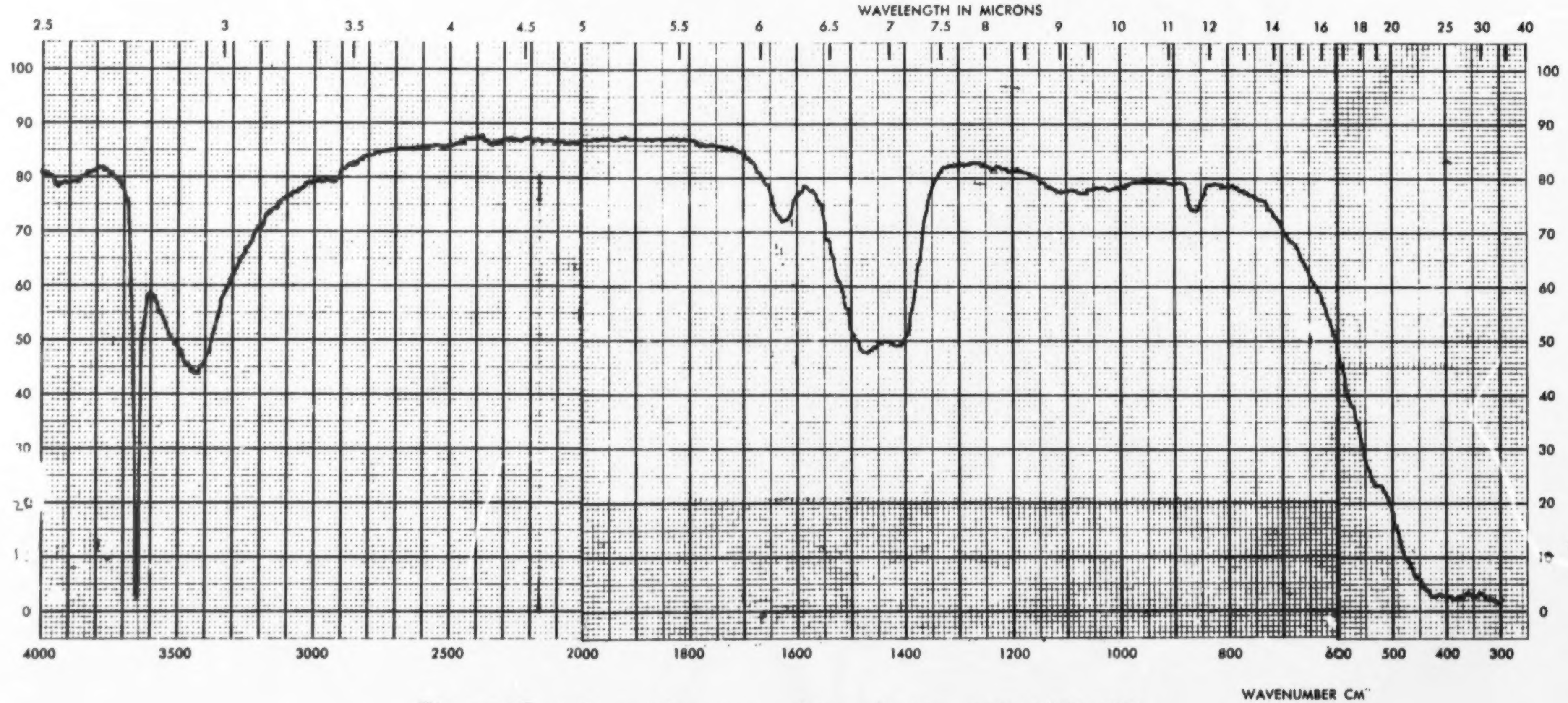

Figure 17. Infrared Spectrum of Sample No. BCR 1699-202
(Unreacted Material)

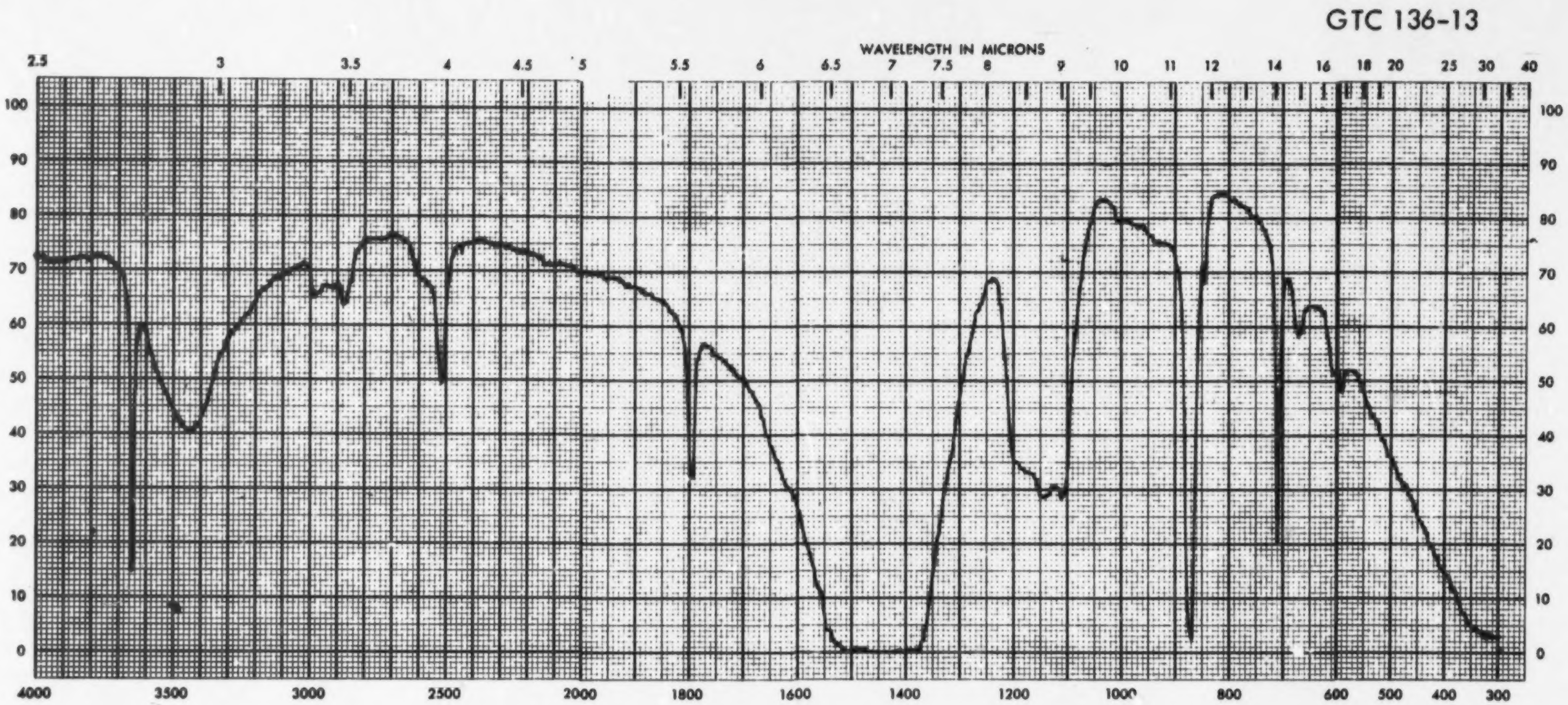

Figure 18. Infrared Spectrum of Sample No. BCR 1699-202
(Reacted Material)

Table VI Infrared Absorption Bands of Sample No. BCR 1684-198

Absorption Bands of Unreacted Material (cm.$^{-1}$)	Absorption Bands of Reacted Material (cm.$^{-1}$)	Relative Intensity*	Assignment
3702	3658	m	O-H stretching
3658			
2926	2922	wb	$CO_3^=$
	2520	w	$CO_3^=$
	2340	vw	?
	1798	w	C-O stretching
1789		vw	?
	1714	w	?
1626	1616	sh	O-H bending
1434	1416	vs	ν_3, $CO_3^=$
	1280	sh	?
	1138	s	ν_3, $SO_4^=$
1080			?
	999	w	?
878	878	vs	$CO_3^=$, deformation out-of-plane mode
	714	w	$CO_3^=$, deformation in-plane-mode

---

*m = medium, sh = shoulder, vs = very strong, w = weak, b = broad

Table VII Infrared Absorption Bands of Sample No. BCR 1362-201

Absorption Bands of Unreacted Material (cm.$^{-1}$)	Absorption Bands of Reacted Material (cm.$^{-1}$)	Relative Intensity*	Assignment
3656	3658	s	O-H stretching
2930	2918	m	$CO_3^=$
	2582	sh	$CO_3^=$
	2520	m	$CO_3^=$
2340		vw	?
	1798	s	C-O stretching
1626		m	O-H bending
1446	1398	vs	ν_3, $CO_3^=$
	1184	sh	
	1132 1110	vs	$SO_4^=$
1230		vw	?
1100		m	?
994		w	?
	956	s	$SO_3^=$
918		sh	?
876	874	s	$CO_3^=$, deformation out-of-plane mode
	716	vs	$CO_3^=$, deformation in-plane-mode
	672	m	$SO_4^=$
	611	w	$SO_4^=$
	598	w	?

---

*m = medium, sh = shoulder, vs = very strong, w = weak, b = broad

Table VIII Infrared Absorption Bands of Sample No. BCR 1342-199

Absorption Bands of Unreacted Material ($cm.^{-1}$)	Absorption Bands of Reacted Material ($cm.^{-1}$)	Relative Intensity*	Assignment
3702			
	3658	m	O-H stretching
3658			
2920	2922	w	$CO_3^=$
2860	2878		
	2520	w	$CO_3^=$
	1799	m	C-O stretching
1620		m	O-H bending
1440	1414	vs	ν_3, $CO_3^=$
	1180	s	$SO_4^=$
	1116		
1050		b	?
	940	sh	$SO_3^=$
865	878	vs	$CO_3^=$, out-of-plane mode
830		w	?
	716	m	$CO_3^=$
	668	sh	$SO_4^=$
	610	vw	$SO_4^=$

---

*m = medium, sh = shoulder, vs = very strong, w = weak, b = broad

Table IX Absorption Bands of Sample No. BCR 1361-200

Absorption Bands of Unreacted Material ($cm.^{-1}$)	Absorption Bands of Reacted Material ($cm.^{-1}$)	Relative Intensity*	Assignments
	3658	s	O-H stretching
3656		vs	O-H stretching
	2990	w	$CO_3^=$
2924	2930	w	$CO_3^=$
	2880	w	
	2598	sh	$CO_3^=$
	2520	m	$CO_3^=$
	2320	vw	?
	1798	s	C-O stretching
1765		vw	?
1710		vw	?
1624		s	O-H bending
1470 1430		vs	ν_3, $CO_3^=$
	1450	vvs	ν_3, $CO_3^=$
	1199	sh	
	1146	vs	ν_3, $SO_4^=$
	1114	vs	
1114		s	?

---

*m = medium, sh = shoulder, vs = very strong, vvs = very, very strong, w = weak, b = broad

Table IX (cont.) Absorption Bands of Sample No. BCR 1361-200

Absorption Bands of Unreacted Material (cm.$^{-1}$)	Absorption Bands of Reacted Material (cm.$^{-1}$)	Relative Intensity*	Assignments
1000		vs	?
	999	vs	?
950		sh	?
	920	sh	$SO_3^=$
916 894		s	?
875	876	s	$CO_3^=$
850	852	w	?
	718	s	$CO_3^=$
	673	w	$SO_4^=$
	610	w	$SO_4^=$
	596	w	?

---

*m = medium, sh = shoulder, vs = very strong, vvs = very, very strong, w = weak, b = broad

Table X Infrared Absorption Bands of Sample No. BCR 1699-202

Absorption Bands of Unreacted Material (cm.$^{-1}$)	Absorption Bands of Reacted Material (cm.$^{-1}$)	Relative Intensity*	Assignment
3656	3658	vs	O-H stretching
	2954	w	$CO_3^=$
	2883	w	$CO_3^=$
	2582	sh	$CO_3^=$
	2520	m	$CO_3^=$
	1798	m	C-O stretching
1628			O-H bending
1470			ν_3, $CO_3^=$
1421			ν_3, $CO_3^=$
	1448	vvs	ν_3, $CO_3^=$
	1190	sh	
	1150	vs	ν_3, $SO_4^=$
	1116	vs	
1094		b	?
	876	vs	$CO_3^=$, deformation out-of-plane mode
874		w	$CO_3^=$, deformation out-of-plane mode
	850	w	$CO_3^=$, deformation out-of-plane mode
	716	s	$CO_3^=$, deformation in-plane mode
	678	w	ν_4, $SO_4^=$
	612	w	ν_4, $SO_4^=$
	598	w	?

---

*vs = very strong, w = weak, sh = shoulder, b = broad

In reacted samples Nos. BCR 1362-201, 1342-199 and 1361-200, sulfite absorption bands were detected in the 956-920 cm.$^{-1}$ region.

The spectra of the unreacted limestone samples showed infrared bands due to carbonate and infrared absorption bands due to the O-H stretching vibrational mode in the 3702-3656 cm.$^{-1}$ and the O-H bending mode in the 1628-1620 cm.$^{-1}$ region. Samples numbers BCR 1342-199 and 1684-198 showed doublets at 3702-3656 cm.$^{-1}$ and 3702-3658 cm.$^{-1}$, respectively. The higher frequency band was attributed to $Mg(OH)_2$ and the lower band to $Ca(OH)_2$. A chemical analysis of these compounds showed that sample No. BCR 1342-199 was composed of 60% CaO and 20% MgO, and sample No. BCR 1684-198 was composed of 57.0% CaO and 39.0% MgO. Hence, upon slaking the calcined material of these two compounds, both the CaO and MgO slaked to give $Ca(OH)_2$ and $Mg(OH)_2$. The carbonate absorption bands found in the slaked samples was attributed to the reaction of the hydroxide with carbon dioxide to give carbonate. For example, when slaked lime, $Ca(OH)_2$ is exposed to air for a long period of time, $CaCO_3$ is formed according to the reaction

$$Ca(OH)_2 + CO_2 \longrightarrow CaCO_3 + H_2O.^{(17)} \qquad (3)$$

The assignment of these infrared absorption bands was based on the following studies. The Raman spectrum of the $SO_4^{=}$ ion has been recorded for $CaSO_4$ and $CaSO_4 \cdot 2\,H_2O$(18). Vibrational modes and frequencies of these compounds are given in Table XI. Also, Bellamy(19) reports that the sulfates possess very strong absorption bands in the region of 1130-1080 cm.$^{-1}$ and medium and weak bands in the 680-610 cm.$^{-1}$ region. In addition, further evidence for the assignment of the absorption bands at 1110-1199 cm.$^{-1}$ to sulfate is found in a paper by Decius(16). His assignments for the $SO_4^{=}$ absorption bands for $CaSO_4$ in KBr and KCl are presented in Table XII.

Table XI Infrared Absorption Bands of $CaSO_4$ and $CaSO_4 \cdot 2H_2O$(18)

Compound	ν_1	ν_2	ν_3	ν_4
$CaSO_4$	1018	415	1108	609
		499	1128	628
			1160	674
$CaSO_4 \cdot 2H_2O$	1006	415	1115	618
		499	1136	622
			1144	672

Table XII Fundamental Frequencies of the Sulfate Ion in Alkali Halides ($cm.^{-1}$)(16)

	$CaSO_4$ in KBr	$CaSO_4$ in KCl
$\nu_2\ (a_1)$	496	--
$\nu_4\ (b_1)$	612	616
$\nu_4\ (a_1)$	627	629
$\nu_4\ (b_2)$	648	651
$\nu_1\ (a_1)$	975.5	982
$\nu_3\ (b_1)$	1080.5	1090
$\nu_3\ (a_1)$	1150.5	1157
$\nu_3\ (b_2)$	1180.5	1186

In the assignment of the carbonate bands, Rao(20) reports three fundamental characteristic bands of the carbonates: the CO_3 asymmetric stretching mode occurs as a strong intensity band in the region of 1450-1410 $cm.^{-1}$, the CO_3 deformation out-of-plane mode is a medium intensity band in the region of 880-850 $cm.^{-1}$, and the CO_3

deformation in-plane mode occurs in the region of 720-680 cm.$^{-1}$. However, the latter assignment is not reliable. The assignment of the 1798 cm.$^{-1}$ absorption band is based on a possible structure for the carbonate ion in organic carbonates. According to Little(21), an infrared absorption band occurs at 1780 cm.$^{-1}$ due to the C=O stretch in the following structure:

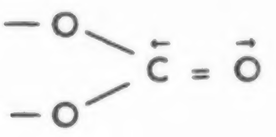

.

b. Infrared Spectra of Limestone Samples Before and After Exposure to Flue Gas at 1800°F

The infrared spectra of samples Nos. BCR 1343, 1351, 1352, 1360, 1697, 1699, and 1360 before and after exposure to 3000 ppm of SO_2 for 3.5 hours at 1800°F are given in Figures 19 through 32. The unreacted samples were prepared by calcining in a rotary kiln at 1800°F for 4 hours. The assignments for the infrared absorption bands in these materials (except samples Nos. 1699 and 1360) are presented in Tables XIII through XVII. The primary absorption bands found in the infrared spectra of these materials is the ν_3 vibrational mode of the sulfate ion in the 1200-1116 cm.$^{-1}$ region and the ν_4 vibrational mode of the sulfate ion in the 627-602 cm.$^{-1}$ region. Reacted samples Nos. BCR 1351, 1352, 1360, and 1697 exhibit carbonate bands in the region from 1438-1420 cm.$^{-1}$ and at 876 cm.$^{-1}$ for samples Nos. BCR 1352 and 1360. No infrared absorption bands were found which could be attributed to sulfite in the 1800°F runs. Hence, the data on these runs at 750°F and 1800°F indicate that sulfur dioxide is adsorbed from the flue gas as both sulfate and sulfite for slaked limestone samples exposed at 750°F, and only sulfate is detected in limestone samples exposed at 1800°F. The mechanism of the adsorption of

GTC 136-35

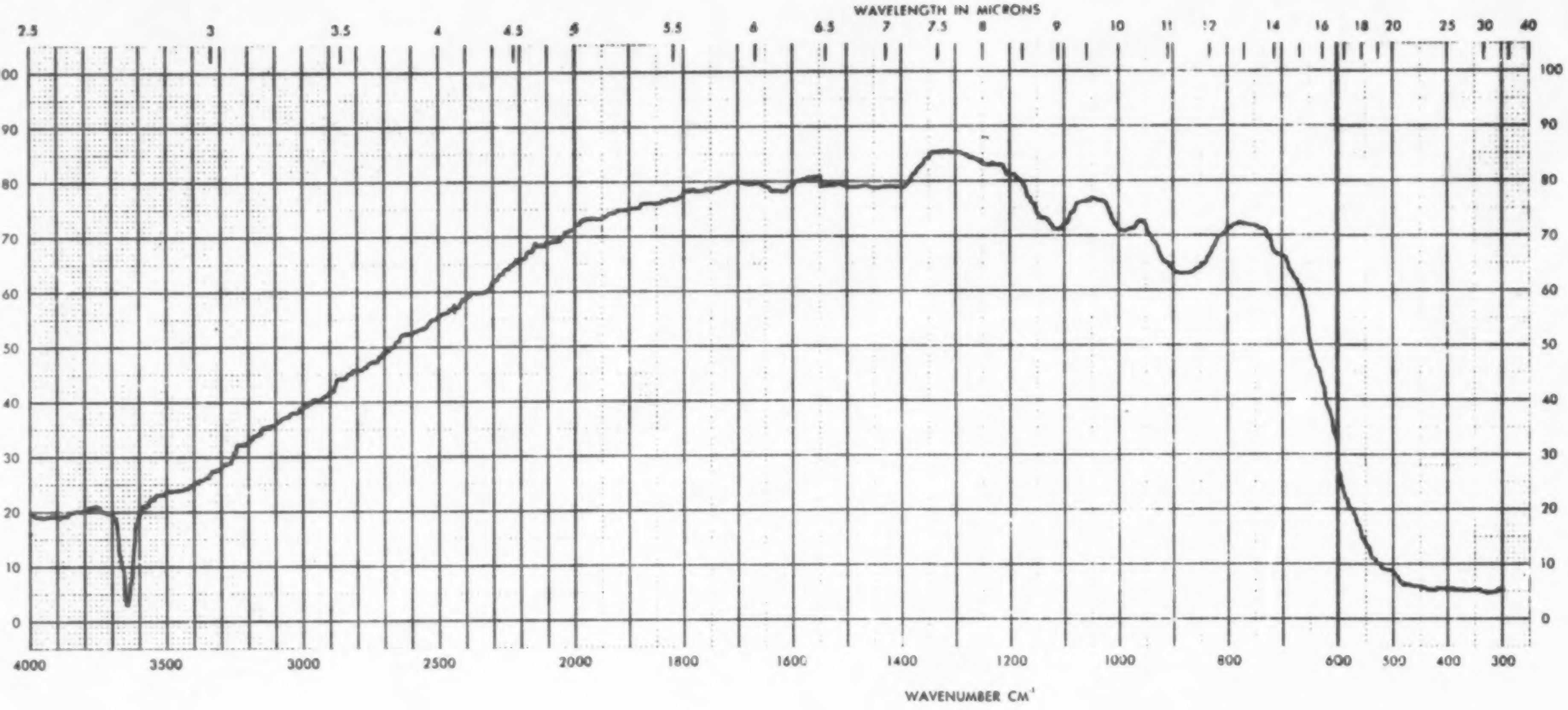

Figure 19. Infrared Spectrum of Sample No. BCR 1343 (Calcined Material)

GTC 136-36

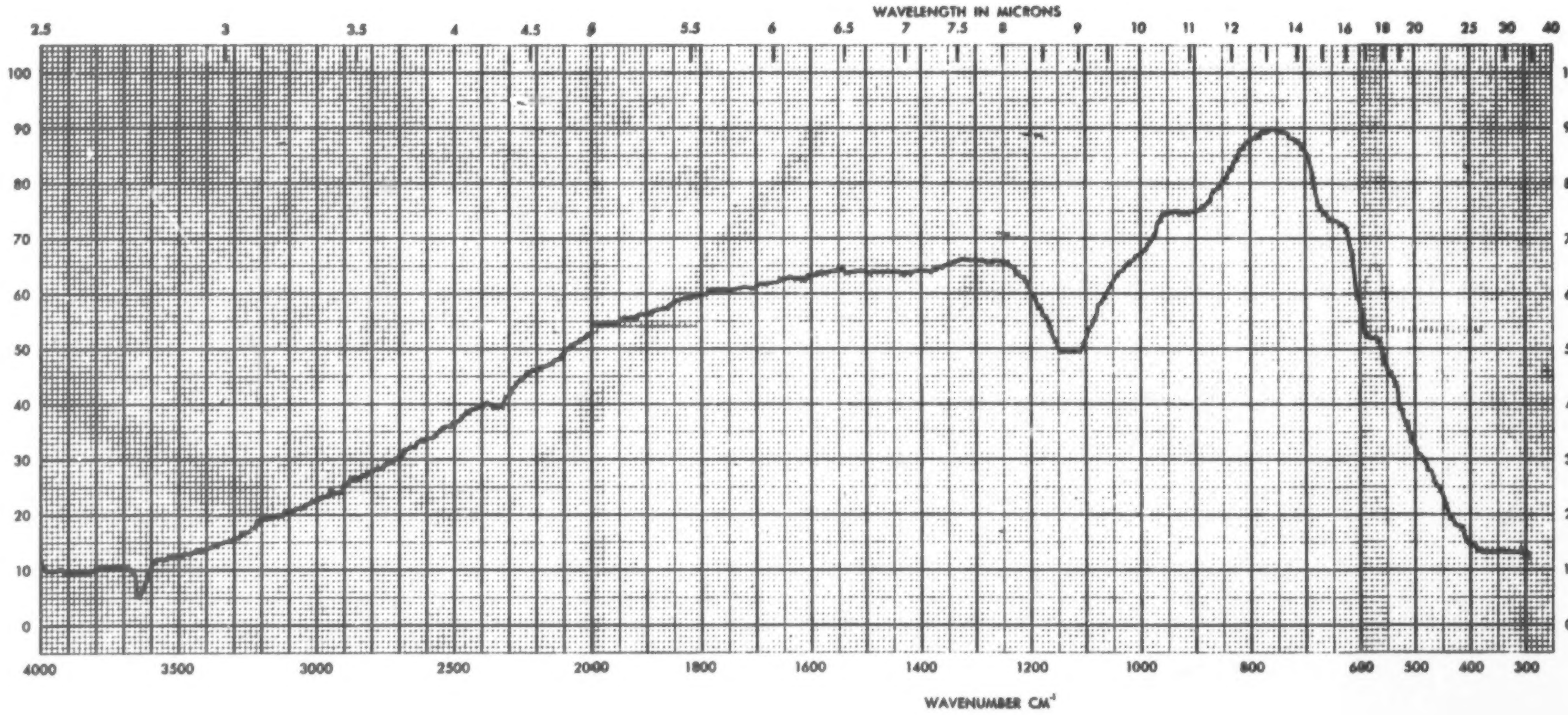

Figure 20. Infrared Spectrum of Sample No. BCR 1343 (Reacted Material)

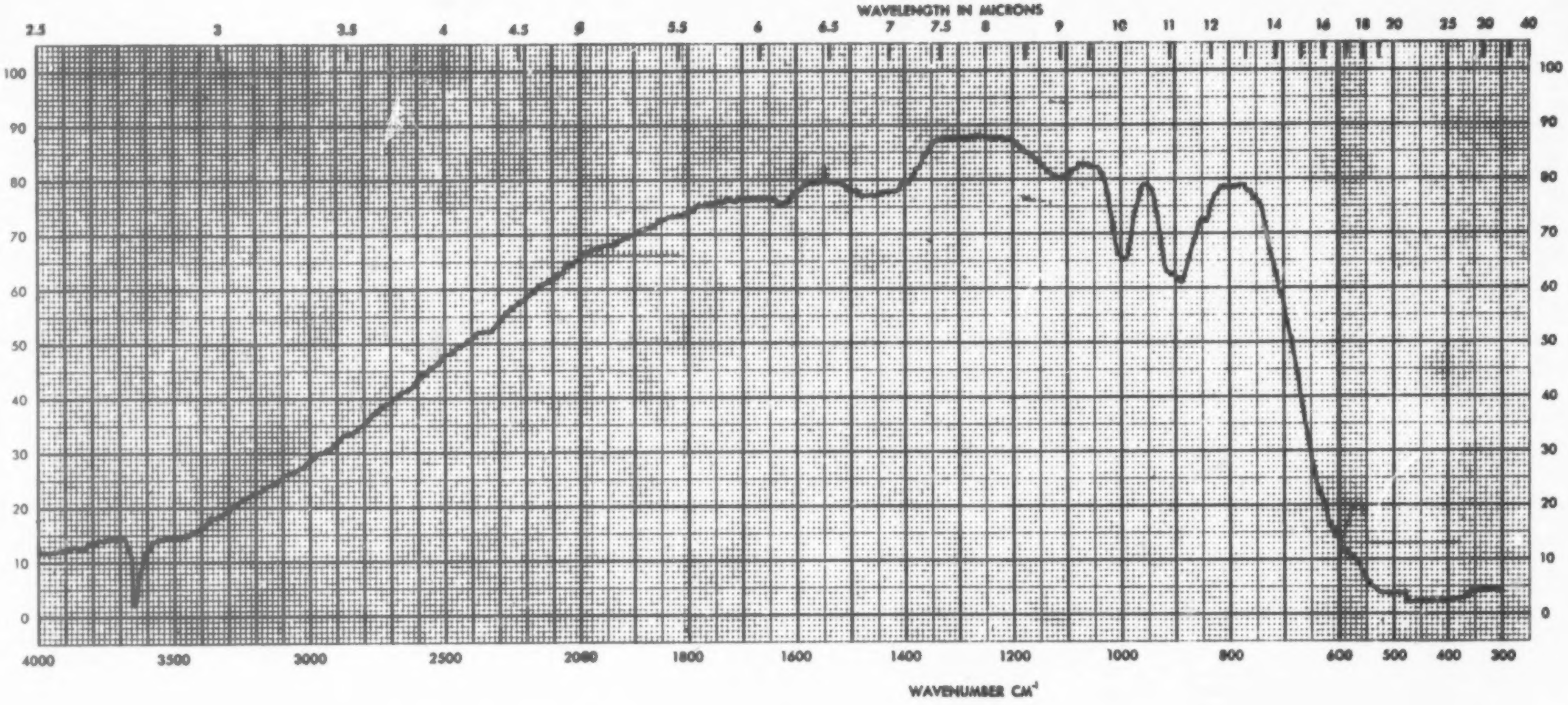

Figure 21. Infrared Spectrum of Sample No. 1351 (Calcined Material)

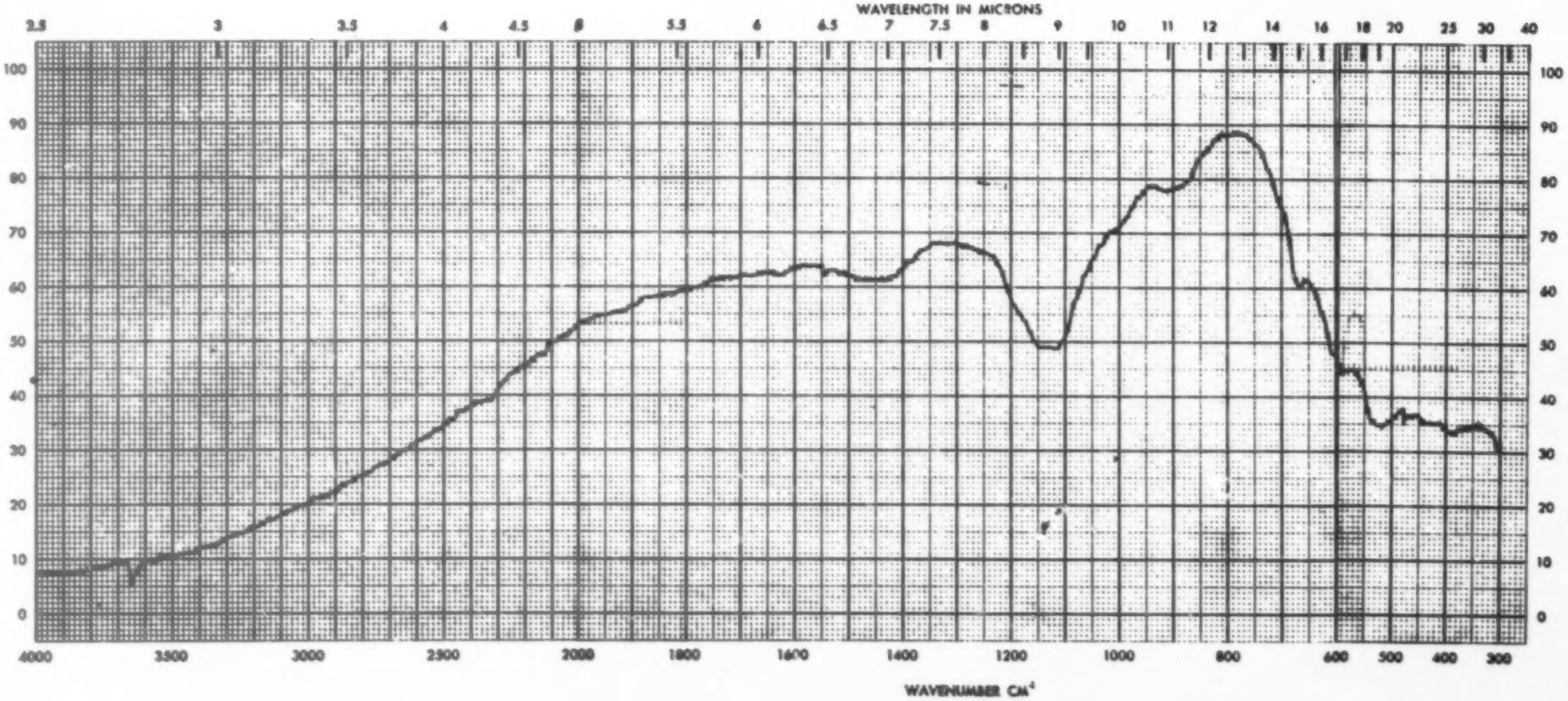

Figure 22. Infrared Spectrum of Sample No. BCR 1351 (Reacted Material)

GTC 136-39

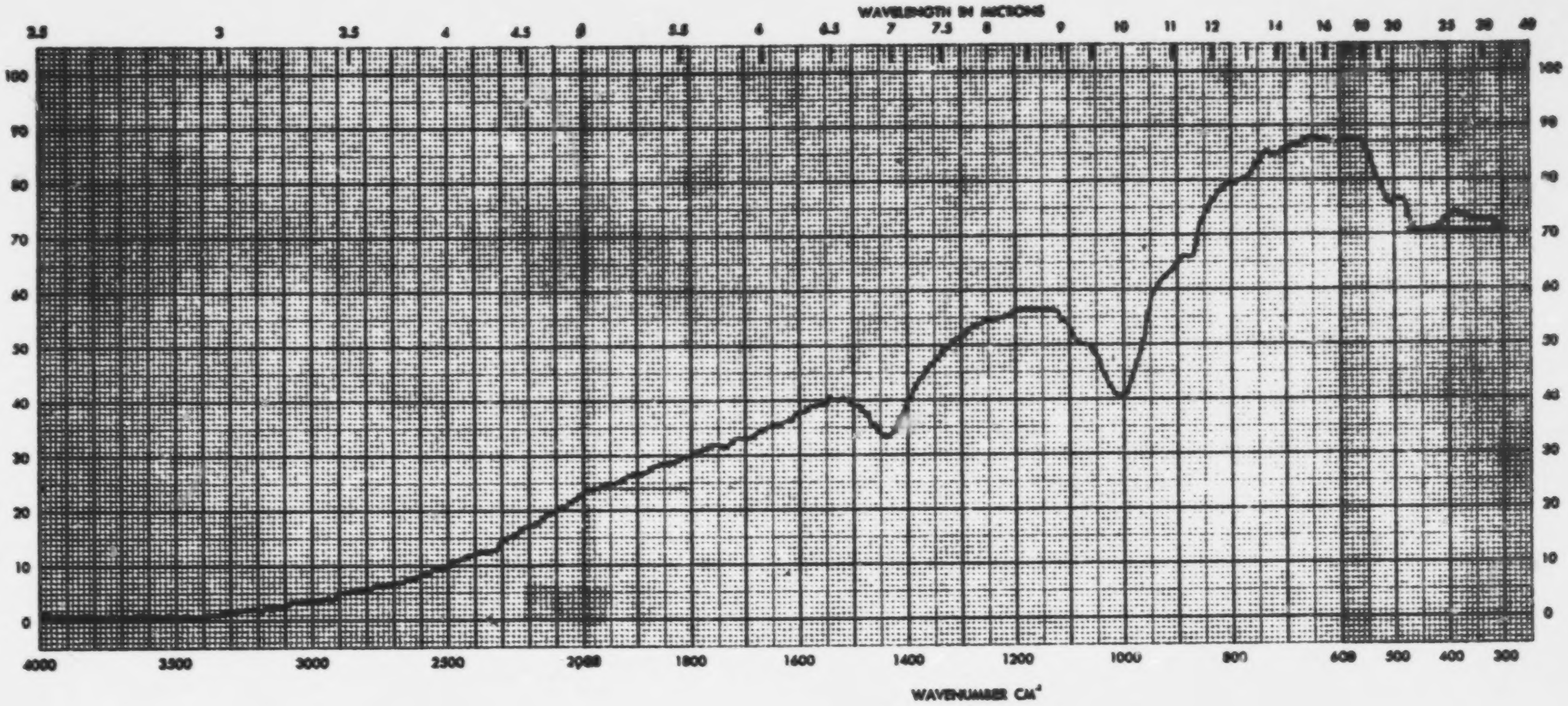

Figure 23. Infrared Spectrum of Sample No. BCR 1352 (Calcined Material)

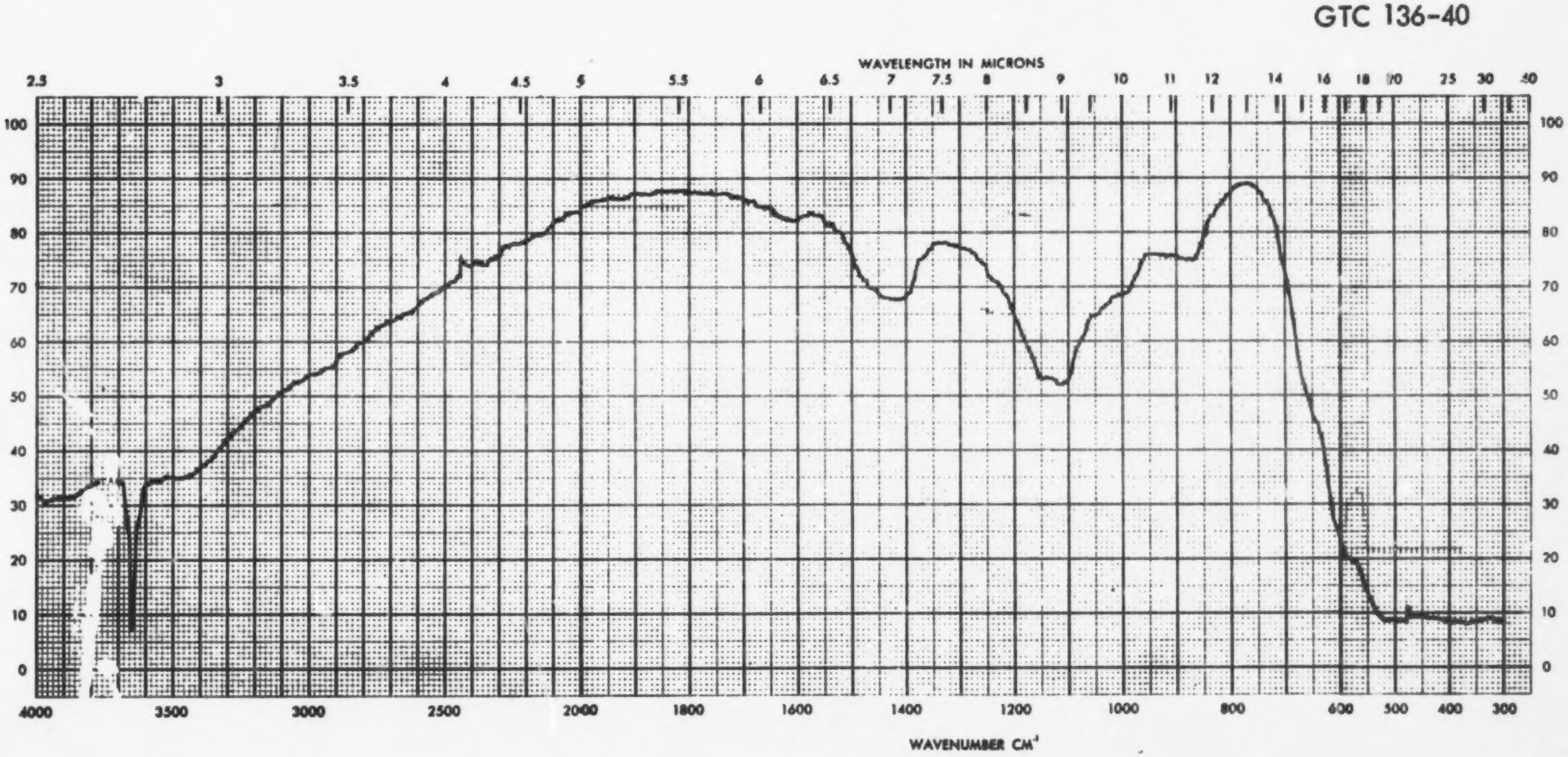

Figure 24. Infrared Spectrum of Sample No. BCR 1352 (Reacted Material)

GTC 136-41

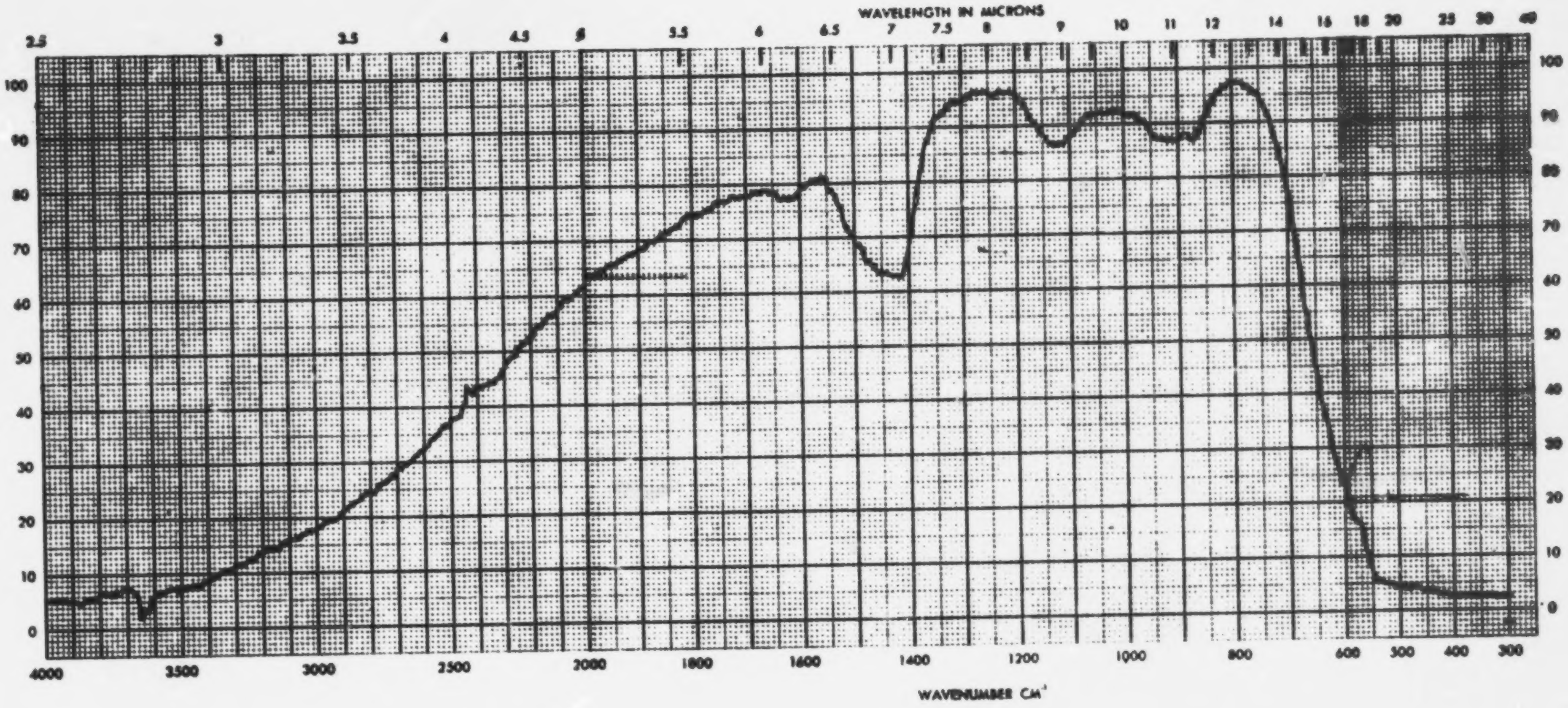

Figure 25. Infrared Spectrum of Sample No. BCR 1360 (Calcined Material)

GTC 136-42

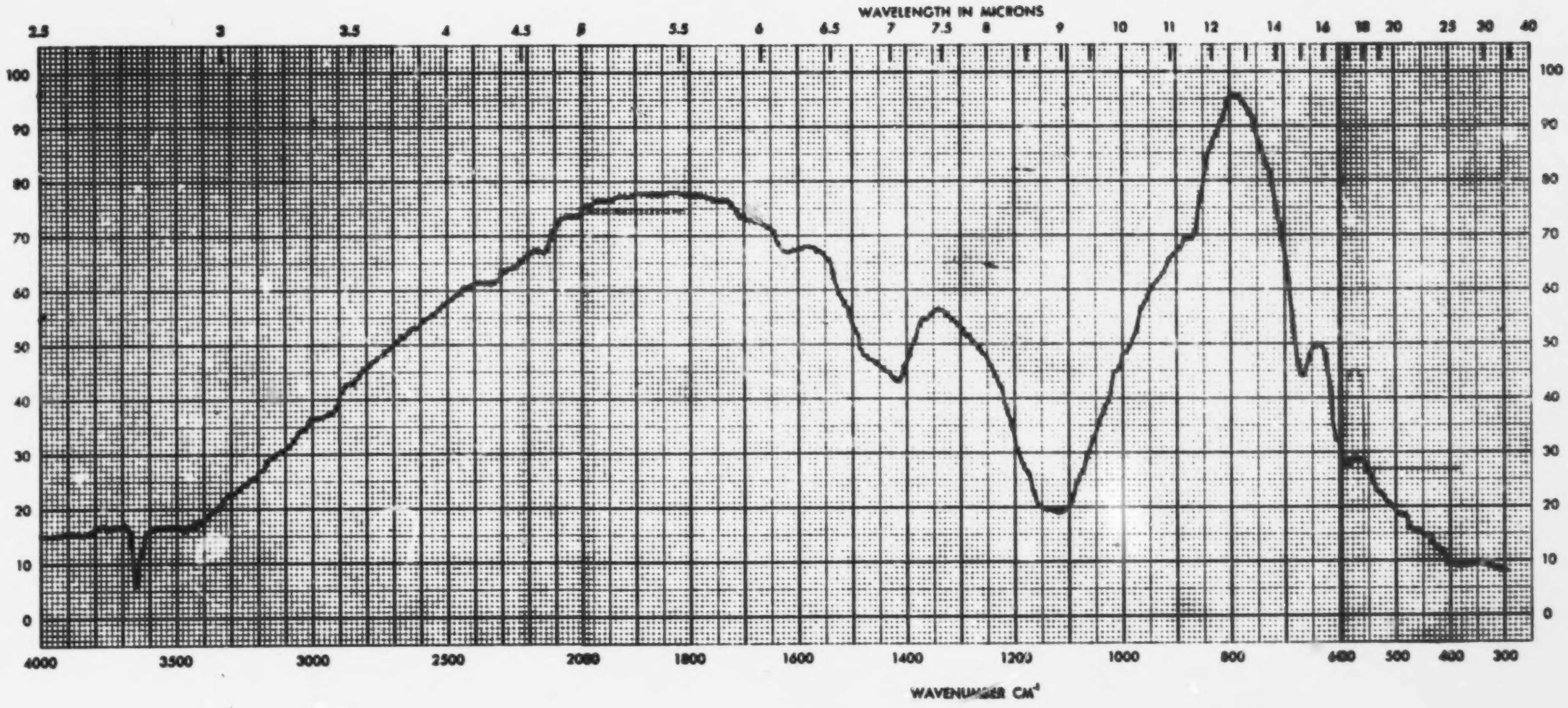

Figure 26. Infrared Spectrum of Sample No. BCR 1360 (Reacted Material

GTC 136-43

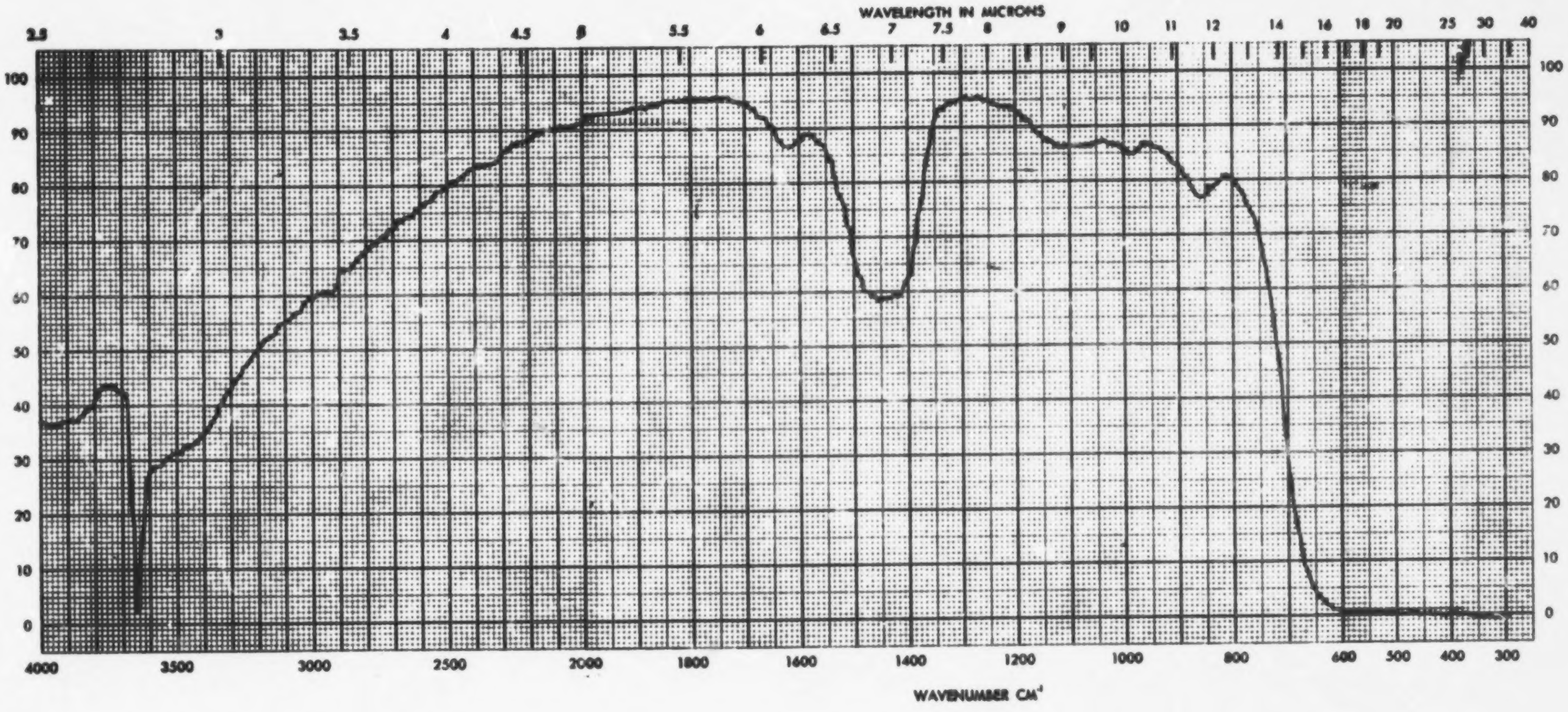

Figure 27. Infrared Spectrum of Sample No. BCR 1697 (Calcined Material)

GTC 136-44

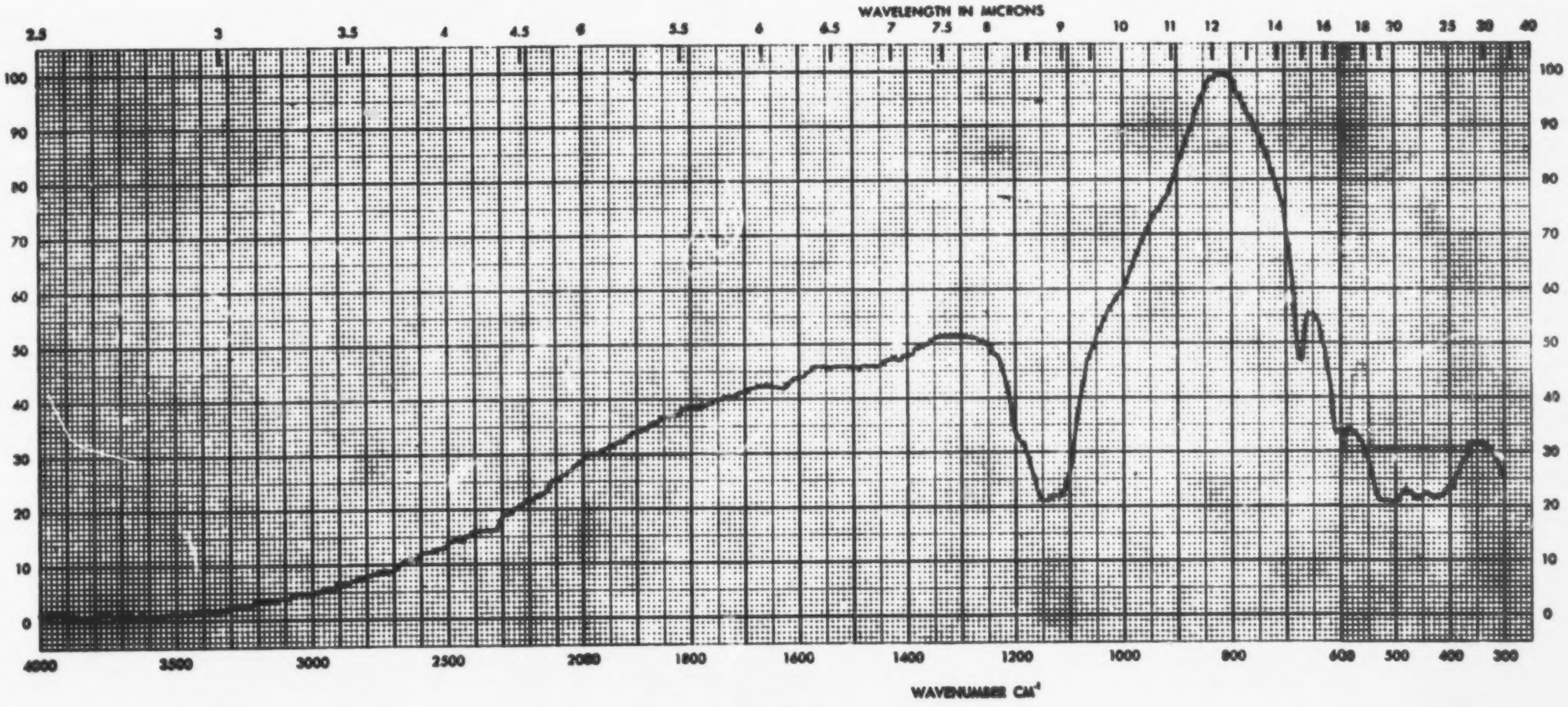

Figure 28. Infrared Spectrum of Sample No. BCR 1697 (Reacted Material

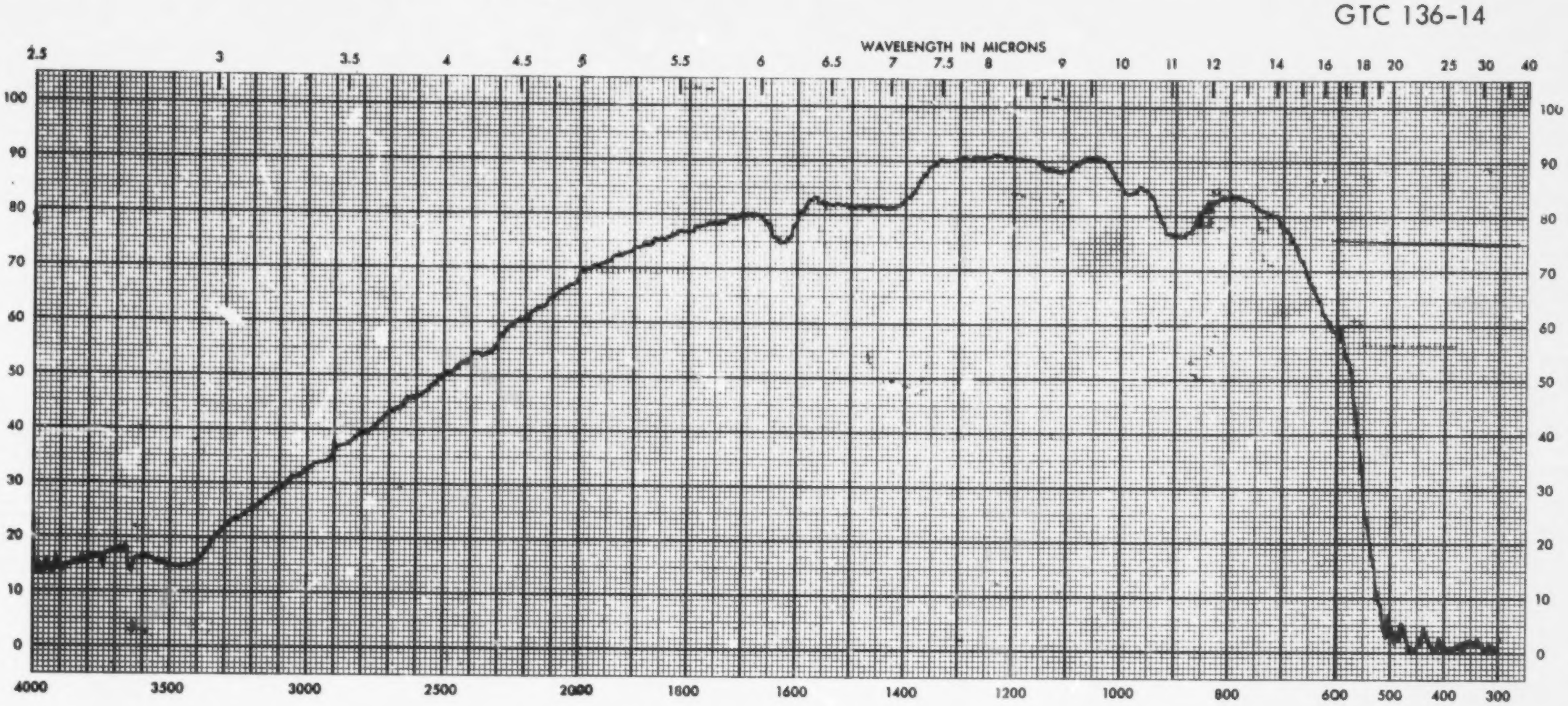

Figure 29. Infrared Spectrum of Sample No. BCR 1699-DB
(Calcined Material)

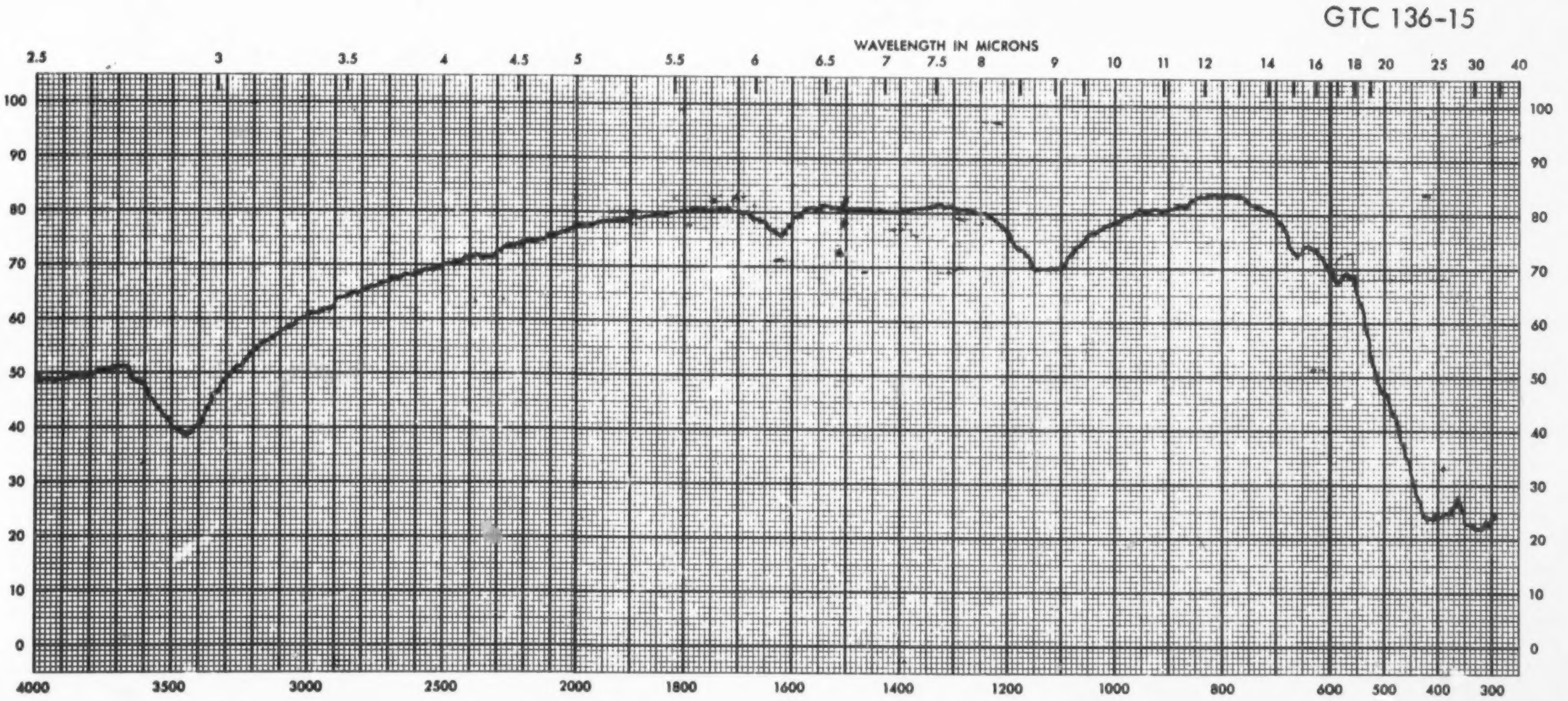

Figure 30. Infrared Spectrum of Sample No. BCR 1699-Run No. 34 DB
(Reacted Material)

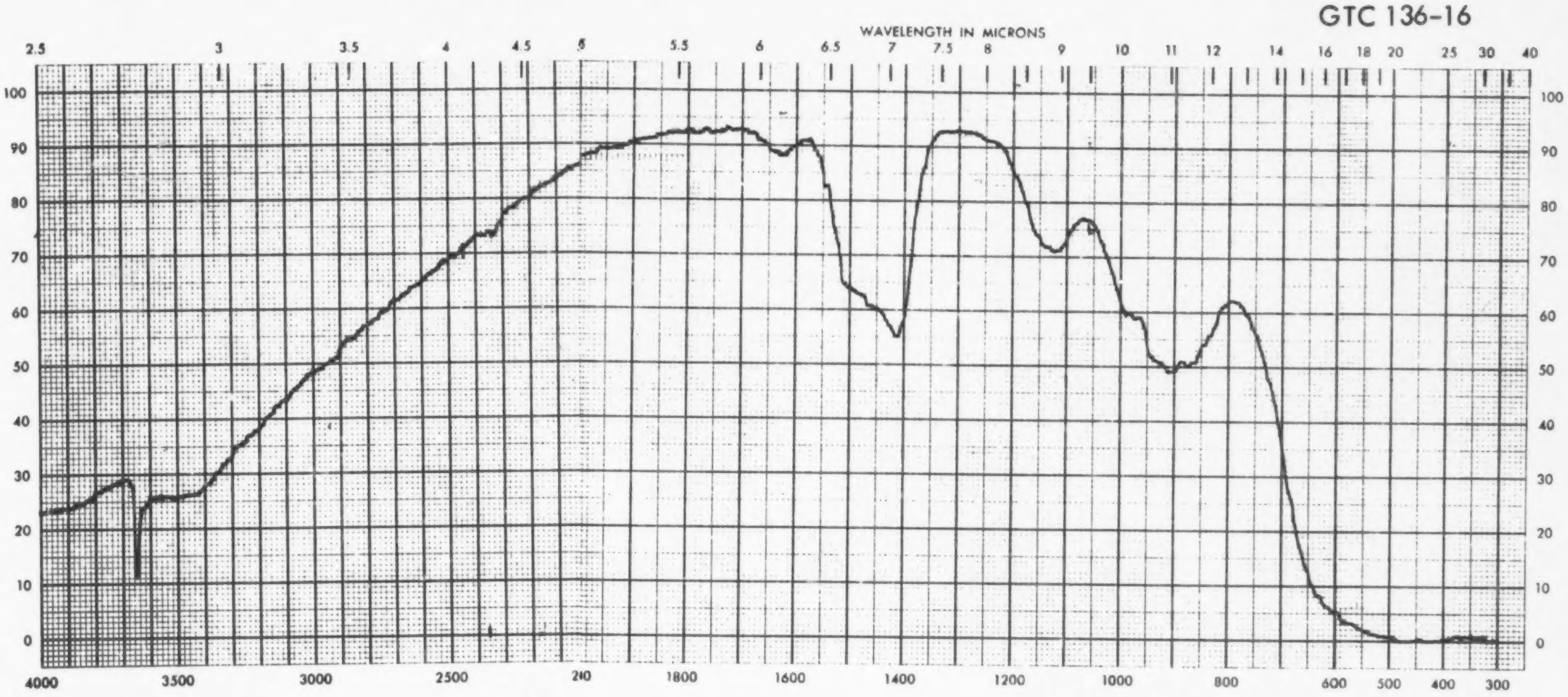

Figure 31. Infrared Spectrum of Sample No. BCR 1360-DB
(Unreacted Material)

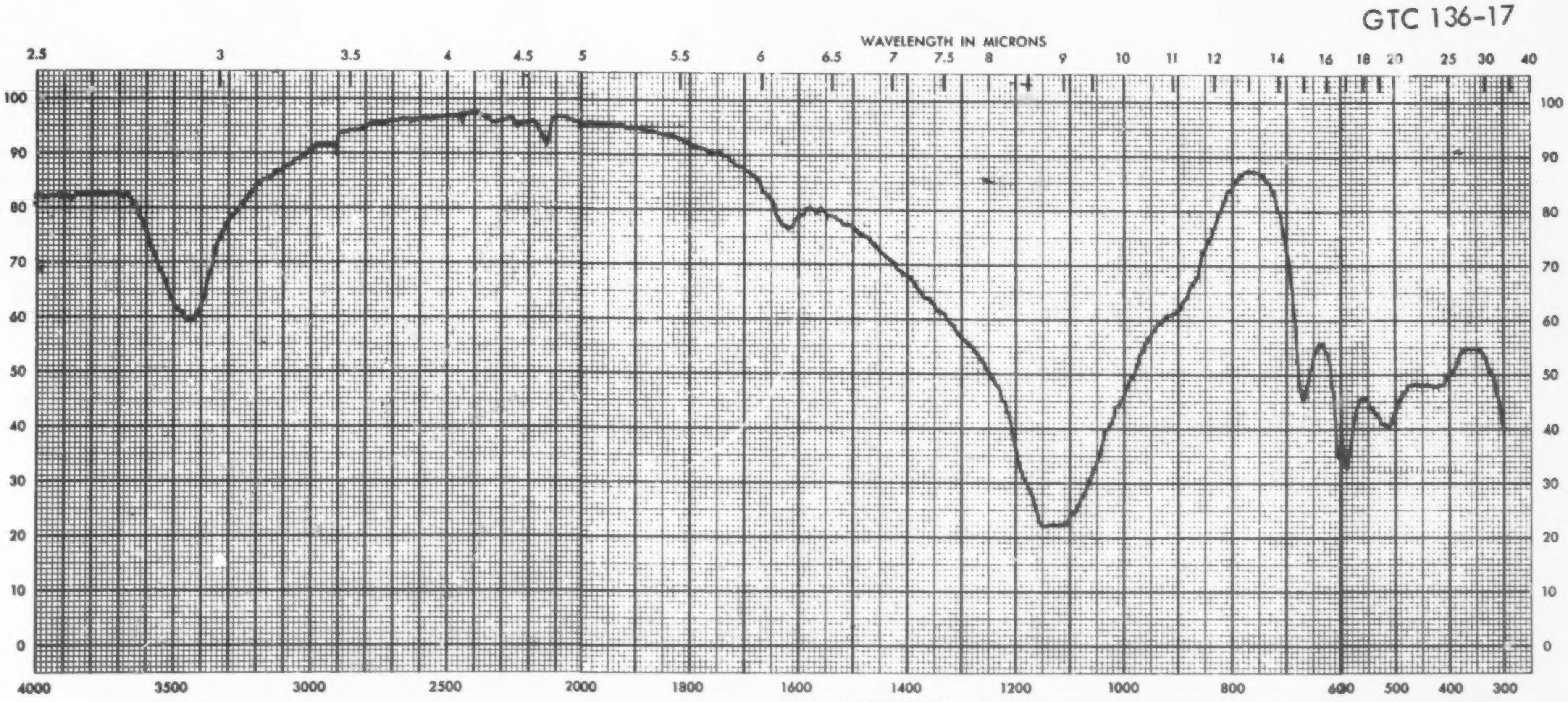

Figure 32. Infrared Spectrum of Sample No. BCR 1360-Run No. 31 DB (Reacted Material)

Table XIII Infrared Absorption Bands of Sample No. BCR 1343

Infrared Absorption Bands of Unreacted Sample (Calcined Material) (cm.$^{-1}$)	Infrared Absorption Bands of Reacted Sample (cm.$^{-1}$)	Assignment
3642 m*	1344 w	O-H stretching
1620 w		O-H bending
1450 1420 } mb		ν_3, $CO_3^=$
1145 sh		?
1113 m		?
	1154 } m	ν_3, $SO_4^=$
	1120	ν_3, $SO_4^=$
	1002 sh	silicates
	916 w	?
	652 w	$SO_4^=$
	610 vvw	$SO_4^=$
	586 vw	?

---

*m = medium, w = weak, vw= very weak, s = strong, vvw = very very weak, b = broad, sh = shoulder

Table XIV Infrared Absorption Bands of Sample No. BCR 1351

Infrared Absorption Bands of Unreacted Sample (Calcined Material) ($cm.^{-1}$)	Infrared Absorption Bands of Reacted Sample ($cm.^{-1}$)	Assignment
3644 m*	3650 w	O-H stretching
1632 w	1629 vw	O-H bending
1460 b	1438 m	ν_{3}, $CO_3^=$
1114 b		?
	1196 sh	ν_3, $SO_4^=$
	1150 1120 } s	ν_3, $SO_4^=$
999 m	1008 wsh	silicates
890 m		silicates ?
848 w		$CO_3^=$
	910 wb	?
	672 m	$SO_4^=$
	602 w	$SO_4^=$
	595 w	?
	522 wb	?

---

*m = medium, w = weak, vw = very weak, s = strong, vvw = very very weak, b = broad, sh = shoulder

Table XV Infrared Absorption Bands of Sample No. BCR 1352

Infrared Absorption Bands of Unreacted Sample (Calcined Material) ($cm.^{-1}$)	Infrared Absorption Bands of Reacted Sample ($cm.^{-1}$)	Assignment
	3656 s*	O-H stretching
1698 w		?
	1626 w	O-H bending
1440 m	1420 m	ν_3, $CO_3^=$
1082 sh		?
1009 m		silicates
910 w		?
892 w		$CO_3^=$
	1202 sh	?
	1152 } s	$SO_4^=$
	1118 } s	$SO_4^=$
	998 sh	silicates
	876 sh	$CO_3^=$
	672 sh	$SO_4^=$

---

*m = medium, w = weak, vw = very weak, s = strong, vvw = very very weak, b = broad, sh = shoulder

Table XVI Infrared Absorption Bands of Sample No. BCR 1360

Infrared Absorption Bands of Unreacted Sample (Calcined Material) (cm.$^{-1}$)	Infrared Absorption Bands of Reacted Sample (cm.$^{-1}$)	Assignment
3640 w*	3644 m	O-H stretching
1621 w	1624 w	O-H bending
1438 m	1422 s	ν_3, $CO_3^{=}$
1128 m		?
	1200 sh	ν_3, $SO_4^{=}$
	1150 } vs	ν_3, $SO_4^{=}$
	1121	ν_3, $SO_4^{=}$
916 b		?
876 w	876 sh	$CO_3^{=}$
	672 m	$SO_4^{=}$
	609 w	$SO_4^{=}$
	591 w	?

---

*m = medium, w = weak, vw = very weak, s = strong, vvw = very very weak, b = broad, sh = shoulder

Table XVII Infrared Absorption Bands of Sample No. BCR 1697

Infrared Absorption Bands of Unreacted Sample (Calcined Material) (cm.$^{-1}$)	Infrared Absorption Bands of Reacted Sample (cm.$^{-1}$)	Assignment
3644 vs*		O-H stretching
2924 vw		$CO_3^{=}$
2860 vw		$CO_3^{=}$
2360 vw		$CO_3^{=}$
1630 w	1620 w	O-H stretching
1460 1430 } s	1430	ν_3, $CO_3^{=}$
1116 wb		?
992 vw	1000 sh	silicates, ?
	1196 sh	ν_3, $SO_4^{=}$
	1140 1116 } s	ν_3, $SO_4^{=}$
866 m		$CO_3^{=}$
	672 m	$SO_4^{=}$
	610 m	$SO_4^{=}$
	598 w	?

---

*m = medium, w = weak, vw = very weak, s = strong, vvw = very very weak, b = broad, sh = shoulder

sulfur dioxide onto the limestone samples will be discussed in more detail in later portions of this report.

The infrared bands due to the O-H stretching vibrational mode in the region of 3644-3540 $cm.^{-1}$ and the O-H bending mode in the 1698-1620 $cm.^{-1}$ region of samples Nos. BCR 1697, 1360, 1352, 1351, and 1343 were attributed to the take up of atmospheric water by the anhydrous calcium oxide samples.

3. INFRARED SPECTRA OF THE REACTION OF FLUE GAS WITH VARIOUS LIMESTONE SAMPLES IN HIGH-TEMPERATURE INFRARED CELL

a. Infrared Spectra of the Reaction of Flue Gas with Limestone Sample No. BCR 1699-202

Limestone sample No. BCR 1699-202 was reacted with a simulated flue gas in the stainless steel infrared cell at two different flow rates, and at temperatures ranging from 201°C to 302°C. The experimental conditions for each of these experiments are given in Table XVIII. The amount of sulfur dioxide adsorbed as sulfate was calculated from the procedure described in Section II-5-b. This method for calculating the amount of sulfate formed in the reaction is very approximate and is only applicable to measuring the relative rates of sulfur dioxide take up from a simulated flue gas by various adsorbents. A more accurate method would be to calculate a molar extinction coefficient for chemisorbed sulfur dioxide and use the coefficient to measure the actual take up of sulfur dioxide. This molar extinction coefficient is calculated by measuring the actual concentration of chemisorbed sulfur dioxide molecules on the surface of the adsorbent using adsorption isotherms or chemical analysis and determining the change in absorbence produced by 1 cc of SO_2 gas. Then one could use equation 4 for calculating the molar extinction coefficient, k,

$$2.303 \log \frac{I_o}{I} = kc \qquad (4)$$

Table XVIII Summary of Experimental Results of the Exposure of Sample No. BCR 1699-202 to Flue Gas in the Stainless Steel Infrared Cell

Experiment Number	%H_2O	%N_2	%CO_2	%O_2	%SO_2	Reaction Temperature (°C.)	Total Flow Rate (cc./min.)	Relative* Amount of SO_2 Adsorbed (moles/cm.^{2})	Reaction Time (min.)
36a	4.9	79.4	12.0	3.4	0.2	264	612.1	$.16 \times 10^6$	17
36b	4.7	79.3	12.3	3.5	0.2	261	620	.30	33
36c	4.2	79.9	12.0	3.7	0.18	262	596.1	.18	57.5
31	5.7	78.9	11.9	3.5	0.2	262	631.3	.75	168
41	5.7	78.3	12.3	3.5	0.17	201	631.1	.17	193
42	5.9	78.6	11.9	3.3	0.18	302	628.1	.51	66
43	5.7	78.6	12.0	3.5	0.2	302	627.3		120
49a	5.5	79.4	11.9	3.0	0.2	262	1281.5	.47	61
49b	5.1	79.5	12.1	3.0	0.2	261	1263.5	.69	76
49c	5.4	79.4	12.0	3.0	0.2	262	1268.6	1.02	138
49d	5.7	79.2	11.8	3.0	0.2	262	1252.5	.96	168
52	6.2	79.0	11.6	2.9	0.2	260	1314.6	.29	23
53a	5.5	79.1	12.0	3.2	0.2	262	633.2	.14	60
53b	5.4	79.3	12.2	2.9	0.2	262	630.2	.36	90
54	5.6	79.4	11.9	2.9	0.2	263	1282.5	.26	62

---

*Measurement of the integrated intensity of the $SO_4^=$ infrared absorption band. The integrated intensity of the sulfate band in $BaSO_4$ was used in this calculation. This value is 28×10^6 moles^{-1} cm.$^{+1}$.

where c is the number of sulfur dioxide molecules in the volume of the sample which is traversed per square centimeter of the infrared band. The value, c, is determined by dividing the total number of molecules chemisorbed by the area of the plated sample. The molar extinction coefficient of sulfur dioxide chemisorbed would be in terms of cm^2/molecule.

The amount of sulfur dioxide chemisorbed per gram of solid adsorbent is determined by dividing the number of moles of chemisorbed sulfur dioxide per cm^2 by the number of mg of plated sample per cm^2 of Irtran 4 window surface. Hence, we have

$$\frac{\text{moles of chemisorbed } SO_2}{cm^2} \div \frac{\text{mg of limestone adsorbent}}{cm^2} = \frac{\text{moles of chemisorbed } SO_2}{\text{mg of limestone adsorbent}}$$

$$\frac{\text{moles of chemisorbed } SO_2}{\text{mg of limestone adsorbent}} \times \frac{1000 \text{ mg}}{g} = \frac{\text{moles of chemisorbed } SO_2}{\text{g of limestone adsorbent}}$$

Figure 33 shows the infrared spectra of limestone Sample No. BCR 1699-202 before and after reaction with sulfur dioxide in a simulated flue gas at 262°C (see Experiment Numbers 36a through 36b in Table XVIII for run conditions). The experimental procedure is given in Section II-1-b. The infrared spectrum of the sample before reaction with sulfur dioxide exhibited infrared bands due to the carbonate ion at 1371 cm.$^{-1}$ and at 857 cm.$^{-1}$. After the sample had been exposed to the flue gas for 2.6 hours at 262°C and the reaction cell had cooled to room temperature, infrared bands appeared at 2320, 1396, 1078, 928, 860, and 638 cm.$^{-1}$. The 2320 cm.$^{-1}$ absorption band was assigned to gas-phase carbon dioxide. The broad infrared band at 1396 cm.$^{-1}$ and the band at 860 cm.$^{-1}$ were assigned to the carbonate ion. The absorption bands at 1078 cm.$^{-1}$ and 638 cm.$^{-1}$ were assigned to the sulfate ion. The absorption band at 928 cm.$^{-1}$ was assigned to $SO_3^=$. A comparison of the relative intensities of the carbonate at 1396 cm.$^{-1}$ and the sulfate

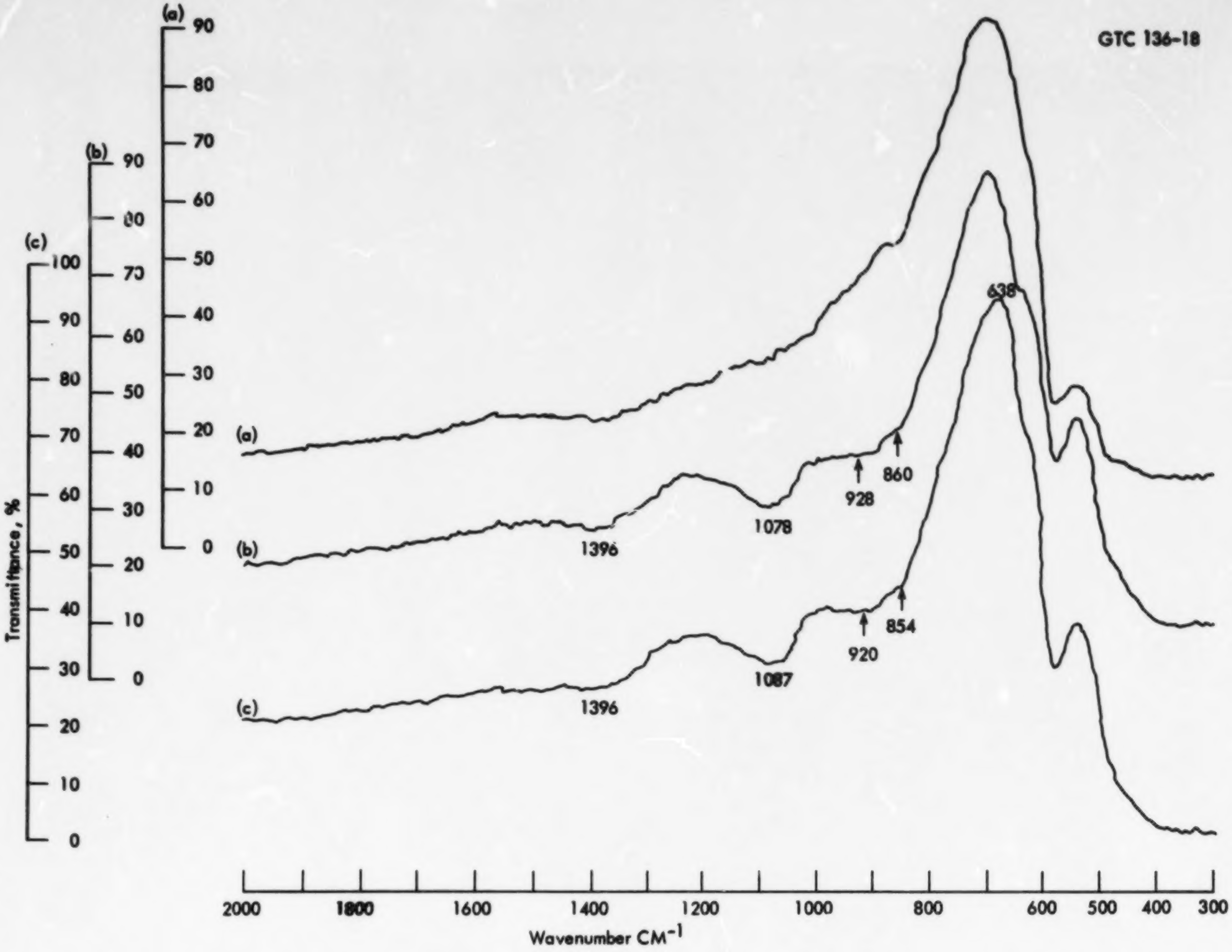

Figure 33. Infrared Spectra of Sample No. BCR 1699-202 Before and After Reaction with Sulfur Dioxide in a Flue Gas at 262°C.

(a) Sample Heated to 106°C. and Evacuated to 24 μ
(b) After Reaction with Sulfur Dioxide at 262°C. for 2.6 Hours and Cooling to Room Temperature
(c) After Evacuation of the Cell to 42 μ. Total Evacuation Time 1.5 Hours

band at 1078 cm.$^{-1}$ indicated that under these particular conditions sulfur dioxide is adsorbed more readily than carbon dioxide. The 1078 cm.$^{-1}$ band of the sulfate ion had an intensity of 0.092 absorbance units and that of the carbonate ion was 0.088 absorbance units.

The evacuation of the cell to 42μ did not reduce the intensities of the infrared bands at 1396, 1078, 928 and 860 cm.$^{-1}$. The 638 cm.$^{-1}$ band appeared as a shoulder after the evacuation of the infrared cell. These results were further evidence for chemical adsorption. The infrared absorption band at 2320 cm.$^{-1}$ disappeared when the cell was evacuated confirming the assignment of this band to gas-phase carbon dioxide.

In establishing the assignments of the infrared absorption bands of limestone Sample No. BCR 1699-202 exposed to sulfur dioxide at 262°C, the spectra from this study were compared with the infrared spectrum of limestone Sample No. BCR 1699-202 reacted with 2800 ppm of sulfur dioxide at 750°F. at the National Air Pollution Control Administration. This sample had been plated from an acetone suspension onto Irtran 4 windows of the stainless steel infrared cell. The spectrum of Sample No. BCR 1699-202 (reacted material) is shown in Figure 34. Infrared bands due to the carbonate ion appear at 1769, 1392, 856 cm.$^{-1}$, and the very weak intensity infrared band at 708 cm.$^{-1}$. Infrared absorption bands at 1090 cm.$^{-1}$ and 672 cm.$^{-1}$ were assigned to the sulfate ion. The shoulder at 950 cm.$^{-1}$ was assigned to SO_3. The results of this spectrum agree very well with those found in Figure 33.

However, one difference is indicated in the spectra of the samples reacted at 262°C. and the sample reacted at 399°C (750°F.). In the spectrum of limestone Sample No. BCR 1699-202 reacted at 750°F., the relative intensity of infrared band due to the carbonate ion at 1392 cm.$^{-1}$ is greater than the intensity of the sulfate ion at 1090 cm.$^{-1}$.

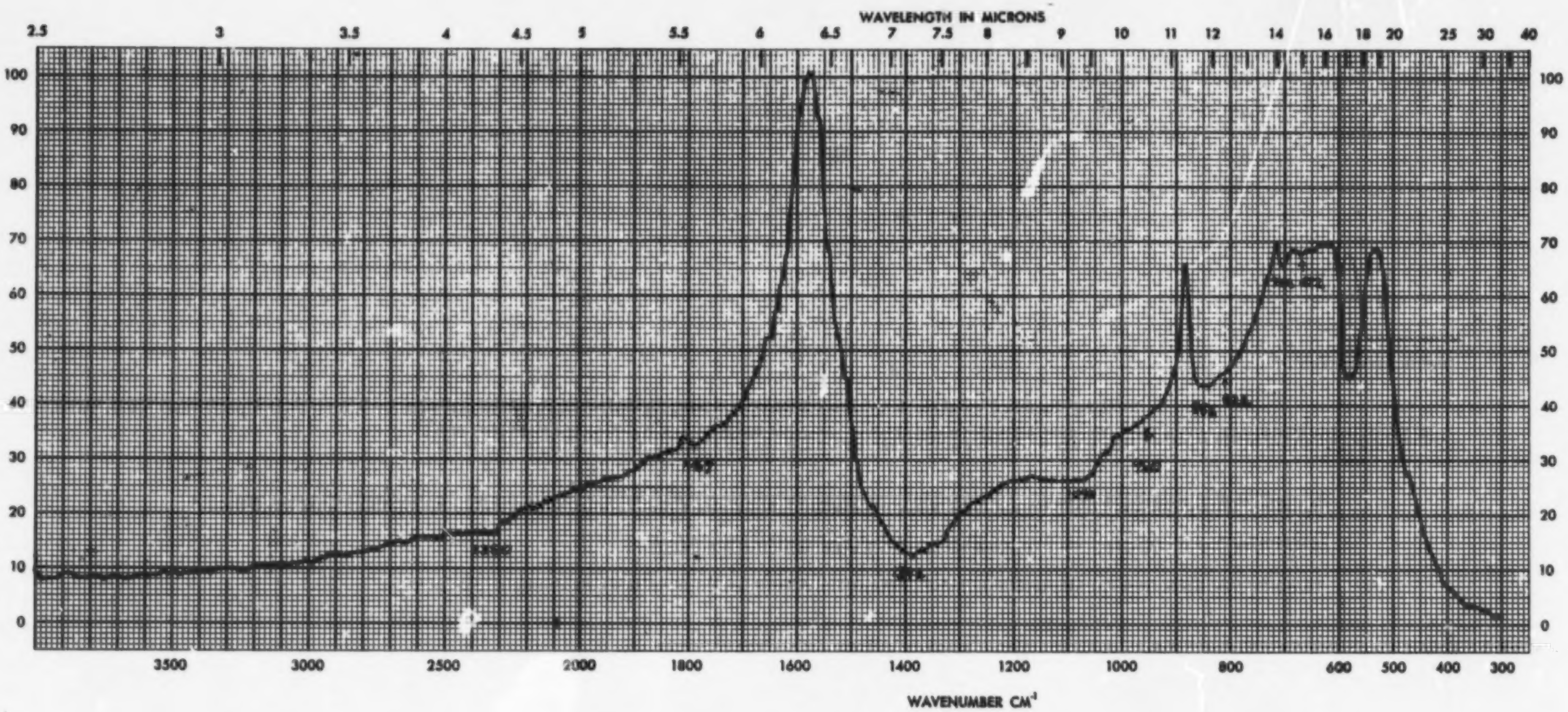

Figure 34. Infrared Spectrum of Sample No. BCR 1699-202 Exposed to 2800 ppm of SO_2 at 750°F. Sample Plated on Irtran 4 Windows of Infrared Cell

As a result, under these conditions carbon dioxide is adsorbed more readily than sulfur dioxide, which is in reverse of the effect observed at 262°C.

An additional check of the infrared bands in the reaction of Sample No. BCR 1699-202 with SO_2 at 262°C. was made by measuring the spectrum of the sample after exposure to a SO_2-N_2-H_2O mixture. The mixture had the following composition: 91.4% N_2, 0.2% SO_2, and 8.4% H_2O*. The total flow rate was 651.2 cc/min. The results of this experiment are shown by the spectra in Figure 35. After the deposit had been exposed to the flue gas mixture for approximately 14 minutes at 261°C. and then allowed to cool to room temperature, infrared bands were observed at 1098 and 856 $cm.^{-1}$. The reaction was interrupted and the deposit was exposed to more of the sulfur dioxide mixture for 3.5 hours at 261°C. The cell was allowed to cool to room temperature and infrared bands were observed at 1080, 862 and 638 $cm.^{-1}$. The infrared bands at 1080 $cm.^{-1}$ and 638 $cm.^{-1}$ were assigned to the sulfate ion. The 862 $cm.^{-1}$ absorption band was assigned to multilayer adsorption of sulfur dioxide since carbon dioxide was not present in the experiment. The absence of carbon dioxide in the experiment was substantiated by the absence of infrared bands due to gas-phase carbon dioxide. Also, there did not appear to be any increase in intensity of the carbonate band at 1380 $cm.^{-1}$.

The infrared spectra of Sample No. BCR 1699-202 before and after exposure to flue gas for 1.1 hours at 301°C. are shown in Figure 36. The infrared absorption band at 1070 $cm.^{-1}$ was assigned to $SO_4^{=}$, and the band at 935 $cm.^{-1}$ was assigned to $SO_3^{=}$. The amount of sulfate found on the surfaces at these temperatures was $.51 \times 10^{-6}$ moles/$cm.^2$.

An example of the effect of infrared emissions for the cell on the observation of the infrared spectrum of adsorbed species is illustrated by the spectrum in Figure 37.

---

*Calculated from ideal gas law.

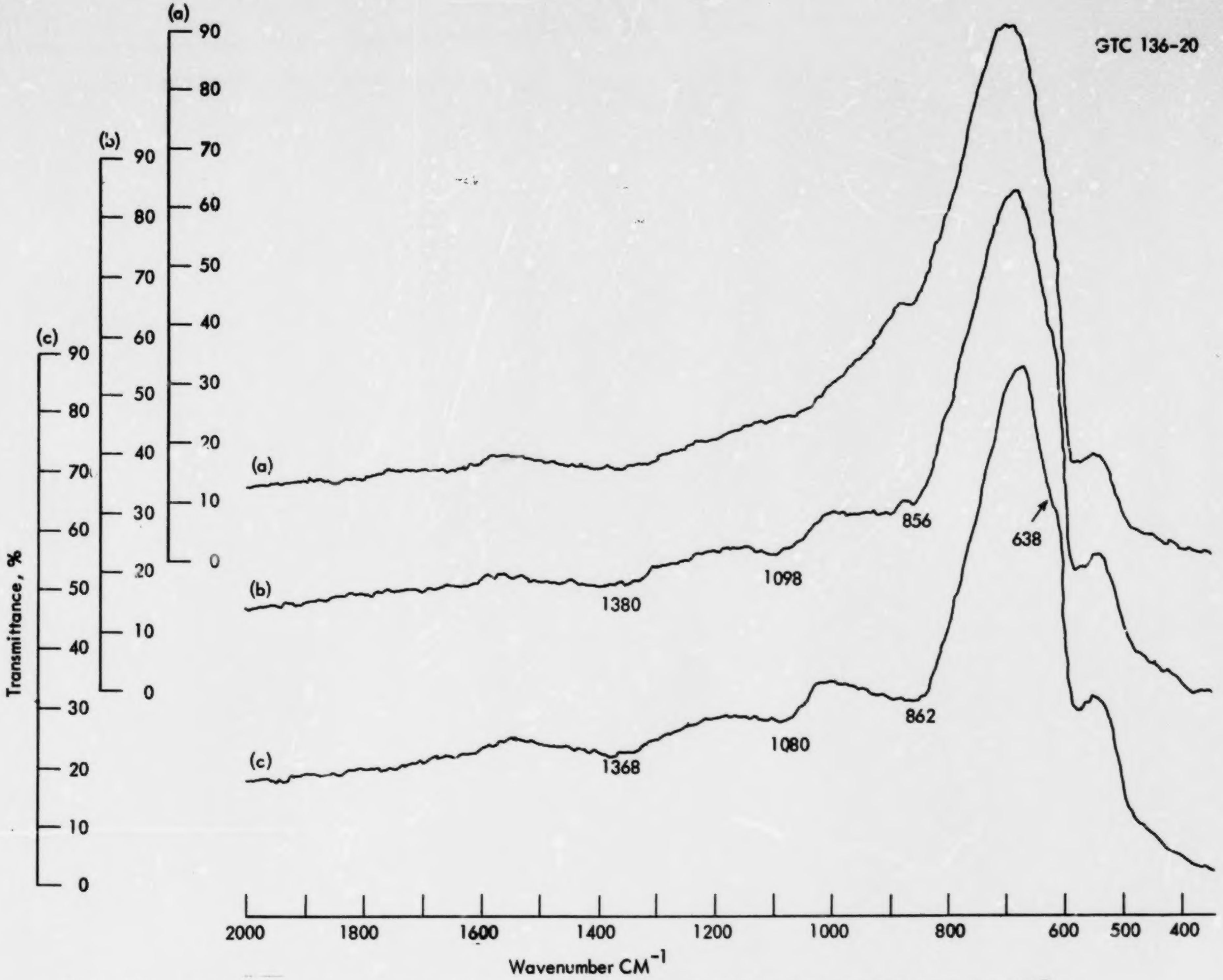

Figure 35. Infrared Spectra of Limestone Sample No. BCR 1699-202 Reacted With a SO_2-N_2-H_2O Mixture at 261°C.

(a) Limestone Deposit Before Reaction with SO_2. Cell Evacuated to 24 μ
(b) After Reaction with SO_2 for Approximately 14 Minutes at 261°C. and Cooling to Room Temperature
(c) After Reaction with SO_2 for an Additional Time of 2.5 Hours at 261°C and Cooling to Room Temperature

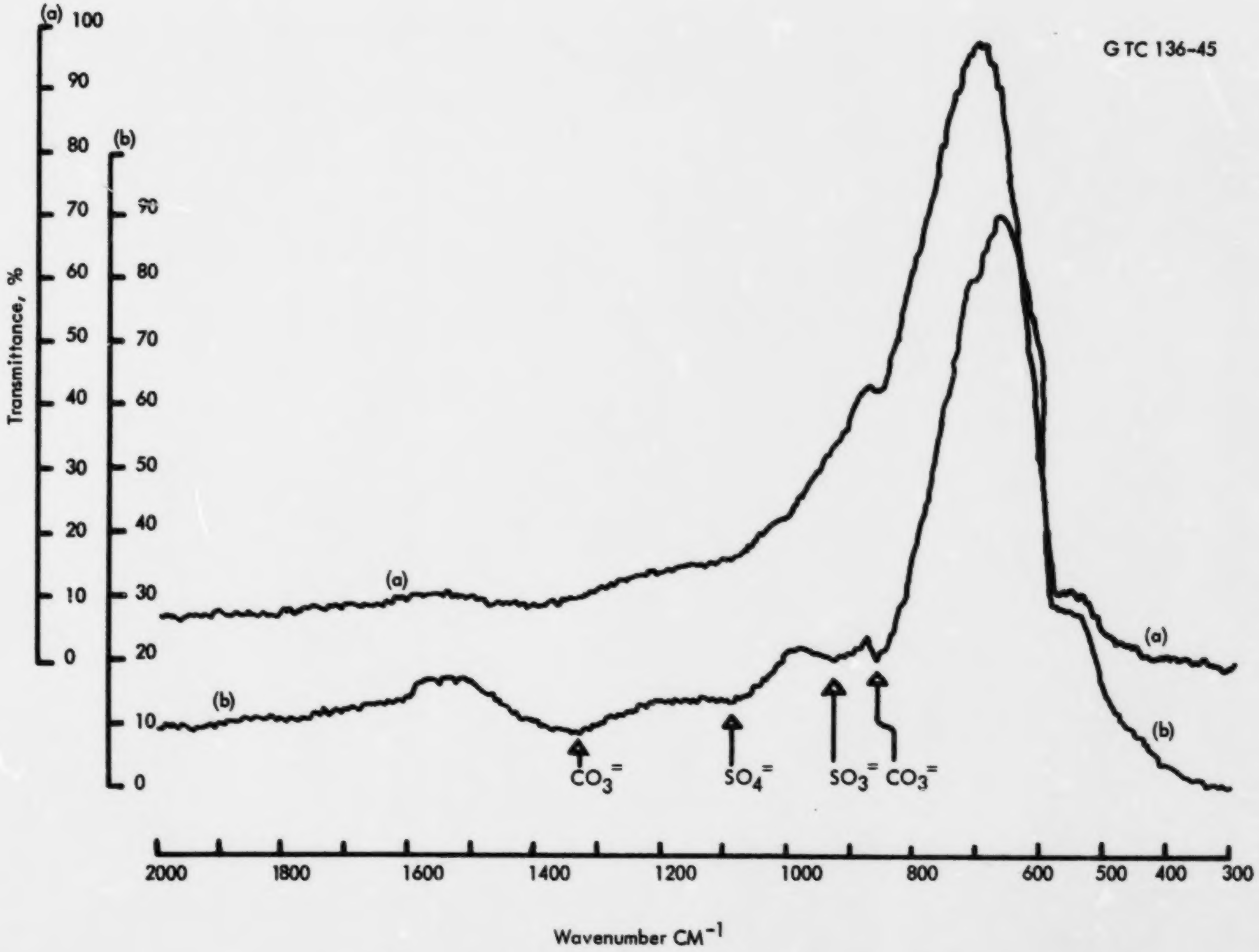

Figure 36. Infrared Spectrum of Limestone Sample No. BCR 1699-202

(a) Before Reaction with Synthetic Flue Gas.
(b) After Reaction with Synthetic Flue Gas for 1.1 Hours at 301°C.

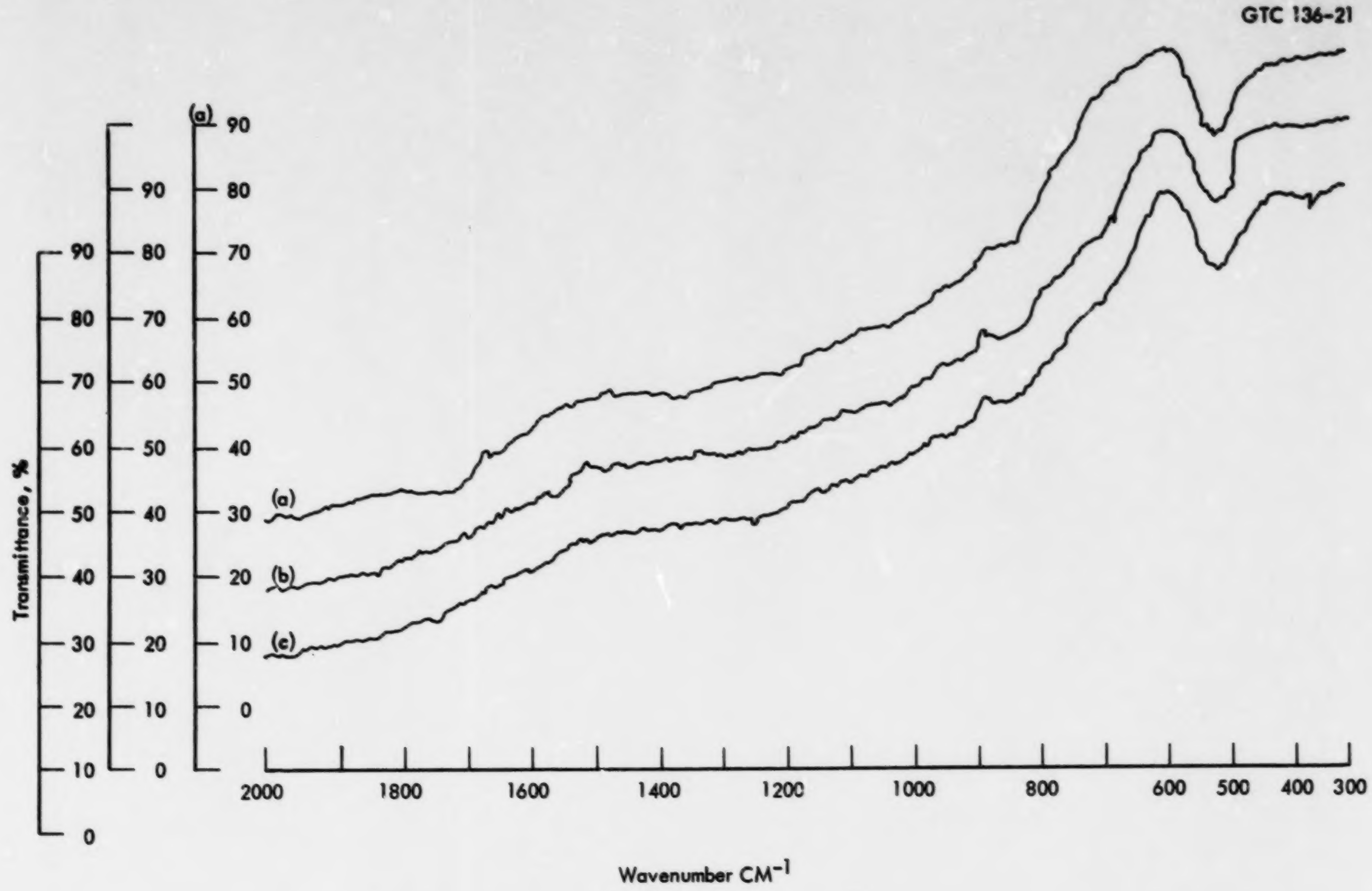

Figure 37. Infrared Spectra of Limestone Sample No. BCR 1699-202 During Exposure to Flue Gas

(a) Background Spectrum of Deposit Heated to 266°C.
(b) After Exposure to Flue Gas for 0.6 Hours at 262°C.
(c) After Exposure to Flue Gas for 1.2 Hours at 262°C.

In this reaction, Sample No. BCR 1699-202 was exposed to a very low flow of flue gas. The gas composition was:

20.0 cc./min.	of N_2 through the humidifier
97.0 cc./min.	of N_2
56.0 cc./min.	of CO_2
10.0 cc./min.	of O_2
.8 cc./min.	of H_2O
183.8 cc./min.	total flow

The SO_2 flue gas was too low to measure under these conditions. The low flow was used to prevent flushing the sample from the Irtran 4 windows. However, as indicated in the experiments discussed previously, this low flow was not necessary since the deposit was not disturbed by the higher flow rates. In the spectra of Figure 37, the growth of a weak band is detected at 850 cm.$^{-1}$. Infrared bands at 1700 cm.$^{-1}$ and 1633 cm.$^{-1}$ were attributed to gas-phase species caused by degassing within the cell since the cell was not pressurized with dry nitrogen prior to heating. The emission from the cell is also indicated from the change in the baseline spectra of the deposit. This is noted when these spectra are compared with the room temperature spectra of the deposit in Figures 34, 35, and 36. During the spectral studies at these temperatures, the baseline is adjusted with the beam attenuator in the reference beam of the spectrophotometer.

An attempt will be made in future studies to make the method more sensitive to the direct observation of the adsorption of sulfur dioxide using a dual cell assembly. In this case, an infrared cell heated to the same temperatures as the reaction cell containing the solid adsorbent will be placed in the reference beam of the infrared spectrophotometer and an external recorder equipped with a scale expanded is used to detect the adsorbed species.

b. Mechanism of the Adsorption of Sulfur Dioxide from a Flue Gas by Limestone Adsorbents

Based on the data obtained from the infrared spectral studies of the adsorption of sulfur dioxide onto limestone samples, the mechanism of the gas-solid interactions is given by equations 5 through 7. For the hydrated limestone samples exposed to flue gas in the temperature range of 200 - 400°C., we have

$$Ca(OH)_2 + SO_2 \longrightarrow CaSO_3 + H_2O \qquad (5)$$

$$CaSO_3 + 1/2\ O_2 \longrightarrow CaSO_4 \qquad (6)$$

In other words, sulfur dioxide is adsorbed as sulfite and the sulfite is oxidized to sulfate. For limestone samples exposed at 1800°F., we have

$$CaO + SO_2 + 1/2\ O_2 \longrightarrow CaSO_4 \qquad (7)$$

In this case, the oxidation step is very fast at these temperatures and only sulfate is detected.

c. Analysis of Infrared Spectroscopic Data Obtained from the Exposure of Slaked Limestone Sample No. BCR 1699-202 to Flue Gas at 201-302°C.

The sulfur dioxide adsorption data in Table XVIII has been subjected to statistical analysis with regard to the variables of time (adsorption rate), total gas flow rate, temperature, and gas phase composition in order to extract significant effects. The results of the extensive calculations and evaluations are summarized below.

Experiments Nos. 31, 36c, 41, and 42 constitute a set having varied temperature but essentially constant flow rate and composition of gas phase. Therefore, they have been examined for the effect of temperature on adsorption per unit time (adsorption rate). The slight variations in gas phase composition in runs 31 and 36c as compared to 41 and 42 are probably not significant and in any event they are at the intermediate temperature and so have very little effect on the calculation of slope (activation energy). Figure 38

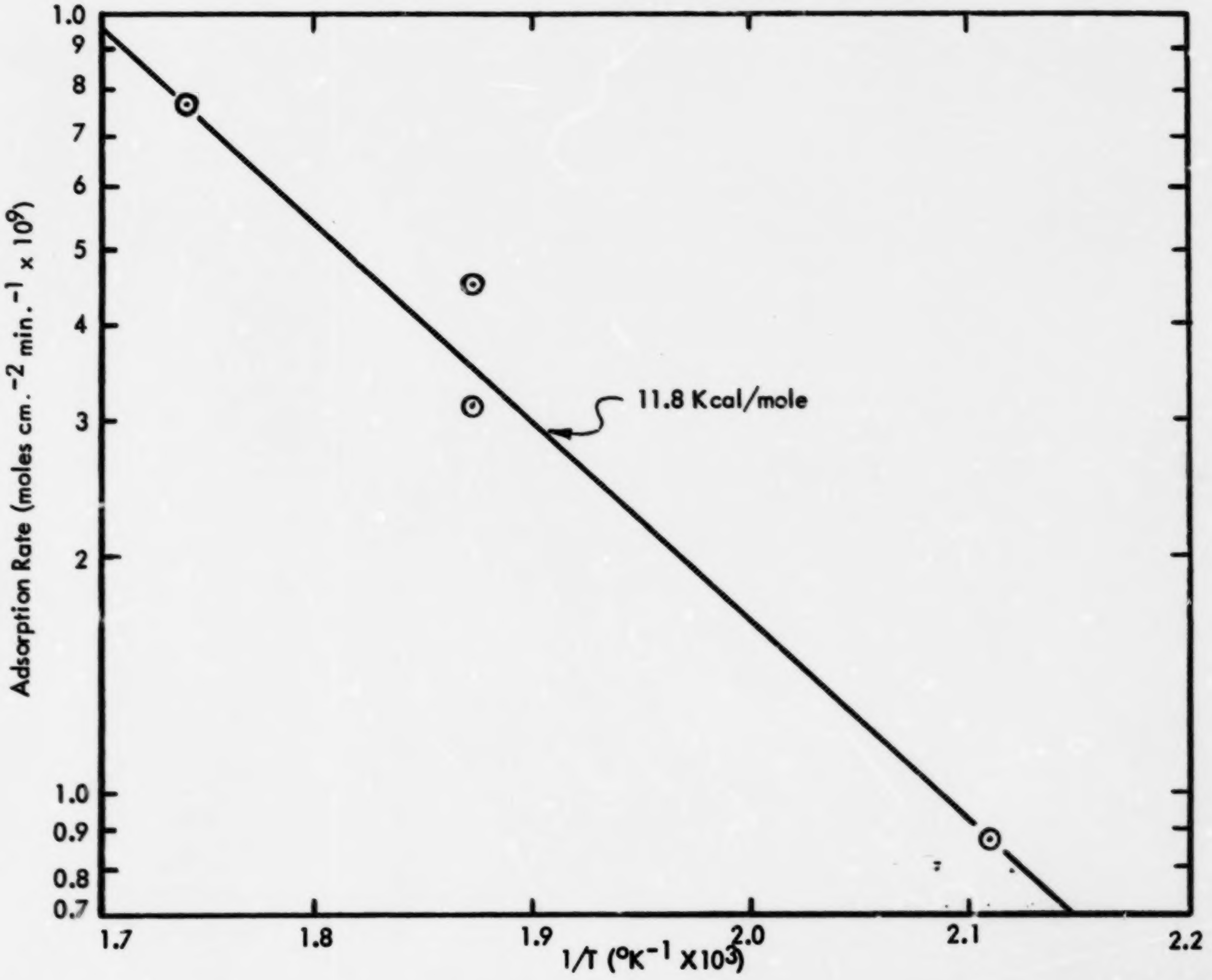

Figure 38. Effect of Temperature on Adsorption Rate

shows these data points plotted in an Arrhenius correlation with a least square line drawn in. An activation energy of 11.8 kcal/mole was calculated from the slope.

The primary concern of this data analysis was to establish the degree of effect that total gas flow rate has upon adsorption rate in order to determine whether or not diffusion through a gas-phase film determines the rate of adsorption in these experiments. Therefore, the rate-temperature data were examined with respect to the presumption that these experiments were diffusion mass-transport-controlled, and the statistical probability of such being the case was calculated.

In order to predict the expected temperature dependency of adsorption rate, assuming diffusion in the gas phase controls rate, the Reynold's "Analogy" equations (see Appendix for derivation of equation) were analyzed for the temperature effect on the constituent parameters:

$$J_D = 0.66\, Re_x^{-1/2} = kg\, P_{BM} \left\{\frac{\mu}{\rho\, D_v}\right\}^{2/3} \qquad (8)$$

$$k_g = 0.66\, Re_x^{-1/2} \left\{\frac{G_M}{P_{BM}}\right\} \left\{\frac{\mu}{\rho\, D_v}\right\}^{-2/3} \qquad (9)$$

$$k_g \sim \frac{X v \rho}{\mu}^{-1/2} \left\{\frac{G_M}{P_{BM}}\right\} \left\{\frac{\mu}{\rho\, D_v}\right\}^{-2/3} \qquad (10)$$

where Re_x = length Reynold's number

k_g = gas-film coefficient, lb. moles/(hr.)(ft.^{2})(atm.)

P_{BM} = logarithmic mean of P_B at phase boundary and P_B in bulk of fluid

P_B = partial pressure of nondiffusing gas B, atm.

G_M = molar gas velocity of stream, lb. mole/(hr.)(ft.^{2})

μ = viscosity, lb./(hr.)(ft.)

ρ = density, lb./ft.^{3}

D_v = molecular diffusivity in gas, ft.^{2}/hr.

Of these parameters, X, G_M, and P_{BM}, being geometrical, are independent of temperature, partial pressure or mass velocity terms. The flow velocity, v, varies with temperature to the first power, based on the gas law. Gas viscosity, μ, is proportional to the 0.5 power of temperature according to kinetic theory. Air viscosity is proportional to temperature to the 0.6 power, in this range. Gas density, as predicted by the gas law, is proportional to T^{-1}. D_v, the molecular diffusivity, is best predicted as a function of T^2 according to Sherwood and Pigford$^{(22)}$. Therefore, we find that:

$$k_g \sim \left\{\frac{T \cdot T^{-1}}{T^{0.6}}\right\}^{-1/2} \left\{\frac{T^{0.6}}{T^{-1}T^{-2}}\right\}^{-2/3} \qquad (11)$$

which reduces to k_g is proportional to $T^{0.57}$. Figure 39 gives the measured data of rate versus temperature together with the predicted diffusion-controlled curve where rate has the above temperature variation. The actual results are so much more temperature sensitive that we must conclude that diffusion is not controlling, but rather chemical reaction rate, which is very highly temperature sensitive. Application of statistical methods to this power-law correlation of the rate-temperature data yields a standard deviation of 1.7 on the empirical power function of 11.1. This value of 11.1 differs from the theoretically predicted diffusion-controlled power of 0.57 by an extent that there is 98% probability that the data do not follow the diffusion-controlling mechanism prediction. We consider this to be very strong evidence of the experiment not being diffusion-controlled in rate. It is very evident that an eddy mass-transfer mechanism of a very effective sort operates in the absorption cell.

Additional evidence indicating that diffusion is not rate controlling is found in the good agreement of data on the activation energies for the sorption of sulfur dioxide

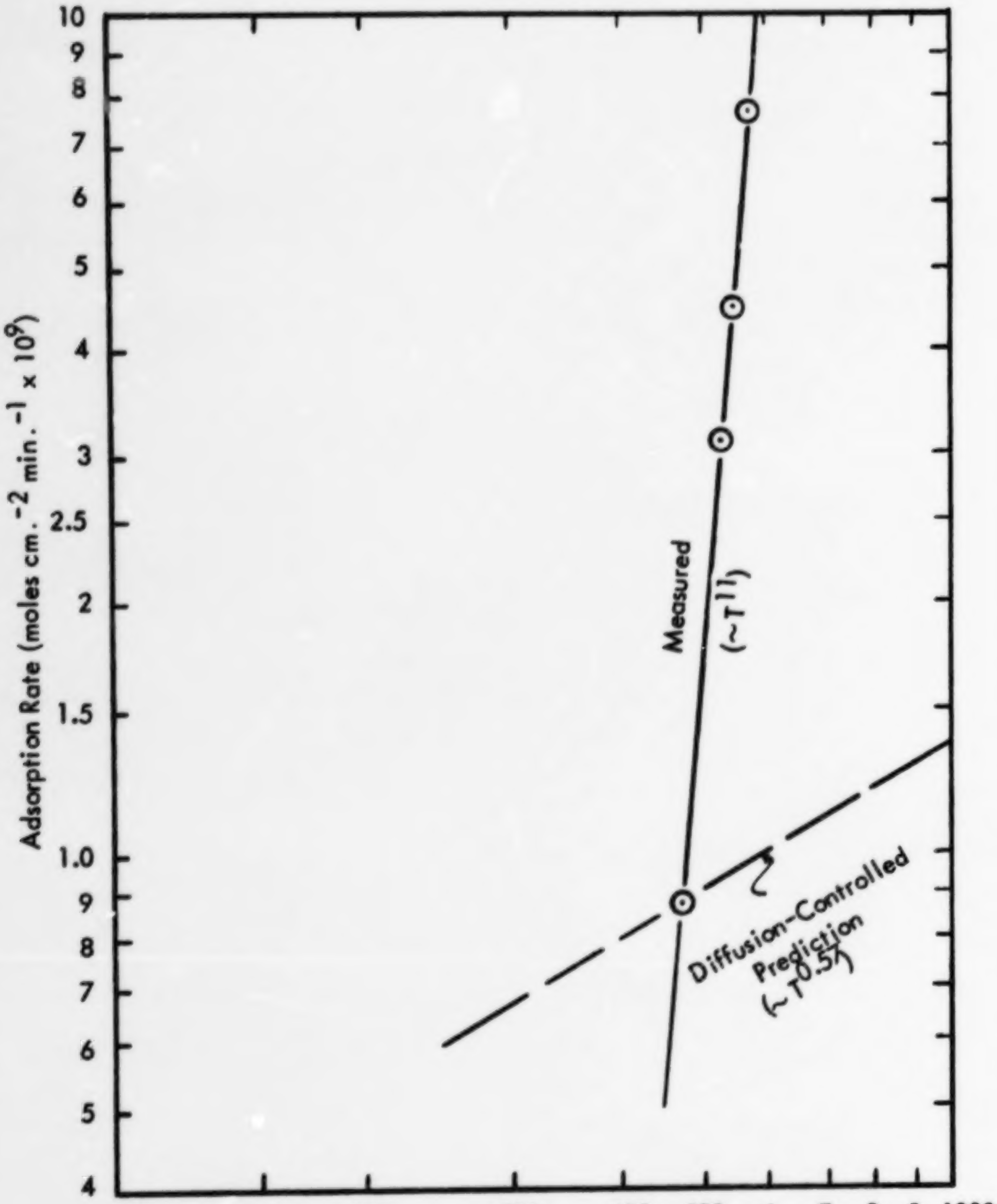

Figure 39. Comparison of Temperature Dependency of Adsorption Rate with Predicted Diffusion Dependency

on limestones in the present work and that conducted by Borgwardt(14) at the National Air Pollution Control Administration using fixed-bed reactors. Borgwardt calculated an activation energy of 14.2 kcal/mole for the sorption of sulfur dioxide onto limestone Sample No. BCR 1699-202 (see Table III), and his values for the several limestones studied range from 8.1 to 18.1 Kcal/mole. The value of 11.8 Kcal/mole in the infrared studies falls well within this range and is quite similar to the 14.2 Kcal/mole value for limestone No. BCR 1343. Hence, the sorption processes occurring in the infrared system are directly relatable to those being conducted in the fixed-bed reactor studies at the National Air Pollution Control Administration in which diffusion through a gas film did not determine the rate measurements.

d. Analysis of Data Obtained at 262°C with Limestone Sample No. BCR 1699-202

The larger volume of data taken at 260° - 264°C. with the Sample No. BCR 1699-202 limestone were also analyzed statistically to determine any effect of the flow rate of flue gas on adsorption rate, the presumption being that if diffusion mass-transfer is not rate-controlling, then the data should be flow-rate insensitive. The first step in this analysis was to normalize the adsorption data to a temperature of 262°C. to eliminate the effect of this variable. The activation energy curve slope of Figure 38 was used to accomplish this. The second step was to normalize with respect to gas phase SO_2 concentration. Three of the runs differed slightly from the normal 0.20% SO_2. Since the gas phase concentration is the driving force for the adsorption, whether controlled by reaction rate or diffusion, the normalization was simple ratioing by the concentration of SO_2. Thus, the lower the SO_2 concentration, the lower the expected adsorption rate. The maximum correction of amount adsorbed due to this effect was 17.7%, for run No. 41.

At this point the remaining varying gas phase parameters believed to be of any significance were % H_2O, % O_2 and % CO_2. Figures 40, 41, and 42 show the corrected adsorptions expressed as adsorption rates (divided by exposure times) plotted versus the gas phase concentration parameters. No correlation was found, except for % H_2O, and the least squares line (X and Y variable) is drawn in which indicates a negative effect of H_2O concentration on adsorption rate at this range. The correlation has a very low statistical significance, $R = 0.28$. However, this does indicate that some of the variability in the adsorption data is due to variation in % H_2O, about 8% of it.

Because of the potential effect of variability in adsorption, the runs 36a, b, and c were eliminated from the correlations for the purpose of determining the flow rate effect because they were markedly lower in % H_2O than the rest (less than 5%). This sample restriction still left five data points at the low total flow and six at the high, sufficient for valid correlation. Least squares analysis of these remaining points, assuming linear correlation of adsorption with time, yielded the curves shown in Figure 43. The adsorption rates calculated from these were:

Flow Rate (cc./min.)	Adsorption Rate (moles $cm.^{-2}$ $min^{-1} \times 10^9$)
627-633	5.5
1253-1315	5.3

The correlation coefficients on these lines are 0.99 and 0.91, both very significant (99% level of confidence).

The correlation lines for the two different levels of flow rate have different intercepts. The physical significance of this may be the difference in cell start-up effects at the two flow rate levels. Thus the initial volume of the cell must be effectively swept

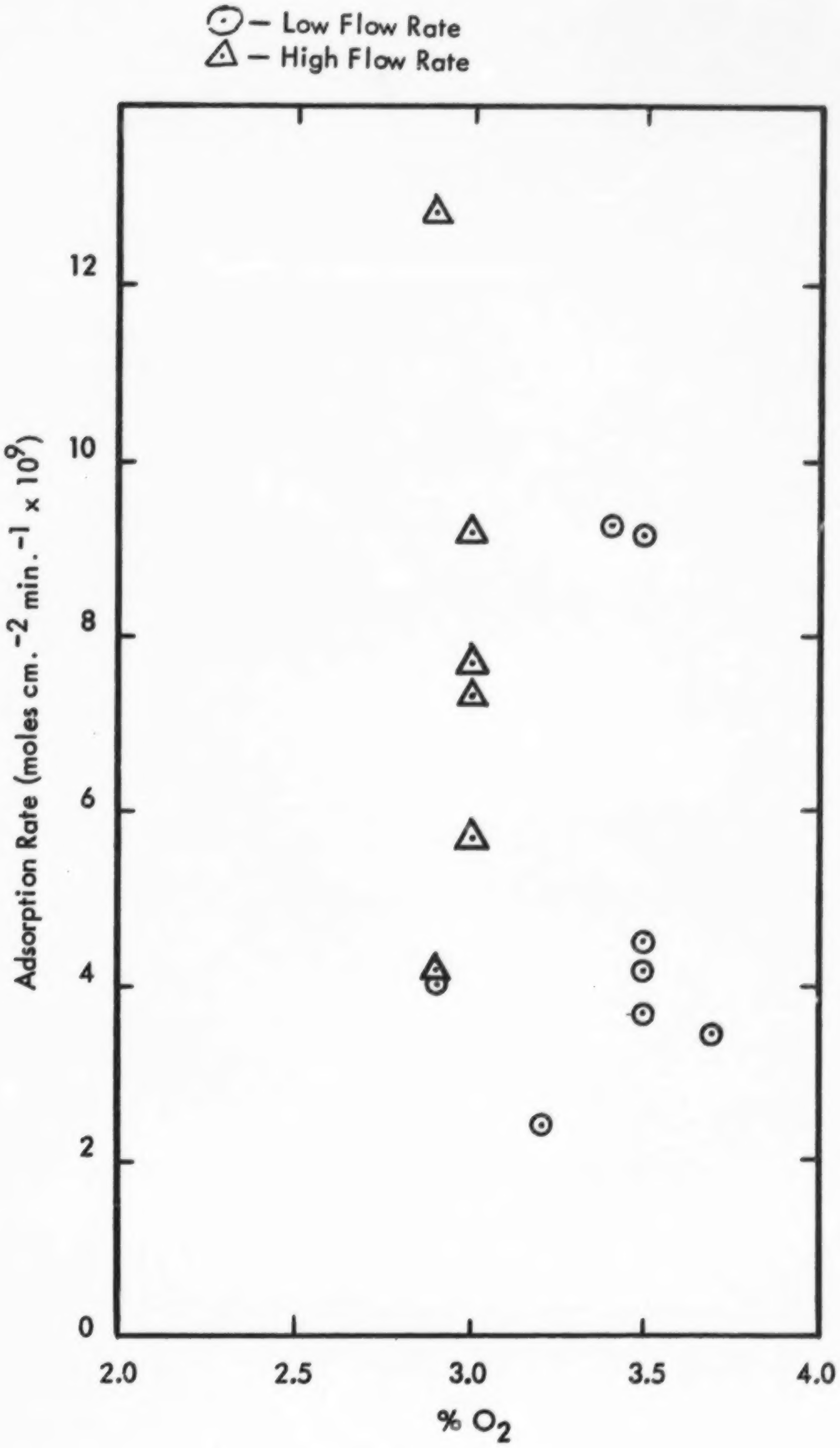

Figure 40. Effect of O_2 Concentration

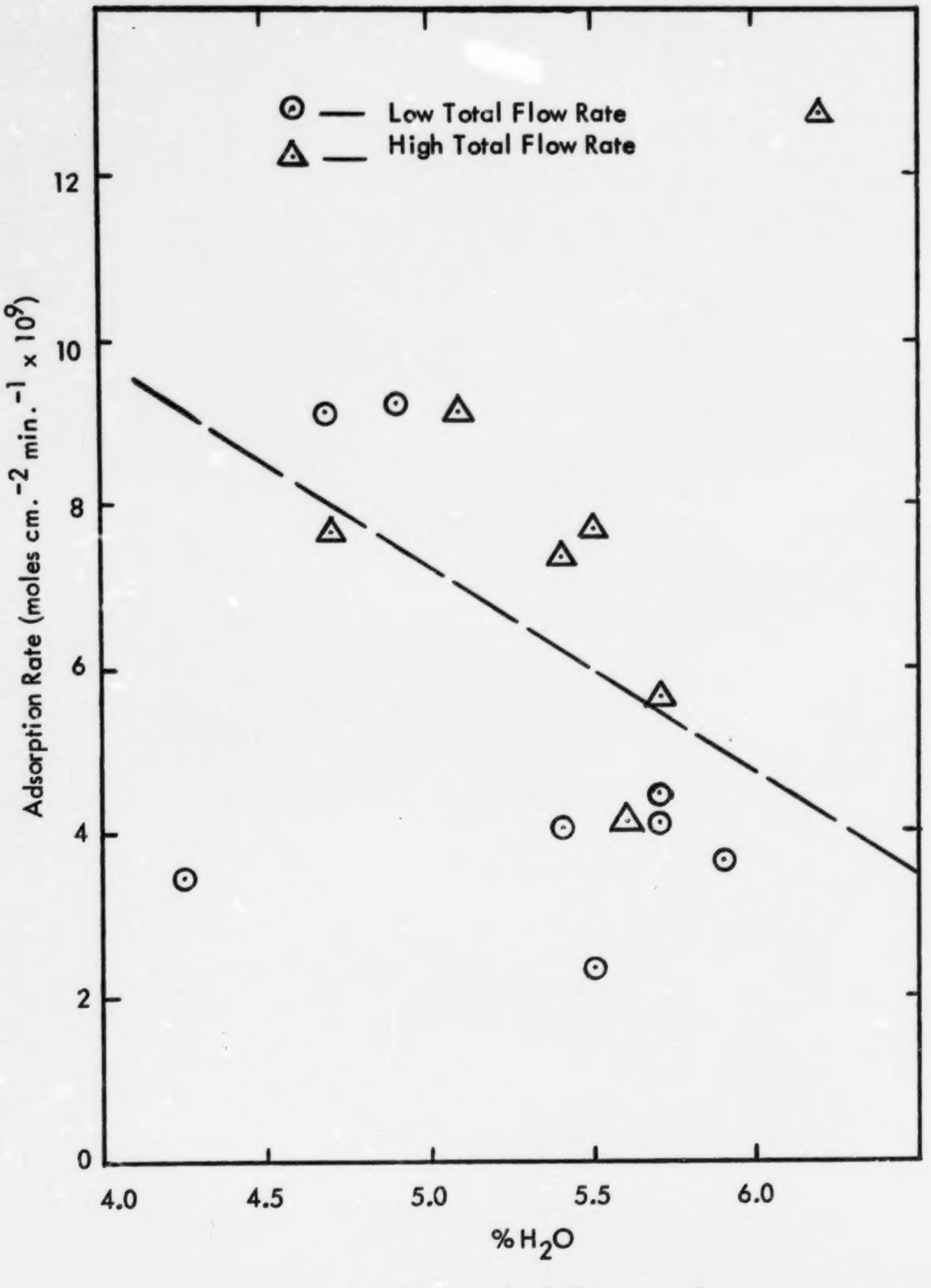

Figure 41. Effect of H_2O Concentration

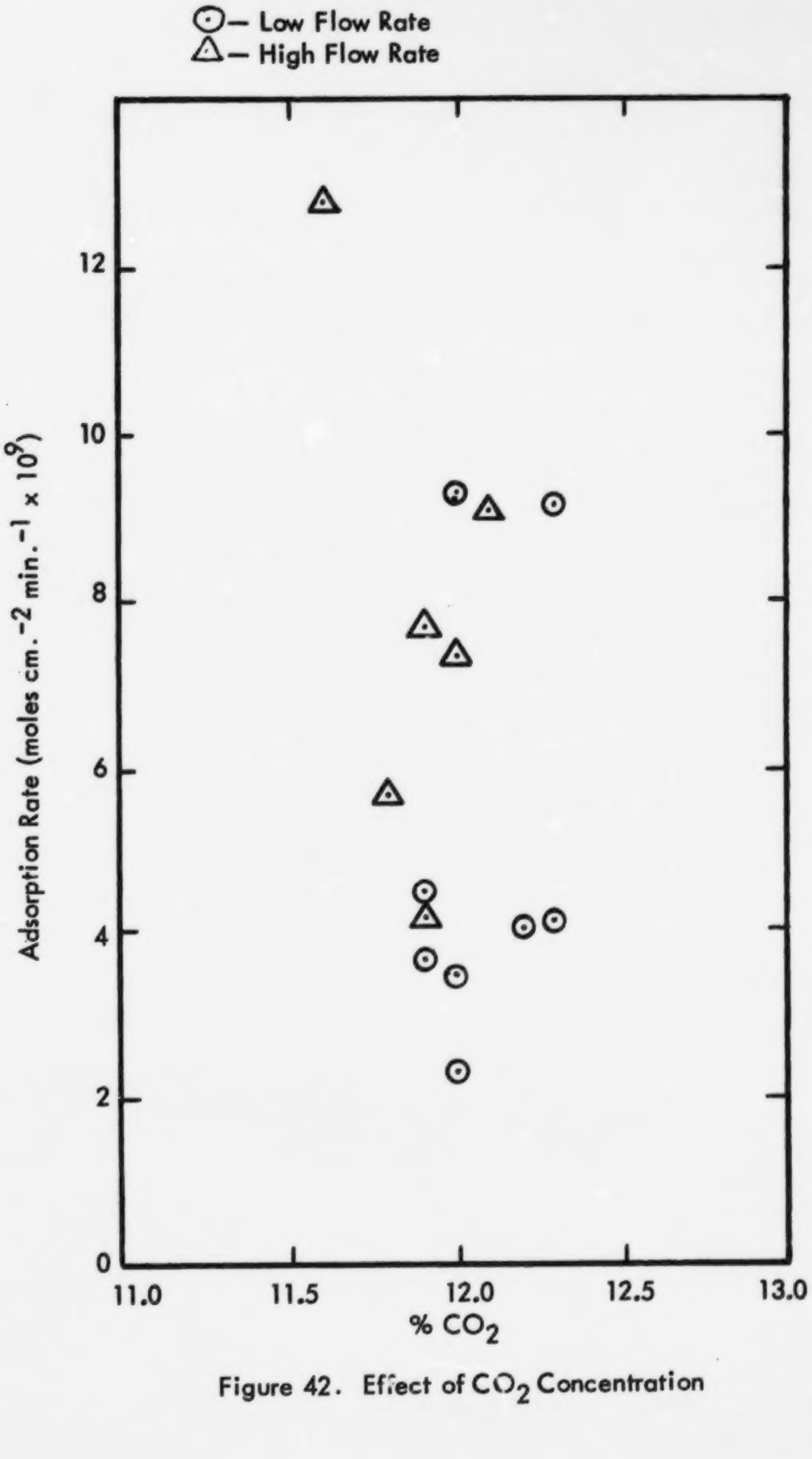

Figure 42. Effect of CO_2 Concentration

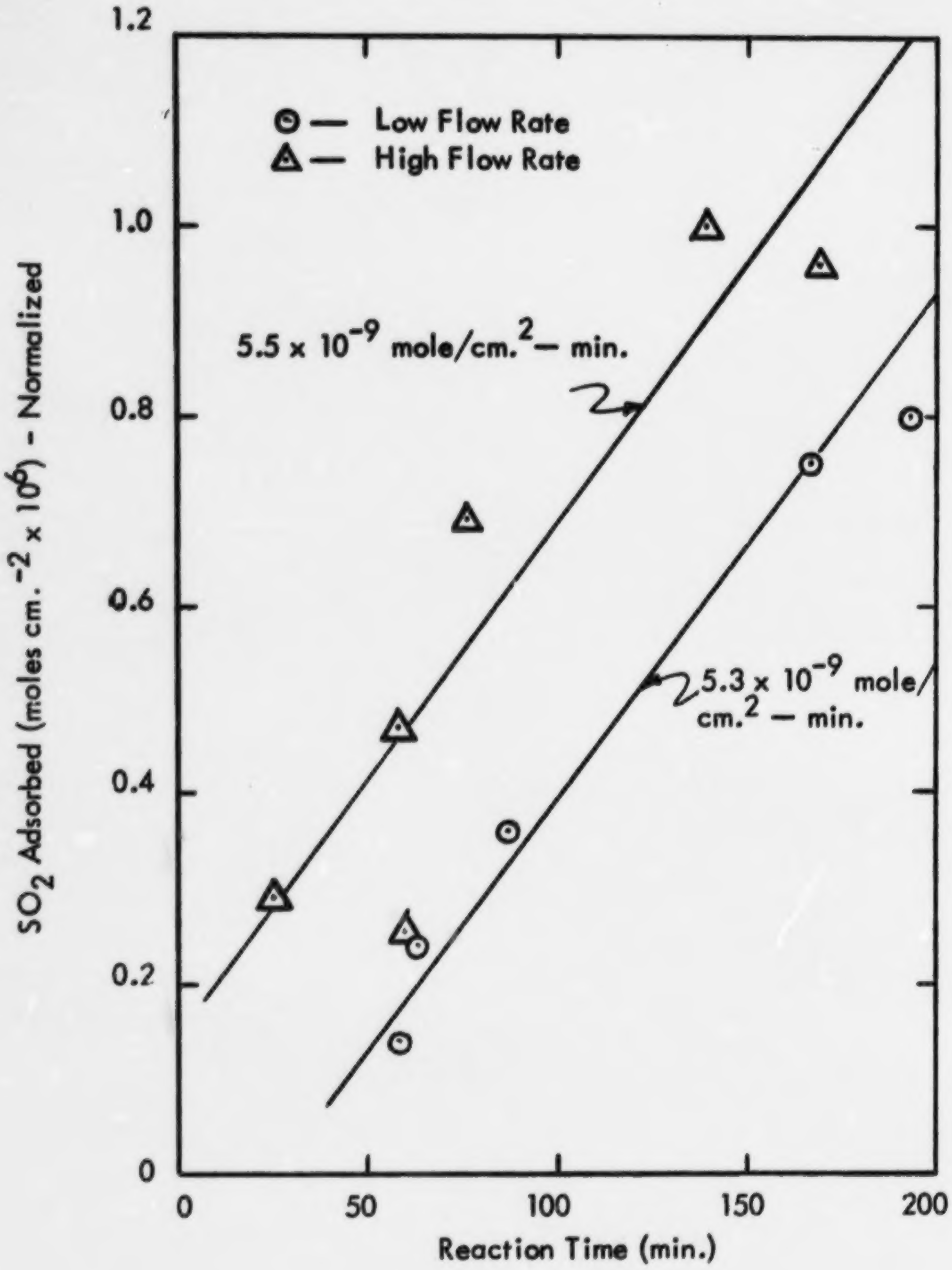

Figure 43. Effect of Total Gas Flow Rate on Adsorption Rate

out and an equilibrium atmosphere established, plus the equilibrium moisture content of the adsorbent film must be established. Such effects as these probably change the shape of the initial portion of the curve, with more delay in establishing steady-state being expected at the lower flow rates.

The reason that diffusion is not controlling despite the low Reynold's Number in the infrared studies conducted at GTC is that the cell chamber is in an eddying condition since the gas flow encounters a sharp change in flow cross section upon entering the cell and the eddy currents are triggered by this action. Therefore, higher adsorption rates, ones in keeping which the chemical reaction effects, have been found with the analytical system.

e. Infrared Spectrum of Sample No. BCR 1362-201 After Reaction with a Simulated Flue Gas at Elevated Temperatures

The infrared spectra of limestone Sample No. BCR 1362-201 before and after reaction with sulfur dioxide in a flue gas for 1.8 hours at 250°C. are shown in Figure 44. Infrared absorption bands attributed to carbonate appear at 1454 and 858 cm.$^{-1}$ in the spectrum of the unreacted sample. After the limestone sample has reacted with sulfur dioxide, an infrared absorption band due to sulfate is observed at 1078 cm.$^{-1}$ and at 635 cm.$^{-1}$. The 635 cm.$^{-1}$ absorption band appears as a very weak shoulder. The 891 cm.$^{-1}$ band has been assigned to a combination of infrared absorptions attributed to $SO_3^=$ and $CO_3^=$ formation.

f. Infrared Spectrum of Alkalized Alumina Before and After Reaction with Flue Gas at Elevated Temperatures

The infrared spectrum of alkalized alumina before and after reaction with sulfur dioxide in a flue gas for two hours at 204°C. is shown in Figure 45. After reaction of the alkalized alumina with sulfur dioxide, an infrared band assigned to sulfate appeared

GTC 136-31

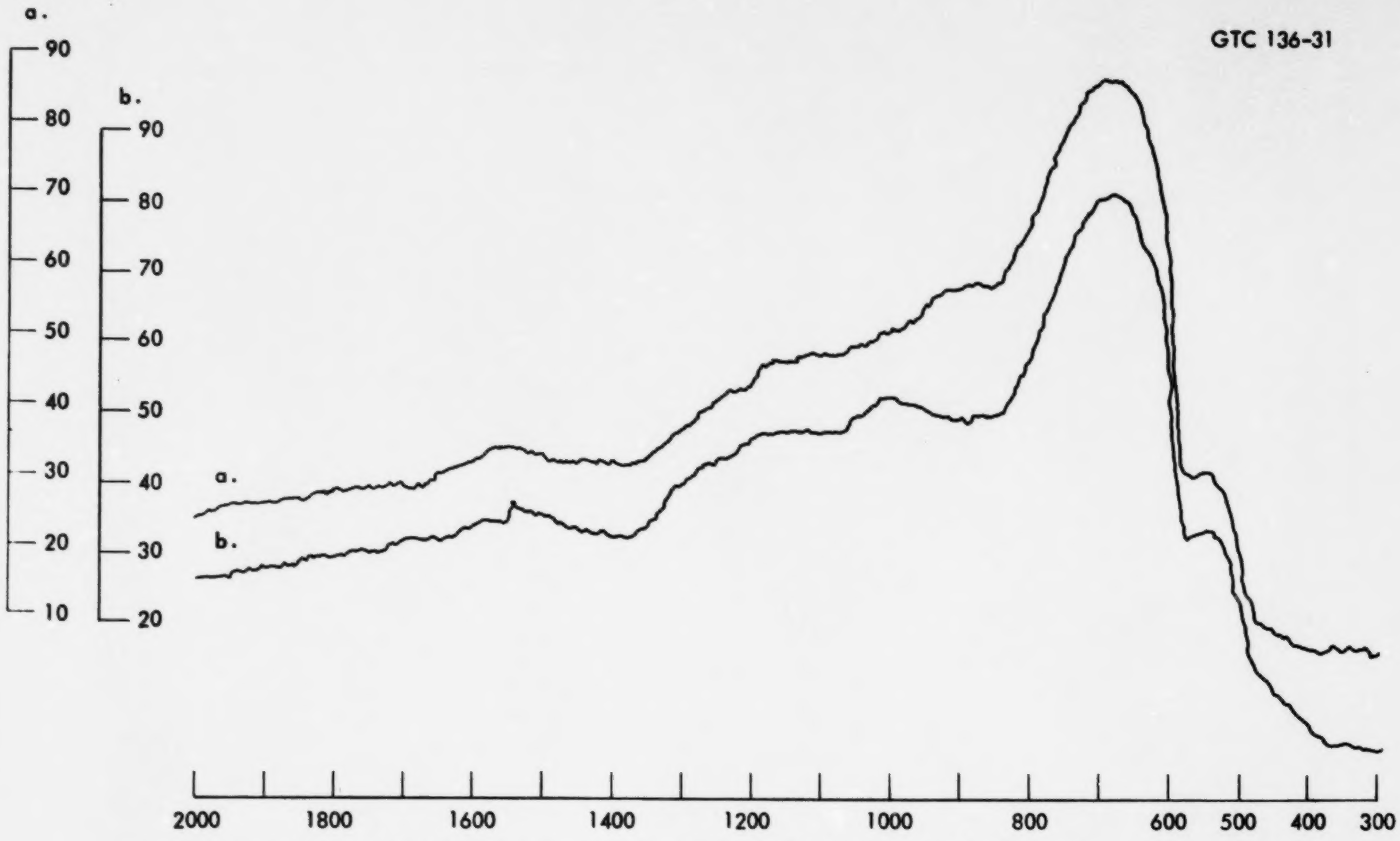

Figure 44. Sample No. BCR 1362-201 Before and After Reaction with SO_2 in a Synthetic Flue Gas. a. Spectral Scan of Sample No. BCR 1362-201 Before Reaction. b. Spectral Scan of Sample No. BCR 1362-201 After Reaction with Sulfur Dioxide in a Flue Gas for 1.8 Hours at 250°C.

GTC 136-30

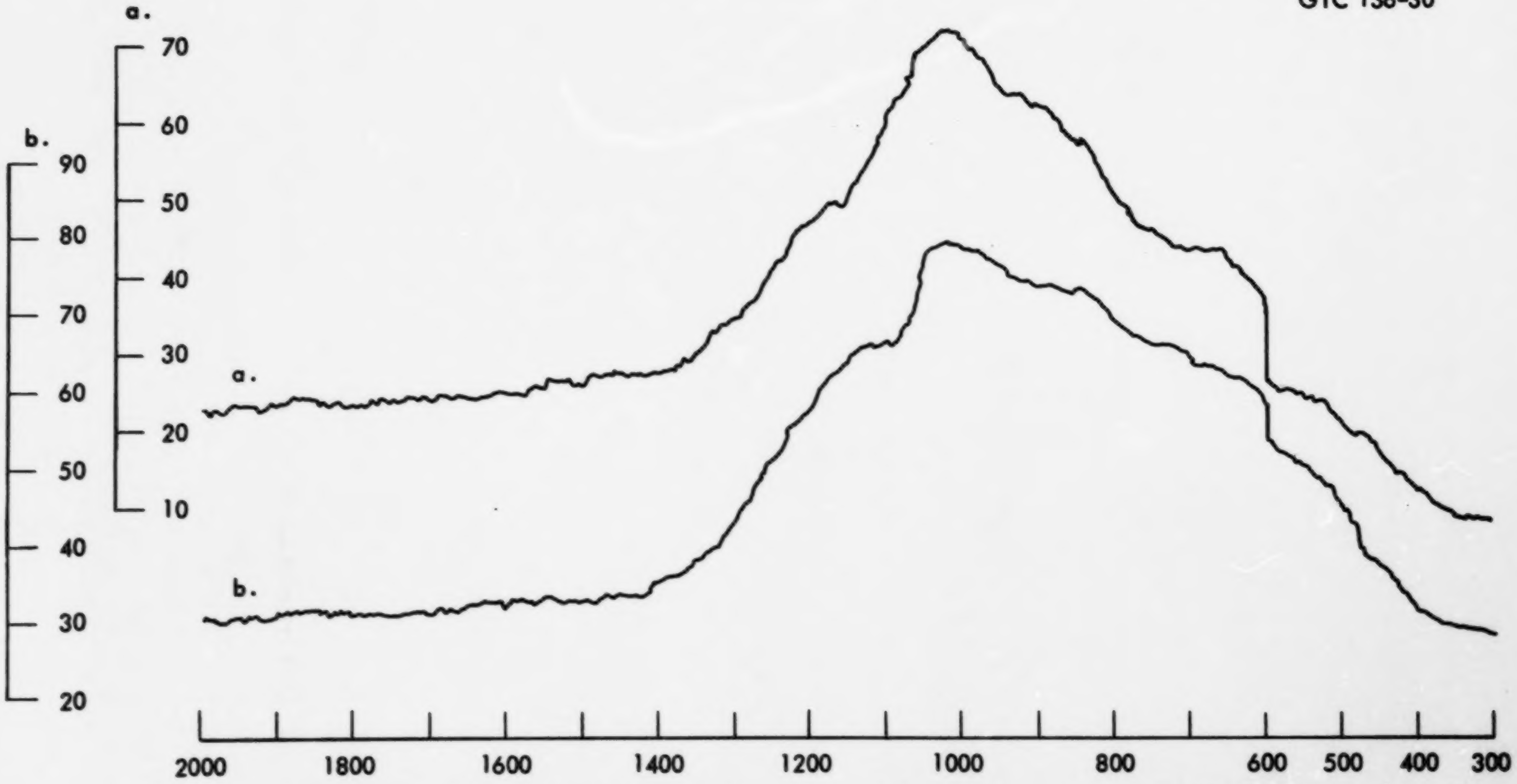

Figure 45. Infrared Spectra of Alkalized Alumina Deposit. a. Infrared Spectrum of Alkalized Alumina Before Reaction with SO_2 in a Flue Gas. b. Infrared Spectrum of Alkalized Alumina After Reaction with SO_2 in a Flue Gas for Two Hours at 204°C

at 1100 cm.$^{-1}$. The amount of sulfate on the surface of the alkalized alumina was calculated to be .56 x 10^{-6} moles/cm.^{2}. The weak absorption band at 930 cm.$^{-1}$ was assigned to $SO_3^=$.

4. PRELIMINARY STUDIES ON THE UTILIZATION OF INFRARED SPECTROSCOPY TO INVESTIGATE "DEAD BURNING"

Infrared spectroscopy was utilized to investigate the phenomenon of "dead burning" in limestone samples. In the investigation of this phenomenon, the infrared spectrum of dead-burned limestone samples obtained from the National Air Pollution Control Administration were studied. The infrared spectra of limestone Sample No. BCR 1363 is shown in Figures 46 and 47. Figure 46 covers the 4000 - 2000 cm.$^{-1}$ region and Figure 47 covers the 2000 - 300 cm.$^{-1}$ region. In each figure, spectrum a. is the dead-burned limestone sample and spectrum b. is the limestone sample containing adsorbed sulfur dioxide.

In the 4000 - 2000 cm.$^{-1}$ region, there are no differences between the spectrum of the dead-burned material and the material containing adsorbed sulfur dioxide. The O-H stretching vibrational mode is present at 3656 cm.$^{-1}$ for the former material and 3650 cm.$^{-1}$ for the latter material. Other infrared absorption bands due to the $CO_3^=$ ion occur at 2924 and 2852 cm.$^{-1}$.

Differences, however, do occur in the spectrum of both materials in the 2000 - 300 cm.$^{-1}$ region. In Spectrum 47b, the presence of the sulfate ion is indicated by the medium intensity absorption band at 1116 cm.$^{-1}$ and the weak intensity infrared absorption band at 640 cm.$^{-1}$. The carbonate ion is indicated by the doublet of the strong intensity absorption band at 1418 - 1454 cm.$^{-1}$. A comparison of the two spectra show that the doublet at 975 - 988 cm.$^{-1}$ in spectrum a. becomes the 1004 cm.$^{-1}$ absorption band of the dead-burned material. In addition, the sulfate ion is not present in the spectrum of

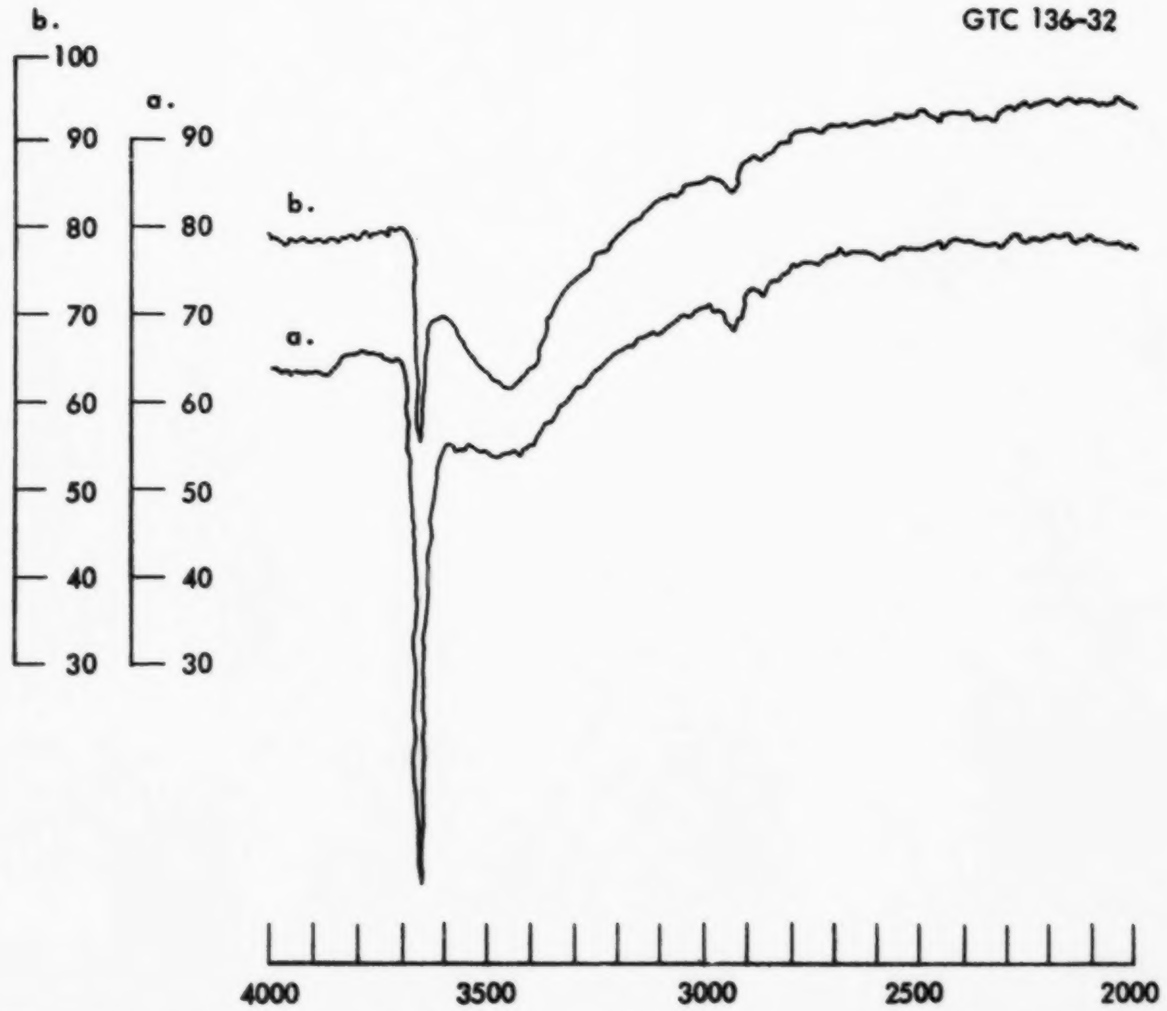

Figure 46. Infrared Spectrum of Sample No. BCR 1363. a. Sample No. BCR 1363 Containing Adsorbed SO2. b. Sample No. BCR 1363 (Dead Burned)

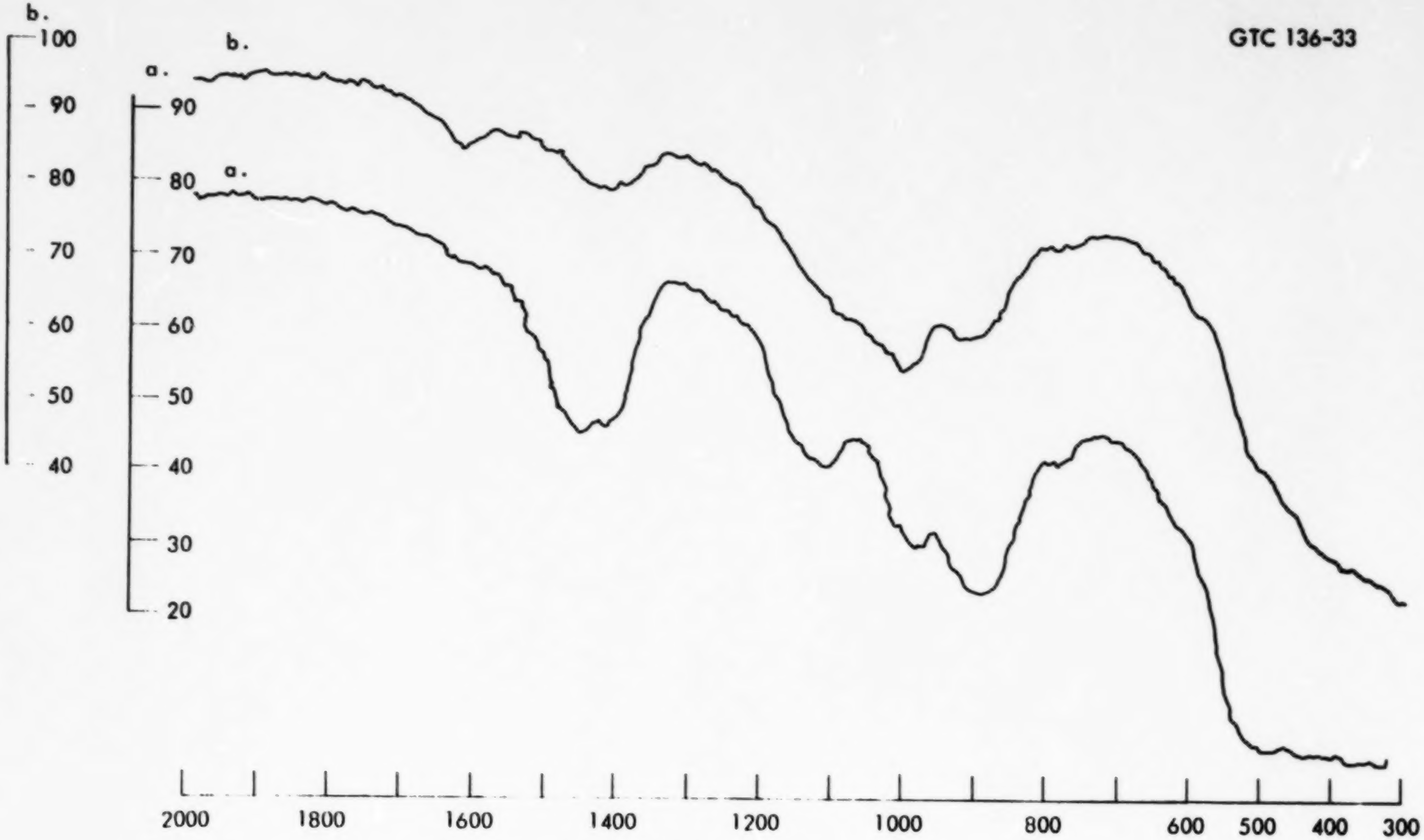

Figure 47. Infrared Spectrum of Limestone Sample No. BCR 1363. a. Sample No. BCR 1363 Containing Adsorbed SO_2. b. Sample No. BCR 1363 (Dead Burned)

the dead-burned material. Furthermore, the medium intensity band at 910 cm.$^{-1}$ decreases in intensity relative to the 982 cm.$^{-1}$ band of Spectrum 47a. One probable assignment of infrared bands in this region is to silicates. Bellamy(23) indicates that silicates absorb in the 1100-900 cm.$^{-1}$ region. For example(24), Tremolite ($(OH)_2Ca_2Mg_5(Si_4O_{11})_{12}$) and actinolite ($(OH)_2Ca(MgFe)_5(Si_4O_{11})_{12}$) exhibit closely related spectra with absorption bands in this region. Hornblend ($Ca(MgFe)_3Si_4O_{12}$; $CaMg_2(AlFe)_2Si_3O_{12}$), however, shows only one band at 1010 cm.$^{-1}$ Hence, based on the foregoing discussion, the doublet at 975 - 988 cm.$^{-1}$ in Spectrum47a and the 1004 cm^{-1} absorption band in Spectrum 47b were assigned to infrared absorption by silicates. This evidence is further substantiated by the presence of absorption bands in this region in limestone samples whose analysis indicates significant amounts of silica are present in the sample.

The infrared spectrum of dead-burned limestone Sample No. BCR 1369 is shown in Figure 48. The silicate absorption band is at 1009 cm.$^{-1}$. The hydroxide absorption band at 3656 cm.$^{-1}$ is due to the adsorption of water by the sample producing calcium hydroxide. The broad adsorption band at 1410 cm.$^{-1}$ and the band at 890 cm.$^{-1}$ are due to the formation of calcium carbonate caused by the reaction of CO_2 with calcium hydroxide. Hence, these preliminary results indicate that silica is present in the dead-burned material.

5. PROPOSED DESIGN OF INFRARED CELL FOR CONDUCTING INFRARED SPECTROSCOPIC STUDIES OF GAS-SOLID INTERACTIONS IN THE TEMPERATURE RANGE OF 1600-2000°F.

A proposed design of a high-temperature cell for the reaction of flue gas with limestone samples in the temperature range of 1600 - 2000°F. is shown in Figure 49. The cell is constructed from fused quartz. It can be fitted with either NaCl or KBr windows since the windows are well removed from the heat zone. In actual operation, the limestone

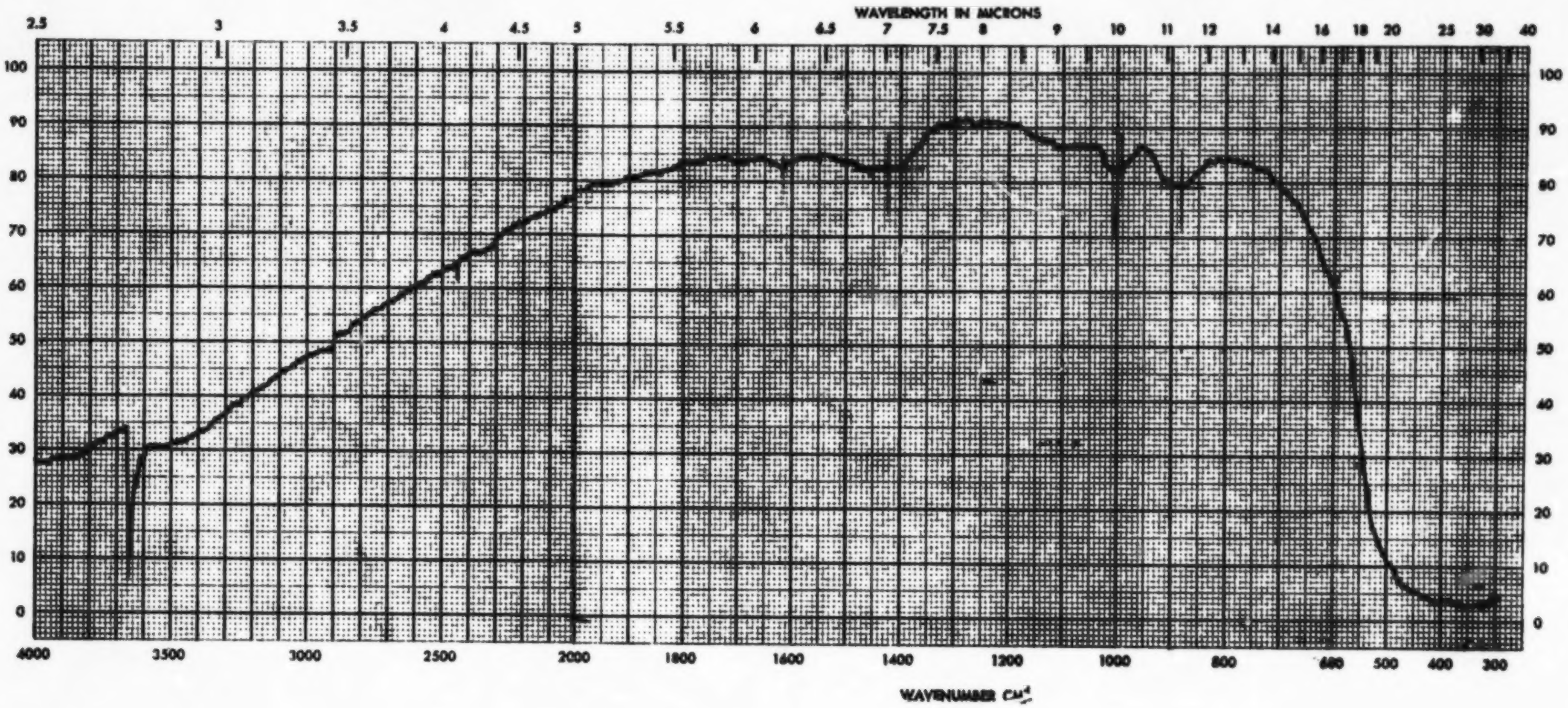

Figure 48. Infrared Spectrum of Limestone Sample No. BCR 1369-DB

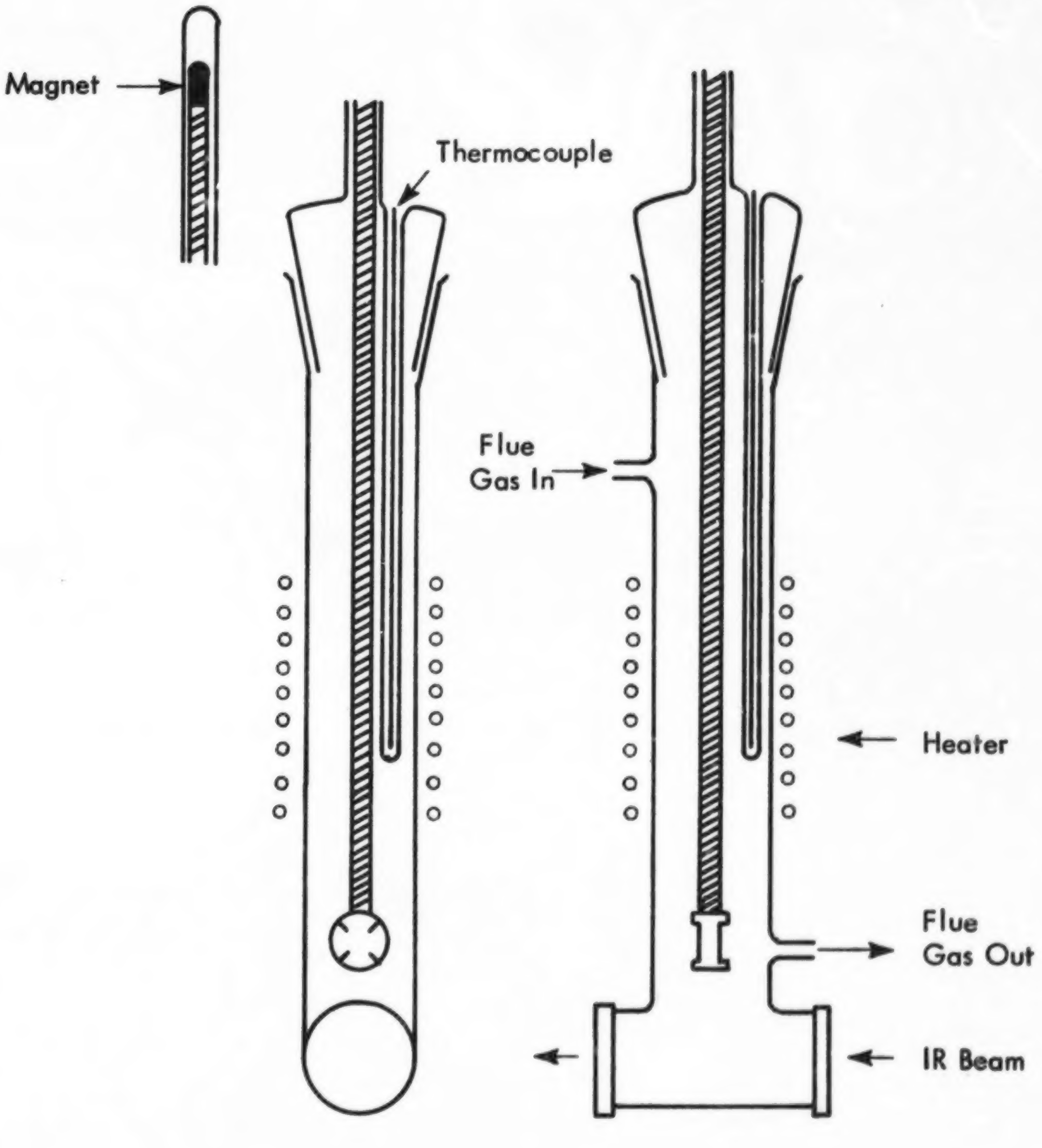
Magnet
Thermocouple
Flue Gas In
Heater
Flue Gas Out
IR Beam

Figure 49. High-Temperature Cell for the Study of Gas-Solid Interactions at Temperatures in Excess of 1800°F.

sample is plated on the Irtran 3 (polycrystalline calcium fluoride) window which is attached to a quartz rod. The cell is assembled and the sample is raised to the heat zone and exposed to flue gas in the temperature range of 1600 - 2000°F. The window is then lowered and placed in the infrared sampling beam of the spectrophotometer to record the spectrum of the sample. The proposed Irtran 3 window of the infrared cell has a useful temperature limit in air around 1000°C. and a useful transmittance range of <0.4 - 11.5 at 25° C.* This particular design is used because the light emissions from the cell window containing the sample would be so great that it would prevent the measurement of the infrared absorption bands of the sample.

---

*Kodak Pamphlet No. U-71, "Condensed Data for Kodak Irtran Infrared Materials," Eastman Kodak Co., Rochester, N. Y.

SECTION IV

CONCLUSIONS AND RECOMMENDATIONS

This study has illustrated the applicability of infrared spectroscopy to the study of gas-solid interactions occurring between sulfur dioxide in a simulated flue gas and various solid adsorbents. Utilizing infrared spectroscopy, it has been possible to determine the mechanism of the gas-solid interaction, determine the relative rates of sulfur dioxide uptake by various limestone adsorbents as a function of time and temperature and to ascertain the thermodynamics of the adsorption process.

The results may be summarized as follows:

1. The slaked limestone samples exposed to flue gas in the temperature range of 200 - 400°C. adsorb sulfur dioxide in a two-step process. Sulfur dioxide is adsorbed as sulfite and the sulfite is oxidized to sulfate.
2. In limestone samples exposed to sulfur dioxide at 1800°F., only sulfate is observed in the reaction product due to the rapid oxidation of the adsorbed sulfite to sulfate.
3. A two-fold increase in the flow rate had little effect on the rate of adsorption of sulfur dioxide by Sample No. BCR 1699-202 at 262°C.
4. Preliminary studies on the spectra of "dead-burned" limestone samples indicated that silica probably plays a role in the "dead-burning" process.
5. The activation energy for the adsorption of sulfur dioxide by limestone Sample No. BCR 1699-202 at 262°C. was found to be 11.8 Kcal/mole.

6. The temperature effect on the adsorption rate was found to be too great to be consistent with a derived diffusion-limiting situation described in the report. Hence, it was concluded that the absorption cell was not diffusion-mechanism rate controlled.

In order to further develop the infrared spectroscopic technique as a more quantitative tool in the study of gas-solid interactions, the following recommendations are made:

1. Actually measure the amount of SO_2 adsorbed by chemical analysis or by use of the B.E.T. adsorption isotherm technique and relate the amount of SO_2 to the absorbence of the ν_3 sulfate absorption band.
2. Use of dual-cell assembly in which a heated cell is also placed in the reference beam of the infrared spectrophotometer to help compensate for the emissions due to the infrared window.
3. Develop better techniques for preparing the solid sample for infrared studies. This would mean incorporating the sample in a pellet or developing better plating techniques to reduce scattering in the sample.
4. Another area of interest would be the measurement of the emission spectrum of solid adsorbents exposed to sulfur dioxide. This would be applicable to the study of gas-solid interactions at temperatures around 2000°F. Data obtained in this manner would be applicable to understanding the chemical reaction occurring during the injection of limestone or lime into the boilers of power plants for the reduction of sulfur dioxide emissions into the atmosphere.

SECTION V

REFERENCES

1. Tennessee Valley Authority, "Sulfur Oxide Removal from Power Plant Stack Gas", PB 178 972, 1968.

2. AVCO Space Systems Division, "Removal of SO_2 from Flue Gas", PB 177 492, November 1, 1967.

3. Little, L. H., "Infrared Spectra of Adsorbed Species", Academic Press, New York, N.Y., 1966.

4. Hair, Michael L., "Infrared Spectroscopy in Surface Chemistry", Marcel Debber, Inc., New York, N. Y., 1967.

5. Eichens, R. P. and Plishin, W. A., Advances in Catalysis, 10, Academic Press, New York, N. Y., 1958.

6. Bertoluzza, A., Bonino, G. B., Fabbi, G. and Lorenzelli, V., J. Chim. Phys., 63, 395-400 (1966).

7. Kiselev, A. V., Quart. Rev., 15, 99-124 (1961).

8. Little, L. H., Ibid., p. 20.

9. Blyholder, George and Neff, Laurence D., J. Phys. Chem., 66, 1464-1469, (1962).

10. Stuart, W. I. and Whateley, T. L., Trans. Faraday Soc., 61, 2763-2771, (1965).

11. Peri, J. B., J. Phys. Chem., 70, 3168, (1966).

12. Ward, J. W. and Habgood, H. W., J. Phys. Chem., 70, 1178-1182, (1966).

13. Crawford, V., Quart. Rev., 14, 378-340, (1960).

14. Borgwardt, R. H., Private communication.

15. Kirkland, J. J., Anal. Chem., 27, 1537-41 (1955).

16. Decius, J. C., Spectrochemica Acta, 21, 15-22, (1965).

17. Frey, Paul R., "College Chemistry", Prentice-Hall, Inc., New York, N.Y., 1955.

18. Nahamoto, Kazu, "Infrared Spectra of Inorganic and Coordination Compounds", John Wiley & Sons, New York, N. Y., 1963, p. 73.

19. Bellamy, L. J., "The Infra-red Spectra of Complex Molecules", Methuen & Co., Ltd., London, England, 1958, p. 344.

20. Rao, C. N. R., "Chemical Applications of Infrared Spectroscopy", Academic Press, New York, N. Y., 1963, p. 343.

21. Little, L. H., "Infrared Spectra of Adsorbed Species", Academic Press, New York, N. Y., 1966, p. 77.

22. Sherwood, Thomas and Pigford, Robert L., "Absorption and Extraction", McGraw-Hill, New York, N. Y., 1952, p. 10.

23. Bellamy, L. D., op. cit.

24. Ibid., pp. 347-348.

SECTION VI

APPENDIX

REYNOLD'S "ANALOGY" EQUATIONS FOR MASS TRANSFER FROM A GAS STREAM TO A FLAT PLATE

The Reynold's "analogy" equation used to investigate the temperature dependence of the adsorption rate can best be understood by considering the following discussions. The mass transfer of an adsorbate from a gas stream to a plane surface may be calculated from an equation derived from Reynold's "analogy" relating heat transfer and friction. For mass transfer from a gas stream to a flat plate, we have the expression:

$$J_D = 0.66\, Re_x^{-1/2} \tag{1}$$

where Re_x = length Reynold's number based on the distance from the leading edge to the downwind boundary as the characteristic dimension. The length Reynold's number, Re_x, is expressed by Equation (2):

$$Re_x = \frac{x v \rho}{\mu} \tag{2}$$

where x = length transversed by the gas stream ft.

ρ = density of the gas mixture, lb./ft.^{3}

v = the velocity of the gas stream, ft./hr.

In addition to equation (1), the following expression holds for J_D:

$$J_D = \frac{k_g P_{BM}}{G_M} \left\{\frac{\mu}{\rho D_v}\right\}^{2/3} \tag{3}$$

where k_g = gas-film coefficient, lb. moles/(hr.)(ft.^{2}) atm

P_{BM} = logarithmic mean of P_B at phase boundary and P_B in bulk of fluid

P_B = partial pressure of nondiffusing gas B, atm.

G_M = molar gas velocity of stream, lb. mole/(hr.)(ft.^{2})

μ = viscosity, lb./(hr.)(ft.)

ρ = density, lb./ft.^{3}

D_v = molecular diffusivity in gas, ft.^{2}/hr.

Combining Equation (1) and (3), we have

$$0.66\,Re_x^{-1/2} = \frac{k_g P_{BM}}{G_M}\left\{\frac{\mu}{\rho D_v}\right\}^{2/3} \tag{4}$$

Solving for k_g and substituting the value of Re_x in Equation (2), k_g is given by Equation (5):

$$k_g = 0.66\left\{\frac{x\,v\,\rho}{\mu}\right\}\frac{G_M}{P_{BM}}\left\{\frac{\mu}{\rho D_v}\right\}^{-2/3}. \tag{5}$$